

**A RAPID KINETIC TECHNIQUE  
FOR MEASURING REACTIVITY  
OF SULPHIDE WASTE ROCK:  
THE OXYGEN CONSUMPTION  
METHOD**

**MEND Project 4.6.5b**

**This work was done on behalf of MEND and sponsored by  
INCO Limited  
Voisey's Bay Nickel Company and  
Waterloo Centre for Groundwater Research**

**December 1997**

A Rapid Kinetic Technique  
for Measuring the Reactivity of Sulphide Waste Rock:  
The Oxygen Consumption Method

A Report Prepared for MEND

With Financial Support from;  
**INCO** Limited  
Waterloo Centre for Groundwater Research  
Voisey' Bay Nickel Company Limited

Prepared by:

Ronald V. Nicholson<sup>(1)</sup>,

Jeno M. Scharer<sup>(2)</sup>

Principal investigators

and

Mark E. Anderson<sup>(2)</sup>

Research Assistant

<sup>(1)</sup>Department of Earth Sciences and  
<sup>(2)</sup>Department of Chemical Engineering  
University of Waterloo  
Waterloo, ON  
Canada, N2L 3G1

December, 1997

## Executive Summary

Assessment of waste rock reactivity involving potential acid generation and/or metal release generally includes kinetic testing methods such as humidity cells and column tests. These tests are generally conducted over periods of tens to hundreds of weeks for the assessment of a single waste rock sample. Each test can provide a single rate of acid generation or rate of metal release. There is clearly a need for additional test methods that can provide more cost effective data to assess waste rock reactivity.

The oxygen consumption method, that was initially developed as a tool to assess reactive tailings in the laboratory and field was adapted to measure reaction rates on waste rock samples in short term experiments. The technique provides reaction rate data that can complement data from humidity cells. Many samples can be processed simultaneously and, therefore, a larger body of kinetic data can be developed for cost-effective statistical assessment and interpretation. This study represents the development of the technique, demonstration of the interpretation and a comparison among several waste rock types from selected mines and exploration projects.

An experimental method was developed to assess the rate of oxygen consumption in sulphide waste rock. The technique involves placing a reactive rock sample in a sealed chamber and measuring the gas-phase oxygen concentration over a period of 2 to 3 days. A research programme was undertaken to investigate the influence of particle size, sulphur content, temperature and inoculation with *Thiobacillus ferrooxidans* on the rate of oxygen consumption of waste rock samples. Waste rock and drill core samples were collected from a number of locations and the oxygen consumption rates of different rock types were compared and contrasted.

The oxygen consumption rate was expected to increase with decreasing particle size, increasing temperature, higher sulphur content and inoculation with *T. ferrooxidans*. The experimental results generally agreed with the expected trends. Particle size effects were studied over a range of sizes from 0.07 to 100 mm. The oxygen consumption rate was a function of  $1/d^n$ , where n was generally between 0.8 and 1.6 for uninoculated samples. Values of n were slightly lower for

inoculated samples, typically between 0.3 and 0.7. The oxygen consumption rate of samples inoculated with *T. ferrooxidans* was linearly related to the total sulphur content of the waste rock. Oxygen consumption rates of uninoculated rock samples did not show a strong dependence on sulphur content. The rate of oxygen consumption in rock containing pyrrhotite as the dominant sulphide mineral increased by a factor of 2 to 10 after inoculation with *T. ferrooxidans* at temperatures of 20 and 30°C. The rates of oxygen consumption in rocks with pyrite as the dominant sulphide increased by as much as a factor of 60 after inoculation. The more pronounced increase for pyrite rates appears to be related to the relatively high rates of pyrrhotite oxidation in the absence of bacteria compared to those for pyrite under similar conditions. At temperatures below 20°C, inoculation did not significantly enhance the rates of oxygen consumption.

Sulphate release rates from selected rock samples were measured on the samples being tested for oxygen consumption and compared to oxygen consumption rates based on the stoichiometry of pyrite and pyrrhotite oxidation. The oxygen consumption rate consistently over-estimated the rate of sulphate release for samples containing pyrrhotite. Partial oxidation of sulphide in the pyrrhotite leading to enrichment of sulphur on the surface may account for 60 to 90% of the total oxygen consumed by pyrrhotite. This is consistent with results observed in more fundamental studies of pyrrhotite oxidation kinetics for early stages of oxidation (weeks to months). Samples containing pyrite as the dominant sulphide mineral exhibit oxygen consumption rates that correlate well with the amount of sulphate released.

Oxygen consumption measurements provide rates of reaction in waste rock samples that can be used to interpret potential acid generation and metal leaching rates. The data can be used to assess depletion rates for sulphide minerals and neutralization potential. Although the method does not give water chemistry, the oxygen consumption values can be used to infer drainage chemistry and can also provide complementary data for other kinetic testing such as humidity cells. In addition, the results of the oxygen consumption tests can be used as input values for sophisticated waste rock models if such methods are required for further evaluation.

## Sommaire

L'évaluation de la réactivité des stériles comportant un risque de production d'acide et/ou de dégagement de métaux fait appel généralement à des méthodes d'essai cinétique, comme les cellules d'humidité et les essais en colonne. En général, ces essais sont effectués sur des périodes allant de dizaines à des centaines de semaines pour l'évaluation d'un seul échantillon de stérile. Chaque essai permet de mesurer une seule vitesse de production d'acide ou de dégagement de métaux. De toute évidence, il y a lieu de disposer d'autres méthodes d'essai qui permettraient d'obtenir des données plus rentables pour évaluer la réactivité des stériles.

Nous avons adapté la méthode de mesure de la vitesse de consommation d'oxygène, initialement mise au point pour évaluer les résidus réactifs en laboratoire et sur le terrain, en vue de déterminer les vitesses de réaction d'échantillons de stérile dans le cadre d'expériences de courte durée. Cette technique permet d'obtenir des données sur les vitesses de réaction qui viennent compléter celles obtenues avec les cellules humidité. Comme elle traite simultanément de nombreux échantillons, cette technique fournit un plus grand nombre de données cinétiques qui permettent de procéder de façon plus rentable à l'évaluation statistique et à l'interprétation. Cette étude porte sur la mise au point de cette technique, sur la démonstration de l'interprétation et sur une comparaison de plusieurs types de stérile provenant de certaines mines et obtenus au cours de certains projets d'exploration.

Nous avons mis au point une méthode expérimentale permettant d'évaluer la vitesse de consommation d'oxygène par les stériles sulfurés. Dans cette technique, on place un échantillon de stérile acidogène dans une enceinte scellée, puis on mesure la concentration d'oxygène dans la phase gazeuse sur une période de 2 à 3 jours. Le programme de recherche avait pour but d'évaluer l'effet de la granulométrie, la teneur en soufre, la température et l'inoculation avec *Thiobacillus ferrooxidans* sur la vitesse de consommation d'oxygène par des échantillons de stérile. Nous avons prélevé des échantillons de stérile et de carotte à un certain nombre d'endroits, puis nous avons

compare et confronté les vitesses de consommation d'oxygene par differents types de roches.

Selon les previsions, la vitesse de consommation d'oxygene augmenterait en presence d'une diminution de la granulometrie, d'une augmentation de la temperature et d'une teneur en soufre plus élevées et apres inoculation avec *T. ferrooxidans*. En general, les résultats expérimentaux concordaient avec les tendances prévues. Les effets de la granulometrie ont été étudiés sur une plage de tailles allant de 0,07 à 100 mm. La vitesse de consommation d'oxygene Ctait une fonction de  $1/d^n$ , où n était generalement compris entre 0,8 et 1,6 inclusivement pour les Cchantillons non inocules. Les valeurs de n etaient légèrement plus faibles pour les echantillons inocules avec *T. ferrooxidans*, se situant normalement entre 0,3 et 0,7. La vitesse de consommation d'oxygene par des echantillons inocules avec *T. ferrooxidans* variait de façon lineaire avec la teneur totale en soufre des stériles. Les vitesses de consommation d'oxygene par des echantillons de roche non inocules ne dependaient pas etroitement de la teneur en soufre. La vitesse de consommation d'oxygene par des roches contenant de la pyrrhotine comme mineral sulfuré principal augmentait par un facteur de 2 à 10 apres inoculation avec *T. ferrooxidans* à des temperatures de 20 et de 30 °C. Les vitesses de consommation d'oxygene par des roches contenant de la pyrite comme mineral sulfuré principal augmentaient par un facteur pouvant atteindre 60 apres inoculation. L'augmentation plus prononcee des vitesses de consommation par la pyrite semblait dependre des vitesses relativement élevées d'oxydation de la pyrrhotine en l'absence de bactéries, en comparaison des vitesses de consommation par la pyrite dans des conditions semblables. À des temperatures inferieures à 20 °C, l'inoculation n'augmentait guère les vitesses de consommation d'oxygene.

Nous avons mesuré les vitesses de degagement de sulfate par certains echantillons de roche utilisés pour determiner la consommation d'oxygene et nous les avons comparées aux vitesses de consommation d'oxygene obtenues à partir de la stoechiometrie de l'oxydation de la pyrite et de la pyrrhotine. La vitesse de consommation d'oxygene surestimait régulièrement la vitesse de dégagement de sulfate par les echantillons

contenant de la pyrrhotine. L'oxydation partielle du sulfure dans la pyrrhotine, qui entraînait un enrichissement en soufre à la surface, permet de rendre compte de 60 à 90 % de la consommation totale d'oxygène par la pyrrhotine, ce qui Concorde avec les résultats obtenus lors d'études plus fondamentales de la cinétique d'oxydation de la pyrrhotine pendant les premières étapes de l'oxydation (allant de semaines à des mois). Les échantillons contenant de la pyrite comme minéral sulfuré principal consomment de l'oxygène à des vitesses qui concordent étroitement avec la quantité de sulfate dégagé.

Les mesures de la consommation d'oxygène permettent de déterminer les vitesses de réaction dans les échantillons de stérile, que l'on peut utiliser pour interpréter les risques de production d'acide et les vitesses de lixiviation de métaux. Les données peuvent servir à évaluer les vitesses d'épuisement des minéraux sulfurés, ainsi que le potentiel de neutralisation. La méthode ne permet pas d'établir la chimie en milieu aqueux, mais les vitesses de consommation d'oxygène peuvent servir à déduire la chimie du drainage et à fournir des données complémentaires lors d'autres essais servant à déterminer la cinétique, comme les cellules d'humidité. De plus, les résultats des déterminations de la consommation d'oxygène peuvent être utilisés dans des modèles perfectionnés simulant les stériles, si de telles méthodes sont nécessaires pour procéder à des évaluations plus poussées.

## **Acknowledgments**

This research would not have been possible without the financial support of Inco Ltd., Voisey's Bay Nickel Company and the Waterloo Centre for Groundwater Research. Special gratitude is extended to Mr. Michael McCann (INCO) and Mr. William Napier (Voisey's Bay) for their interest in this study.

The authors would also like to thank those who provided assistance during the project, including; Edmund Kwong, Phil Tibble, Mike Janzen, David Stuienberg, Gary Williams, Charlie Magnusson, Iringo Scharer and Joyce Hui.

# Table of Contents

<b>1. INTRODUCTION .....</b>	<b>1</b>
<b>2. BACKGROUND .....</b>	<b>4</b>
<b>2.1 Oxidation of Iron Sulphides .....</b>	<b>4</b>
<b>2.2 Laboratory-scale Measurement of Oxidation Rate .....</b>	<b>5</b>
2.2.1 Humidity Cells .....	5
2.2.2 Waste Rock Columns.. .....	.8
<b>2.3 Field Scale Measurement of Oxidation Rate .....</b>	<b>9</b>
<b>2.4 Factors Influencing the Oxidation Rate of Sulphide Minerals .....</b>	<b>12</b>
2.4.1 Temperature .....	12
2.4.2 Particle Size .....	13
2.4.3 Presence of Iron-oxidizing Bacteria .....	15
2.4.4 Field and Laboratory Studies using the Oxygen Consumption Method.. .....	18
<b>3. MATERIALS AND METHODS .....</b>	<b>22</b>
<b>3.1 Materials .....</b>	<b>22</b>
3.1.1 Whistle Mine Waste Rock .....	.22
3.1.2 Voisey's Bay Rock Samples.. .....	.23
3.1.3 Additional Rock Samples.. .....	.24
<b>3.2 Particle Size .....</b>	<b>27</b>
<b>3.3 <i>Thiobacillus ferrooxidans</i> Cultures .....</b>	<b>27</b>
<b>3.4 Reactor Configurations .....</b>	<b>29</b>
3.4.1 Oxygen Sensor .....	30
3.4.2 Acrylic Reactor .....	30
3.4.3 Glass Reactor .....	31
3.4.4 Large Volume Reactors .....	32

<b>3.5 Oxygen Consumption Method for Waste Rock .....</b>	<b>35</b>
35.1 Detection Limit.....	<b>.36</b>
3.5.2 Data Analysis .....	37
3.5.3 Reproducibility and Precision .....	<b>.39</b>
<b>4. RESULTS .....</b>	<b>40</b>
<b>4.1 Particle Size .....</b>	<b>41</b>
4.1.1 Initial Tests on Whistle Mine Samples .....	41
4.1.2 Voisey's Bay Tests .....	43
4.1.3 Tests on Additional Rock Samples .....	44
<b>4.2 Temperature .....</b>	<b>48</b>
4.2.1 Initial Tests on Whistle Mine Samples .....	48
4.2.2 Voisey's Bay Tests.....	<b>.49</b>
4.2.3 Tests with Additional Rock Samples .....	49
<b>4.3 Sulphide Content .....</b>	<b>51</b>
4.3.1 Initial Tests on Whistle Mine Samples.....	<b>.51</b>
4.3.2 Voisey's Bay Tests .....	<b>.51</b>
4.3.3 Tests on Additional Rock Samples .....	54
<b>4.4 Inoculation with <i>Thiobacillus ferrooxidans</i> .....</b>	<b>57</b>
4.4.1 Initial Tests on Whistle Mine Samples .....	57
4.4.2 Voisey's Bay Tests .....	57
4.4.3 Tests on Additional Rock Samples .....	58
<b>4.5 Measured Sulphate Release Rates .....</b>	<b>62</b>
4.5.1 Initial Tests on Whistle Mine Samples .....	62
4.5.2 Voisey's Bay Tests .....	<b>.62</b>
4.5.3 Tests on Additional Rock Samples .....	65
<b>5. DISCUSSION .....</b>	<b>67</b>
<b>5.1 Error Analysis .....</b>	<b>.67</b>
<b>5.2 Multivariable Linear Regression .....</b>	<b>70</b>
5.2.1 Comparison to Field Data.....	<b>.73</b>

5.3 Particle Size .....	74
5.4 Temperature .....	77
5.5 Sulphide Content .....	78
5.6 Inoculation with <i>Thiobacillus ferrooxidans</i> .....	83
5.7 Measured Sulphate Release.. .....	.86
5.8 Comparison of Rates with those in the Literature	88
<b>6. SUMMARY OF CONCLUSIONS .....</b>	<b>91</b>
<b>7. REFERENCES .....</b>	<b>94</b>
<b>APPENDICES .....</b>	<b>99</b>
Appendix A: Measured oxygen consumption rates	
Appendix B: Oxygen consumption rate vs. nominal particle size for Voisey's Bay COMP samples	
Appendix C: Arrhenius plots	
Appendix D: Oxygen consumption rate vs sulphur content for Voisey's Bay COMP samples	
Appendix E: Normalized oxygen concentration vs time for 17L tests	
Appendix F: Summary of statistical output from SYSTAT®	
Appendix G: Analytical reports	

## List of Tables

Table 2.1 Sulphate release rates from Cinola Gold humidity cells .....	.7
Table 2.2 Reported values of $E_a$ for sulphide minerals.. .....	.12
Table 2.3 Effect of grain size on surface area (from Morin and Hutt, 1994) .....	.13
Table 3.1 Sulphide and carbonate content of Whistle waste rock samples.....	2 3
Table 3.2 Sulphide and carbonate content of Voisey's Bay rock samples.....	2 4
Table 3.3 Total sulphur and carbonate content for the additional rock samples .....	26
Table 3.4 Standard US Sieve Sizes.. .....	.27
Table 4.1 Values of n for Voisey's Bay COMP samples .....	.44
Table 4.2 Activation energies for Whistle waste rock samples.. .....	.49
Table 4.3 Activation energies for Voisey's Bay waste rock samples.. .....	.50
Table 4.4 Activation energies for different rock types.. .....	.50
Table 5.1 Estimated random error of measurements.. .....	.68
Table 5.2 Estimates of parameters in Equation 5.1 .....	.71
Table 5.3 Estimates of parameters in Equation 5.1 for inoculated rates.. .....	.72
Table 5.4 Dissolved metals and sulphate in leachate from Faro waste rock.. .....	.82
Table 5.5 Literature values of intrinsic Oxidation Rates .....	.90

## List of Figures

Figure 3.1 Schematic representation of oxygen consumption equipment.....	3 0
Figure 3.2 Scale drawing of acrylic reactor.. .....	. 31
Figure 3.3 Scale drawing of glass reactor.. .....	. 32
Figure 3.4 Scale drawing of 17L reactor.. .....	. 34
Figure 3.5 Sensor output for Whistle medium sulphide, 8 mm size, T=30°C.....	3 9
Figure 4.1 Oxygen consumption rate vs. size - Whistle massive sulphide at 20°C .	42
Figure 4.2 Oxygen consumption rate vs. size - Whistle high S norite at 20°C .....	.42
Figure 4.3 Oxygen consumption rate vs. size - Whistle medium S norite at 20°C...	4 3
Figure 4.4 Oxygen consumption rate vs. size - ED and WE composites.. .....	. 45
Figure 4.5 Oxygen consumption rate vs. size - Faro waste rock .....	. 45
Figure 4.6 Oxygen consumption rate vs. size - Mine Doyon waste rock.. .....	. 46
Figure 4.7 Oxygen consumption rate vs. size - Whistle high S norite .....	. 46
Figure 4.8 Oxygen consumption rate vs. size - Whistle low S norite .. .....	. 47
Figure 4.9 Oxygen consumption rate vs. size - Pamour waste rock.. .....	. 47
Figure 4.10 Oxygen consumption rate vs. size - KZK waste rock.. .....	. 48
Figure 4.11 Oxygen consumption rate vs. sulphide content -Whistle waste rock, 22 mm size at 20°C.. .....	. 51
Figure 4.12 Oxygen consumption rate vs. sulphide content - Whistle waste rock, 14 mm size at 20°C.. .....	. 52
Figure 4.13 Oxygen consumption rate vs. sulphide content - Whistle waste rock, 7 mm size at 30°C.. .....	. 52
Figure 4.14 Oxygen consumption rate vs. sulphide content - Whistle waste rock, 7 mm size at 10°C.. .....	. 53
Figure 4.15 Oxygen consumption rate vs. sulphide content - Whistle waste rock, 7 mm size at 30" inoculated with <i>T. ferrooxidans</i> .....	. 53
Figure 4.16 Oxygen consumption rate vs. sulphide content - ED and WE composites .....	54
Figure 4.17a Oxygen consumption rate vs. sulphide content - Ovoid samples .....	55

Figure 4.17b Oxygen consumption rate vs. sulphide content - Ovoid samples excluding HC8 .....	55
Figure 4.18 Oxygen consumption rate vs. sulphide content - 6 rock types, 8 mm size .....	56
Figure 4.19 Oxygen consumption rate vs. sulphide content - 6 rock types, 3 mm size .....	56
Figure 4.20 Scanning electron micrograph of <i>T. ferrooxidans</i> on Whistle massive sulphide material .....	69
Figure 4.21 Relative rate of oxygen consumption after inoculation - Whistle waste rock, 30°C, 8 mm size fraction .....	60
Figure 4.22 Relative rate of oxygen consumption after inoculation - Voisey's Bay COMPs, all size fractions .....	60
Figure 4.23 Relative rate of oxygen consumption after inoculation - ED and WE composites, 8 mm size fraction .....	61
Figure 4.24 Relative rate of oxygen consumption after inoculation - 6 rock types, 8 mm and 3 mm size fractions .....	61
Figure 4.25 Oxygen consumption rate vs. sulphate release rate - initial Whistle tests .....	63
Figure 4.26 Oxygen consumption rate vs. sulphate release rate - Voisey's Bay COMPs .....	63
Figure 4.27 Oxygen consumption rate vs. sulphate release rate - Voisey's Bay ED, WE and Ovoid samples .....	64
Figure 4.28 Oxygen consumption rate vs. sulphate release rate from humidity cells - ED and WE composites at 20°C .....	64
Figure 4.29 Oxygen consumption rate vs. sulphate release rate - 6 rock types . . . .	65
Figure 4.30 Oxygen consumption rate vs. sulphate release rate - pyrrhotite samples only .....	66
Figure 4.31 Oxygen consumption rate vs. sulphate release rate - pyrite samples only .....	66
Figure 5.1 Comparison of rate for 3 mm size rock from Mine Doyon and Faro.....	83

## **1. Introduction**

The mining of base and precious metals is a corner-stone of the Canadian economy. The mining and mineral industry accounts for \$20 billion annually and makes up 15% of Canada's exports (Dickie, 1995). The economic impact of mining is obvious, however there are also environmental issues related to the mining industry. It was not until relatively recently that the production, release and impact of acidic, metal laden leachates from sulphide bearing mine wastes was recognized as an environmental liability with significant ramifications. Attempts are now being made to repair the damage that has been done and identify new waste disposal technologies that will reduce the potential impact of mining on the environment.

Sulphide minerals are mined in order to recover metals, such as copper, nickel, lead and zinc, which have economic value. Gold, silver and uranium are examples of metals that can also occur in deposits associated with sulphide minerals. The main environmental concern with the mining of sulphide ores is the production and release of acidic drainage which results from the oxidation of sulphide minerals when they are brought into contact with atmospheric oxygen and water. Mobilization of potentially toxic heavy metals, sulphate and acidity can negatively impact surface water adjacent to the mine property as well as contaminating regional groundwater. The effects of acid mine drainage on the local biosphere can manifest in many ways including bioaccumulation of heavy metals introduced into lower levels of the food chain, a decline in fish fecundity due to high acidity in surface water and the contamination of local water rendering it unusable for agricultural, industrial or municipal use.

Tailings and waste rock are commonly the most significant sources of acid mine drainage. Tailings are comprised of finely ground, sand- to silt-sized particles that are separated from the economically desirable constituents in the ore. Tailings are typically deposited into impoundments as a slurry. Waste rock is composed mainly of material that is removed in order to gain access to an ore body or associated

sub-economic rock material. In contrast to tailings, waste rock can be more heterogeneous in terms of the sulphide content, particle size and permeability to air and water.

### ***1.1 Waste Rock Characterization***

Development of an effective disposal strategy for sulphide bearing mine wastes relies on an ability to accurately predict the future behaviour of the waste material under ambient conditions. The first stage in this process is the characterization of the mine waste to assess the potential acid production and loading rates of associated contaminants. The most commonly used and accepted methods of characterizing mine wastes can be grouped into two broad categories, namely static and kinetic tests.

Static tests are commonly performed as an initial screening exercise in the development of new mining properties or the expansion of existing facilities. These tests simply quantify and compare the relative amounts of acid-producing and acid-consuming minerals present in representative samples. Samples which indicate a net acid-producing potential are usually subjected to kinetic testing as the next stage of the assessment process.

Kinetic tests are designed to simulate the natural weathering process and differ from static tests in that they can demonstrate potential differences between the relative rates of acid generation and consumption. Kinetic tests can provide important insight into the oxidation processes occurring at a given site and give an explicit description of the overall rates of acid production and metal release. The major drawbacks to kinetic testing are the long time scale of the test, typically 20 weeks or more, and the concomitant high cost of approximately \$100 to \$250 per sample per week. In light of the drawbacks of conventional kinetic tests, the need to develop a rapid, inexpensive method for the assessment of the acid-producing potential of mine wastes is obvious.

### *1.2 Objectives and Scope of Research*

The objectives of this study were two-fold; first, to develop a method for the determination of the oxidation rate of sulphide minerals in waste rock and second, to use this method to investigate some of the fundamental parameters influencing the rate of oxidation in waste rock.

The oxygen consumption method was originally developed to measure the oxygen flux from the ground surface into tailings. This method was modified and adapted for use with waste rock as the initial stage of this investigation. Once a protocol was established, an experimental programme was initiated to study the effects of particle size, temperature, sulphide content and the presence of *Thiobacillus ferrooxidans* on the rate of oxygen consumption in sulphide-bearing waste rock.

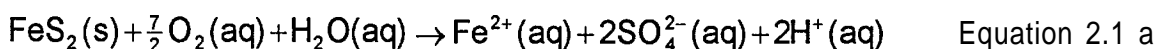
## 2. Background

In comparison to the vast amount of literature to quantify and model the production of acid mine drainage from finely ground, processed tailings, comparatively little information has been published in the area of waste rock. Much of the information available on waste rock is in the form of environmental assessment studies prepared by environmental consultants for mining companies; very few studies have been reported in refereed journals. Several researchers have reported studies on the oxidation of pure sulphide mineral phases using material representative of tailings (McKibben and Barnes, 1986; Nicholson *et al.*, 1988; Rimstidt *et al.*, 1994; Janzen, 1996; Kwong, 1996) and several major reviews indicate the volume of work in this area (Lowson, 1982; Nordstrom, 1984; Nicholson, 1994; Evangelou and Zhang, 1995). Waste rock, especially the large volumes produced by open-pit mining practices, can also be a significant source of environmental contamination and must be considered in the initial permitting and planning stages of a mining operation.

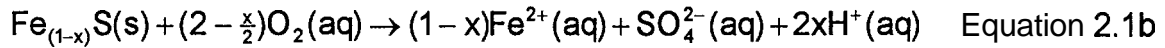
The work conducted with tailings is difficult to translate directly to waste rock due to the different hydrologic conditions in waste rock piles compared to tailings and the relative heterogeneous nature of waste rock. This heterogeneity is expressed in the wide range of particle size, distribution of sulphide minerals in the host rock and presence of accessory minerals which may alter the geochemistry in the proximity of sulphide grains.

### **2.1 Oxidation of Iron Sulphides**

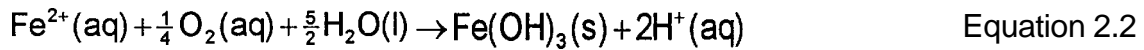
The dominant acid generating reactions in tailings and waste rock are the oxidative weathering of iron sulphide minerals, particularly pyrite and pyrrhotite. Pyrite oxidizes according to the following reaction (Stumm and Morgan, 1981);



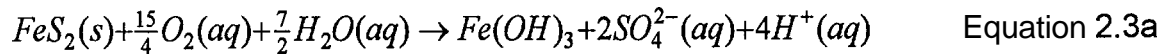
and pyrrhotite reacts with molecular oxygen in the following manner (Nicholson and Scharer, 1994);



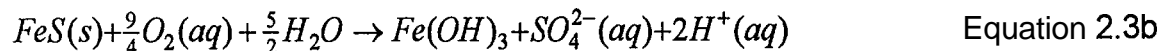
where x may vary from 0 (i.e. FeS) to 0.125 (i.e. Fe<sub>7</sub>S<sub>8</sub>) due to iron deficiency in the crystal lattice. Pyrite oxidation produces 2 moles of H<sup>+</sup> for every mole of pyrite oxidized and pyrrhotite produces between 0 to ¼ moles of H<sup>+</sup> for every mole oxidized, depending on the iron content. In both cases, the resulting aqueous ferrous iron is available for further oxidation in the presence of excess oxygen and can precipitate as amorphous ferric hydroxide to form more acid as shown in Equation 2.3.



Complete oxidation of the sulphide minerals, that includes oxidation of ferrous to ferric iron with precipitation of ferric hydroxide can be represented by the following reactions for pyrite;



and for a simplified pyrrhotite formula (ie. X=0), by;



Oxygen is the key oxidant in these equations, all of which can be catalyzed by iron- and sulphur-oxidizing bacteria, in particular *Thiobacillus ferrooxidans*. Aqueous ferric iron can also act as an oxidant. However, oxygen is required to oxidize ferrous iron in solution to ferric iron. Oxygen remains the primary oxidant and is ultimately the electron acceptor in these reactions.

## 2.2 Laboratory-scale Measurement of Oxidation Rate

### 2.2.1 Humidity Cells

Humidity cells have been used to mimic the weathering environment in waste rock piles. The weathering process has been simulated by subjecting a sample of crushed material to alternating three day cycles of humid and dry air and weekly flushing with water to remove oxidation products (Sobek *et al.*, 1978). The sample is flushed with a known volume of water which is collected and analysed for various indicators of oxidation, including pH, acidity, alkalinity, dissolved sulphate and metals. These tests have typically been conducted for a period of 20 weeks or more, however it is often necessary to run tests for much longer periods in order to observe depletion of buffering minerals and the consequent onset of acidic leachate production even in materials with excess acid potential.

Lapakko and Antonson (1994) reported rates of sulphate release from Duluth Complex rock samples containing pyrrhotite. The humidity cells were operated for periods of 69 to 150 weeks in an environmental chamber which maintained the temperature at an average of 26°C and relative humidity of 60%. Rates ranged from  $1.4 \times 10^{-13}$  to  $52.7 \times 10^{-13}$  mol  $\text{SO}_4 \cdot (\text{g rock})^{-1} \cdot \text{s}^{-1}$  ( or  $5.0 \times 10^{-10}$  to  $1.8 \times 10^{-8}$  mol  $\text{O}_2 \cdot (\text{kg rock})^{-1} \cdot \text{s}^{-1}$ , from Equation 2.2 for pyrrhotite,  $\text{FeS}$ , 2 moles of oxygen consumed per mole of sulphate produced). The reaction rate, expressed in mol  $\text{SO}_4 \cdot (\text{g rock})^{-1} \cdot \text{s}^{-1}$ , was found to be approximately first-order with respect to the solid-phase sulphur content (in percent) of the sample as follows;

$$\left[ \frac{d(\text{SO}_4)}{dt} \right]_{\text{avg}} = 5.97 \times 10^{-13} S^{0.984} \quad \text{Equation 2.2}$$

for samples with total sulphur contents (%S) between 0.18 and 3.12 percent.

White and Jeffers (1994) determined sulphate release rates from humidity cells for three rock samples containing 1.5, 3.5 and 13% sulphide-S present as subhedral/framboidal, euhedral and framboidal pyrite respectively. These cells were operated with alternating three day cycles of dry and humid air. For pH values

greater than 3.5, the rates of sulphate release were 23, 162 and 423 mg  $\text{SO}_4 \cdot \text{kg}^{-1} \cdot \text{wk}^{-1}$  (or  $6.9 \times 10^{-10}$ ,  $4.9 \times 10^{-9}$  and  $1.3 \times 10^{-8}$  mol  $\text{O}_2 \cdot (\text{kg rock})^{-1} \cdot \text{s}^{-1}$ , from Equation 1.1 for pyrite, 1.75 moles of oxygen consumed per mole of sulphate produced) with the rate increasing with sulphide content. These results are consistent with the first-order relationship between reaction rate and sulphide content proposed by Lapakko and Antonson (1994). The rate of sulphate release was noted to increase significantly as the pH of the leachate dropped below 3.5. At this pH, ferric iron can become an important oxidizing agent and it is thought that *Thiobacillus ferrooxidans* becomes a significant factor by catalyzing the rate-limiting step by oxidizing aqueous ferrous to ferric iron. No attempt was made to quantify or verify bacterial catalysis although the authors proposed this as a possible explanation for the increase in sulphate release rate with decreasing pH.

Norecol Environmental Consultants (1988) reported significant differences in the rate of sulphate release from humidity cells operated with alternating cycles of humid and dry air from those running continuously with humid air. The second series of tests using a continuous stream of humid air was conducted because this situation was thought to be more representative of the conditions in the waste rock pile. The waste rock samples were taken from three test piles that had been constructed previously at the Cinola Gold Project site. The resulting sulphate release rates are summarized in Table 2.1.

Table 2.1: Sulphate release rates from Cinola Gold humidity cells

Sampling Location	Sulphide (%S)	Sulphate Release humid/dry cycles mg $\text{SO}_4 \cdot \text{kg}^{-1} \cdot \text{wk}^{-1}$ (mol $\text{O}_2 \cdot \text{kg}^{-1} \cdot \text{s}^{-1}$ )	Sulphate Release humid air only mg $\text{SO}_4 \cdot \text{kg}^{-1} \cdot \text{wk}^{-1}$ (mol $\text{O}_2 \cdot \text{kg}^{-1} \cdot \text{s}^{-1}$ )
Waste Rock Pad 1	0.3	4.3 ( $2.6 \times 10^{-10}$ )	4.9 ( $3.0 \times 10^{-10}$ )
Waste Rock Pad 2	1.28	7.7 ( $4.6 \times 10^{-10}$ )	56 ( $3.4 \times 10^{-9}$ )
Waste Rock Pad 4	1.64	4.8 ( $2.9 \times 10^{-10}$ )	81 ( $4.9 \times 10^{-9}$ )

Differences in the rate of sulphate production for samples from Pad 2 and 4 suggested that the release of sulphate was impeded during the testing using humid and dry air cycles. The authors suggested that this may have been due to the encapsulation of sulphide minerals by gypsum or ferric hydroxide which may have precipitated during the drying cycle. Waste rock from Pad 1 did not show the same behaviour presumably because this material had already been weathering for five years at the mine site. This may have resulted in the removal of readily reactive sulphide minerals and the development of oxidation product layers on the reactive surfaces. The difference in sulphate release between the two methods indicates that the results of humidity cell tests may be misleading in some cases using the standard method of humid and dry air cycles.

Humidity cell testing is one of the most commonly used and accepted techniques for measuring the acid-producing potential of tailings and waste rock samples although very little work has been conducted to evaluate the reliability of the measurement. Coastech Research Inc. (1989) compared the results of humidity cell tests to actual acid mine drainage behaviour of waste rock and tailings. The authors found that humidity cell tests gave reliable predictions of the acid generating behaviour of 11 out of 12 samples when compared to minesite drainage quality data. Drawbacks to this method include the high cost and length of time to complete the test, the lack of field verification, and possible misleading results under some conditions.

### **2.2.2 Waste Rock Columns**

Stromberg *et al.* (1994) performed a study on six columns filled with approximately 1500 kg of waste rock from the Aitik Mine in northern Sweden. These columns were 0.8 m in diameter and 2 m high. Water was added at a rate of  $0.7 \text{ m}\cdot\text{yr}^{-1}$  to simulate natural precipitation and the columns were maintained at  $5^{\circ}\text{C}$  to simulate the field conditions at the site. These columns approached the complexity of the actual waste rock pile in terms of the range of particle size, variability of mineralogy, and possibility of heterogeneous flowpaths while retaining the ability to do precise mass and hydrologic balances by sampling the effluent from the columns. The waste rock

contained pyrite as the dominant sulphide with lesser amounts of pyrrhotite and chalcopyrite. Previous measurements of oxygen consumption by the waste rock yielded rates of  $(2.4 \pm 0.8) \times 10^{-10} \text{ mol O}_2 \cdot \text{kg}^{-1} \cdot \text{s}^{-1}$ . A mass balance approach was used to determine the rate of oxidation of pyrite and chalcopyrite using this value and the average chemical composition of the leachate. Values for the oxidation of pyrite and chalcopyrite were  $5.5 \times 10^{-11} \text{ mol FeS}_2 \cdot \text{kg}^{-1} \cdot \text{s}^{-1}$  ( $2.1 \times 10^{-10} \text{ mol O}_2 \cdot \text{kg}^{-1} \cdot \text{s}^{-1}$ ) and  $6.9 \times 10^{-12} \text{ mol CuFeS}_2 \cdot \text{kg}^{-1} \cdot \text{s}^{-1}$  ( $2.9 \times 10^{-11} \text{ mol O}_2 \cdot \text{kg}^{-1} \cdot \text{s}^{-1}$ ), respectively. The authors concluded that pyrite oxidation dominated the consumption of oxygen in this material.

### **2.3 Field Scale Measurement of Oxidation Rate**

A number of researchers have attempted to estimate the intrinsic oxidation rate of waste rock in actual waste rock piles. The intrinsic oxidation rate was defined by Ritchie (1994b) as the loss of oxygen from the gas phase by oxidation reactions in the material comprising the dump. Harries and Ritchie (1981) were among the first to report estimates of intrinsic oxidation rates from temperature measurements in waste rock dumps. Temperature profiles were measured in the White's and intermediate dumps at the Rum Jungle mine site in Australia and from these profiles the oxidation rates were inferred. They utilized the exothermic nature of the pyrite oxidation reaction along with a one dimensional heat transport model to determine the distribution of heat sources, and hence oxidation sites, within the waste rock pile. Estimated oxidation rates for this site ranged from  $0.3 \times 10^{-8}$  to  $8.8 \times 10^{-8} \text{ kg O}_2 \cdot \text{m}^{-3} \cdot \text{s}^{-1}$  ( $5.6 \times 10^{-11}$  to  $1.6 \times 10^{-9} \text{ mol O}_2 \cdot \text{kg}^{-1} \cdot \text{s}^{-1}$ ) for the dumps which contained approximately 3% S as pyrite (Ritchie, 1994). Most regions within the dump showed temperatures of 33 to 37°C with the notable exception of one borehole which had temperature values over 45°C and a peak value of 56°C.

In a similar study at a waste rock pile at La Mine Doyon, Quebec, Gélinas *et al.* (1991) determined the rate of oxidation of pyrite using temperature profiles. The waste rock pile in this case contained between 1.5 and 7% S, depending on the rock type and averaged about 3.5% S for the entire pile. The maximum

temperatures measured in the boreholes were in the range of 40 to 66°C resulting from the exothermic oxidation reaction. Using the average temperature profile from 5 boreholes, the overall heat generation rate for the pile was calculated to be  $0.6 \text{ W}\cdot\text{m}^{-3}$ . This was translated into an oxygen consumption rate of  $3.17 \times 10^{-10} \text{ mol O}_2 \cdot \text{kg}^{-1} \cdot \text{s}^{-1}$ . The loading of sulphate in toe drains from the pile was also measured and it was determined that sulphate was being liberated at a rate of  $4.37 \text{ mg SO}_4 \cdot \text{kg}^{-1} \cdot \text{wk}^{-1}$ . This indicates a rate of oxygen consumption of  $2.63 \times 10^{-10} \text{ mol O}_2 \cdot \text{kg}^{-1} \cdot \text{s}^{-1}$  based on sulphate release. One of the possible reasons that sulphate may underestimate the rate of oxygen consumption is that dissolved sulphate is not always conservative. Sulphate often precipitates as gypsum or jarosite, both of which were detected in the waste rock pile at this site. The loss of sulphate from solution would lead to an underestimation of the rate of oxidation. Another possible reason that the oxidation rate based on heat production overestimates the actual value is the simplicity of the model used to describe the temperature gradients. The model assumes that the oxidation rate is greatest at the surface and decreases linearly with depth. The authors also state that the model must be revised to include air convection due to thermal gradients, **advective** heat transport by infiltrating water and the latent heat of vapourization and fusion of water. The quality and precision of the field data did not warrant these amendments.

Bennett *et al.* (1994) utilized the same methods of inferring the rate of oxidation by measuring oxygen and temperature gradients, as well as independent measurements of sulphate loading from a pyritic waste rock dump at the Aitik Copper Mine in northern Sweden.

Oxygen gradients can be used in much the same manner as temperature gradients. Modelling of the steady-state oxygen transport in one dimension, assuming that oxygen is moving only by diffusion leads to the following equation;

$$D \frac{\delta^2 C}{\delta x^2} (x) = 0 \quad \text{Equation 2.3}$$

where  $D$  is the effective diffusion coefficient of oxygen in  $\text{m}^2\cdot\text{s}^{-1}$ ,  $C$  is the concentration of oxygen in  $\text{mol}\cdot\text{m}^{-3}$ ,  $x$  is the distance in  $\text{m}$  and  $R$  is the rate of oxygen consumption per unit volume in  $\text{mol}\cdot\text{m}^{-3}\cdot\text{s}^{-1}$ . By fitting the measured field data to an analytical function, the rate of oxidation is easily found using the above equation.

The temperature data collected at this site was not useful for calculating oxidation rates. The heat produced by the oxidation of pyrite was too small to yield coherent thermal gradients and this problem was compounded by large seasonal fluctuations in temperature. The oxygen gradient method, however, gave some promising results. Two distinct regions were identified within the dump; one region where the oxygen gradients were large and indicative of a significant rate of reaction and another area where the oxygen gradients were low. The oxidation rates calculated for the reactive region of the waste rock dump ranged from  $3.1\times 10^{-9}$  to  $4.3\times 10^{-8}$   $\text{kg O}_2\cdot\text{m}^{-3}\cdot\text{s}^{-1}$  ( $6.5\times 10^{-11}$  to  $9.0\times 10^{-10}$   $\text{mol O}_2\cdot\text{kg}^{-1}\cdot\text{s}^{-1}$ ) with an average close to  $1\times 10^{-8}$   $\text{kg O}_2\cdot\text{m}^{-3}\cdot\text{s}^{-1}$  ( $2.1\times 10^{-10}$   $\text{mol O}_2\cdot\text{kg}^{-1}\cdot\text{s}^{-1}$ ). Rates were not calculated for the less reactive zone. Sulphate loading calculations indicated that only  $12.1 \text{ t SO}_4\cdot\text{ha}^{-1}\cdot\text{yr}^{-1}$  ( $3.1\times 10^{-11}$   $\text{mol O}_2\cdot\text{kg}^{-1}\cdot\text{s}^{-1}$ ) were being discharged from the rock dump. From this information the authors concluded that only 14% of the dump was actively contributing to the sulphate output, given that it was oxidizing at a rate of  $1 \times 10^{-8}$   $\text{kg O}_2\cdot\text{m}^{-3}\cdot\text{s}^{-1}$ .

The authors did not give any reason for the apparent large range of oxidation rates observed in individual bore holes. Oxygen profiles changed significantly over the fifteen month observation period and consequently, oxygen consumption rates calculated from a single bore hole differed by more than one order of magnitude. This casts into doubt the 14% figure that the authors calculated. Despite this, the sulphate loading from the dump implies that even material with a relatively low oxygen consumption rate (on the order of  $10^{-11}$   $\text{mol O}_2\cdot\text{kg}^{-1}\cdot\text{s}^{-1}$ ) can generate significant amounts of acid rock drainage.

The temperature and oxygen profiles in a waste rock dump can be measured with precision and can provide a direct indicator of the rate of sulphide oxidation. The instrumentation required is relatively inexpensive, however installation and monitoring costs can be substantial. The construction cost of a probe hole for oxygen and temperature measurement depends on the depth and construction of the waste rock pile, as well as the rock type. Calculation of the oxidation rate from temperature profiles is complicated by the need to account for seasonal fluctuation in surface temperature and uncertainties about the boundary conditions at the surface and base of the dump. Oxygen profiles can also be difficult to interpret if diffusion is not the primary transport mechanism.

## 2.4 Factors Influencing the Oxidation Rate of Sulphide Minerals

### 2.4.1 Temperature

The oxidation of sulphide minerals, like most chemical reactions, responds to changes in temperature according to the Arrhenius relationship. Several researchers have calculated activation energies for a variety of sulphide minerals, these are summarized in Table 2.2.

Table 2.2: Reported values of  $E_a$  for sulphide minerals

Sulphide	Conditions	Activation Energy (kJ·mol <sup>-1</sup> )	Reference
Pyrite (FeS <sub>2</sub> )	pH 2-4	57	McKibben and Barnes, 1986
Pyrite (FeS <sub>2</sub> )	3-60°C, O <sub>2</sub> as oxidant, pH 7-8	88	Nicholson et al., 1988
Pyrrhotite (FeS)	10-33°C, O <sub>2</sub> as oxidant	52 (pH 4) 100 (pH 6)	Nicholson and Scharer, 1994
Galena (PbS)	25-60°C, 10 <sup>-2</sup> -10 <sup>-3</sup> molal Fe(III) as oxidant, acid pH	40	Rimstidt et al., 1994
Chalcopyrite (FeCuS <sub>2</sub> )	25-60°C, 10 <sup>-2</sup> -10 <sup>-5</sup> molal Fe(III) as oxidant, acid pH	63	Rimstidt et al., 1994
Sphalerite (ZnS)	25-60°C, 10 <sup>-2</sup> -10 <sup>-3</sup> molal Fe(III) as oxidant, acid pH	27	Rimstidt et al., 1994

From Table 2.2 it would appear that the activation energy depends on the reaction conditions and the sulphide mineral in question. In general, the magnitude of the activation energies given above would suggest that the reactions are not controlled by diffusion, except perhaps in the case of sphalerite. Lasaga (1981) has suggested that the activation energy for a diffusion-controlled heterogeneous reaction should be less than approximately  $20 \text{ kJ}\cdot\text{mol}^{-1}$ .

### 2.4.2 Particle Size

Morin and Hutt (1994) presented a theoretical argument that suggested that the influence of large rock particles (0.2 m) on the total surface area, and hence, rate of oxidation, is minor relative to small rock particles (0.0032 m). The authors assumed that the rock particles were cubes and have a bulk density of  $1800 \text{ kg}\cdot\text{m}^{-3}$ . A given mass of waste rock consisting of 80 wt% large rock fragments and 20 wt% small particles would have a total surface area of  $221 \text{ m}^3\cdot\text{tonne}^{-1}$  with these assumptions. The 0.2 m size particles contributed only 6% of the total surface area in this case, as illustrated in Table 2.3.

Table 2.3 Effect of grain size on surface area (adapted from Morin and Hutt, 1994)

0.2 m size fraction (wt%)	0.0032 m size fraction (wt%)	Total Surface Area ( $\text{m}^2\cdot\text{tonne}^{-1}$ )	% of area from 0.2 m fraction
0	100	1040	0
20	80	835	0.40
40	60	631	1.05
60	40	426	2.34
80	20	221	6.04
90	10	119	12.5
100	0	16.6	100

This simple analysis exemplifies the importance of smaller particles in terms of their contribution to the reactive surface area in waste rock piles. The authors have used this argument to support their claim that rates obtained from humidity cell tests using 0.0032 m size material can be applied directly to entire piles with no concern for particle size effects. While this approach can be used to give very general

predictions of the acid generation behaviour of a waste rock pile, a more detailed analysis of the relationship between particle size and oxidation rate is necessary to make more accurate predictions.

Sheremata et al. (1991) studied the oxidation of waste rock samples from the Heath Steele Mine in New Brunswick. The waste rock contained on average 6.6% S as pyrite and it was segregated into three size fractions; 1.8 - 10 mm, 10 - 25 mm and 25 - 50 mm. A 10 kg sample of each size fraction was packed into a 15 cm diameter column which was maintained at 27°C and 80% relative humidity. Water was continuously recirculated through the column by allowing it to trickle down over the rock bed into a collection vessel at the base of the column and then pumped back to the top of the column by means of a peristaltic pump. The water in the collection vessel was sampled every week for total acidity and pH. Every 4 weeks the entire 2L volume of water was replaced with fresh deionized water. The cumulative acidity loading from each column increased with decreasing particle diameter. This effect was attributed to an increase in the surface area of oxidizable material associated with a decrease in particle diameter.

A report by Synergetic Technology (1996) presented a theoretical analysis of the effects of particle size on the oxidation rate of sulphides in waste rock. Given that the rate of sulphide oxidation is directly proportional to the effective surface area per unit volume, any scaling law relating a change in surface area to a change in particle diameter will also apply to the oxidation rate. The shrinking core model is a commonly used conceptualization that assumes that the rock particles are regular geometric objects for which the surface area is given by  $\alpha d^2$ , where  $\alpha$  is a coefficient ranging between  $\pi$  for a sphere to 6 for a cube, and  $d$  is the characteristic diameter of the rock particle. The shrinking core model postulates that the oxidation reaction takes place in a narrow zone which moves toward the centre of the particle as the reactants are consumed. Oxygen must diffuse through an accumulating oxidation product layer in order to reach the reaction zone.

Since the volume of a regular geometric object is proportional to  $d^3$ , this leads to the scaling axiom;

$$R \propto \frac{A}{V} \propto \frac{d^2}{d^3} = \frac{1}{d} \quad \text{Equation 2.4}$$

According to the authors, this law applies to rock particles for which the diameter is larger than the average distance between sulphide grains, i.e.  $>10^{-2}$  m for material with 10% sulphide. The authors also suggest that this law only holds during the early “surface-dominated” leaching stage when the reaction takes place primarily on the surface of the particle. At later times, reactive sulphide has depleted from the surface, the reaction zone moves into the particle and the process is said to become “volume-dominated”. At this point, the reaction is controlled by the relatively slow diffusion of oxygen through a sulphide-depleted zone to the interior of the particle and the rate becomes proportional to  $1/d^2$ . The arguments presented by Synergetic Technologies infer that the rate of oxidation of waste rock should initially be inversely proportional to the particle diameter but this relationship changes in the presence of a diffusive resistance to oxygen transport and eventually becomes a function of  $1/d^2$ .

### 2.4.3 Presence of Iron-oxidizing Bacteria

A number of bacterial species that can oxidize reduced iron and sulphur compounds have been identified. They include both chemolithotrophic and chemoorganotrophic species of aerobic bacteria. Autotrophic acidophilic bacteria that obtain carbon from dissolved carbon dioxide and have an optimal growth range less than pH 4 are expected to predominate in waste rock. *Thiobacillus ferrooxidans* is an autotrophic acidophile that has been extensively studied due to its ubiquitous nature and its role in acid generation from mine wastes.

*T. ferrooxidans* obtains energy for cellular metabolism from the oxidation of reduced iron (i.e. ferrous iron) and sulphur species such as thiosulphate, sulphide and

elemental sulphur. Its primary role in the generation of acid mine drainage is thought to be the catalysis of aqueous ferrous iron oxidation to ferric iron. This is considered to be the rate limiting step in the oxidation of sulphide minerals and is catalyzed by *T. ferrooxidans* at pH values below 4.5 (Gould et al., 1994). In an inter-laboratory study, Olson (1991) found that *T. ferrooxidans* enhanced the oxidation rate of pyrite tailings by a factor of 10 to 100 times. Based on field data, the enhancement of the acid generation rate due to iron-oxidizing bacteria was estimated to be between 5 and 20 times greater than the rate due solely to chemical oxidation mechanisms (Morin et al., 1990).

Field measurements of *T. ferrooxidans* populations cited by Ritchie (1994) fall into the range of  $10^2$  to  $10^4$  cells·(g rock)<sup>-1</sup>. This value is quoted as being at least two orders of magnitude lower than the values commonly used in experiments involving microbially catalyzed sulphide oxidation. This difference was noted to be about the same order of magnitude as the difference found between field and laboratory measurements of the rate of biotic pyrite oxidation.

Stromberg and Banwart (1994) developed a model of the geochemical processes active in a waste rock pile at the Aitik Mine in Sweden which was validated using measured flowrates and dissolved metal concentrations of leachate from the pile. Published kinetic data were used in the model to describe the oxidation of sulphide minerals and the dissolution of primary silicate phases. The pH of the drainage and net flux of cations, such as calcium, magnesium and sodium, measured at the site were consistent with the model results. The field data suggested, however, that the oxidation of ferrous to ferric iron in the rock pile was three orders of magnitude faster than can be explained by published abiotic reaction rate constants. The authors interpreted this to mean that iron-oxidizing bacteria were active at this site. Numerous other researchers have documented or alluded to the presence of iron-oxidizing bacteria at various mine sites (Ritchie, 1994; Gélinas et al., 1991; Golder Associates, 1996; Morin et al., 1990)

Watzlaf (1988) investigated the inhibitory effects of sodium lauryl sulphate, potassium benzoate and potassium sorbate on iron-oxidizing bacteria and hence, the production of acidity from a waste rock sample. The bactericidal effects of similar anionic surfactants on *T. ferrooxidans* was previously documented by Kleinmann (1981). The waste rock material containing 4% pyritic sulphur was collected from a mine in British Columbia, Canada. The material was used as collected, i.e. containing particles ranging in diameter from sand (<1 mm) to cobble (15 cm) size and hosting an indigenous population of bacteria. Two parallel experiments were conducted on 100 kg and 7 kg samples of the waste rock. Due to a limited supply of waste, only two of the inhibitors, sodium lauryl sulphate and potassium benzoate, were tested on the 100 kg scale using a dosage of 600 mg of inhibitor per kg of rock. High and low doses of the three inhibitors, equivalent to 600 and 60 mg·kg<sup>-1</sup>, were applied to the 7 kg samples. Bacterial populations were measured in water collected from the 100 kg samples using the multiple tube, most probable number technique according to the method described by the American Public Health Association using a medium suitable for the growth of iron-oxidizing bacteria. The control had a constant population of approximately 10<sup>3</sup> cells/ml. The results showed a decrease in the number of iron-oxidizing bacteria below the detection limit of the procedure (<1 cell·mL<sup>-1</sup>) for 182 and 231 days for rock samples treated with sodium lauryl sulphate and potassium benzoate, respectively. The cumulative acidity loading from the treated waste rock was reduced by more than 85% over the period of 250 days relative to the control. However, the bacterial populations re-established themselves and acidity production increased after 250 days for both treated samples. The results from the 7 kg columns showed similar results, acidity loadings were reduced by more than 50% for 343 days for samples treated with 600 mg·kg<sup>-1</sup> of sodium lauryl sulphate. Potassium benzoate and potassium sorbate were both effective in reducing acidity loadings by more than 50% for 147 days. Acidity loadings were reduced by more than 50% for the 7 kg columns for 63 and 77 days for the columns treated with 60 mg·kg<sup>-1</sup> of sodium lauryl

sulphate and potassium benzoate. Potassium sorbate did not appear to have any effect on the acidity loading at the low dosage. The results indicate that all three compounds were effective in inhibiting the growth of iron-oxidizing bacteria on the waste rock and reducing the amount of acidity produced.

#### **2.4.4 Field and Laboratory Studies using the Oxygen Consumption Method**

Elberling *et al.* (1994), Nicholson *et al.* (1995) and Elberling and Nicholson (1996) and Tibble and Nicholson (1997) have used oxygen as the reaction progress variable to measure the oxidation of sulphide tailings in the laboratory and in the field. Laboratory studies (Elberling *et al.*, 1994) involved the estimation of sulphide oxidation rates using three different methods; the flux of oxygen across the surface estimated from oxygen concentration gradients, the rate of oxygen consumption at the tailings surface and the total sulphate removed from the columns by flushing with water.

The oxygen gradient method was used to calculate the flux of oxygen across the tailings surface using Fick's law by measuring the oxygen gradient over the top 0.2 m. At steady state Fick's law states;

$$F = -D_{\text{eff}} \frac{dC}{dz} \quad \text{Equation 2.5}$$

where  $F$  is the flux of oxygen,  $D_{\text{eff}}$  is the effective diffusion coefficient of oxygen,  $C$  is the concentration and  $z$  is the distance in the direction of transport. An effective diffusion coefficient of oxygen in the partially saturated porous media was calculated using water saturation as a weighting parameter. A semi-empirical technique was employed to estimate the effective diffusion coefficient,  $D_{\text{eff}}$ , as a weighted average of the diffusion of oxygen through the water and air phases (Elberling *et al.*, 1994). The oxygen concentration gradient was approximated by measuring the oxygen concentration at a depth of 20 cm and assuming atmospheric oxygen concentration at the surface. Substituting the calculated  $D_{\text{eff}}$  and measured oxygen concentration gradient into Equation 2.4 allowed the flux of oxygen to be

calculated. Assuming steady state conditions, the flux of oxygen across the surface should be equal to the consumption of oxygen by the tailings.

The oxygen consumption technique involves the measurement of oxygen concentration in a fixed headspace over time. At steady state, Fick's second law and a first order kinetic term yields;

$$D_{\text{eff}} \frac{\delta^2 C}{\delta z^2} - k C = 0 \quad \text{Equation 2.6}$$

From this, the flux through the surface of the sulphide waste becomes;

$$F = C_o (kD_{\text{eff}})^{0.5} \quad \text{Equation 2.7}$$

given that  $C(z) = C_o$  at  $z = 0$  and  $C(z) = 0$  as  $z \rightarrow \infty$ . If a fixed-volume chamber is placed over the tailings, the oxygen concentration will decrease due to consumption according to:

$$\frac{dC}{dt} = \frac{A}{V} C (kD_{\text{eff}})^{0.5} \quad \text{Equation 2.8}$$

where  $A$  is the surface area of the tailings and  $V$  is the headspace volume. Integrating this equation gives;

$$\ln\left(\frac{C}{C_o}\right) = -(kD_{\text{eff}})^{0.5} \frac{A}{V} t \quad \text{Equation 2.9}$$

if  $C=C_o$  at  $t=0$ . The slope of a plot of  $\ln(C/C_o)$  vs. time will yield  $(kD_{\text{eff}})^{0.5}$ , if  $\frac{AV}{A}$  is measured. Substituting back into Equation 2.6 gives the flux of oxygen through the surface.

The third method to determine the oxidation rate is simply to flush any oxidation products out of the column using a measured amount of water and analyzing the effluent for sulphate. The amount of sulphate produced will be directly related to the oxidation rate by the stoichiometry of the oxidation reaction.

The results of the studies by Elberling *et al.* (1994) showed that the oxygen gradient method gave consistently higher rates than either of the other two methods. This

was attributed to the possibility that layering may have resulted in highly saturated layers that could not be properly characterized. The method used to measure water saturation may have underestimated the actual saturation in these layers because the method samples a larger volume than the scale of the layers. Consequently, the effective diffusion coefficient would be overestimated and the oxidation rate would also be overestimated.

The oxygen consumption method gave results that were higher than those indicated by the sulphate release method. One reason for this is that the sulphate release method gives an average rate over the experimental period, whereas the oxygen consumption and oxygen gradient methods are instantaneous measures of the oxidation rate. It was shown that the oxidation rate measured using the oxygen consumption method increased during the first two days of the test and remained constant for the next 5 days. In light of this evidence, it should not be surprising that the sulphate release rate gives lower oxidation rates. Another reason for the lower rates based on sulphate is the possible adsorption of sulphate onto ferric hydroxides. Over the course of three months the rates based on sulphate and oxygen consumption methods approached each other suggesting saturation of the sorption sites.

Based on the results of the laboratory investigations, the oxygen consumption method was recommended for field use because it eliminates the need to determine water saturation in order to estimate the effective diffusion coefficient of oxygen. The oxygen consumption method also takes into account *in situ* effects such as recent precipitation events, temperature conditions, and indigenous bacterial populations.

Results of field investigations by Nicholson et al. (1995), Elberling and Nicholson (1996) and Tibble and Nicholson (1997) showed that the oxygen consumption method works well for measuring the flux of oxygen into tailings. The data

demonstrated an expected decreasing trend in oxygen flux with decreasing depth to the water table, an increase in the oxygen consumption rate with the addition of a 20 cm layer of fresh tailings at the surface and a decrease in the rate with the addition of a 20 cm layer of fine non-reactive sand over the reactive tailings. The rate of sulphate production was also measured and showed a much closer correlation to the rate of oxygen consumption than those measured in the laboratory by Elberling *et al.* (1994). Oxygen consumption rates lower were closely correlated to the measured pore-water sulphate concentrations.

In light of the promising results obtained from both laboratory and field investigations using the oxygen consumption method, the current research was undertaken to adapt the method for use with waste rock. The experimental methods and the waste rock materials used are described in detail in the following sections.

## 3. Materials and Methods

### 3.1 Materials

#### 3.1.1 Whistle Mine Waste Rock

Initial method development and testing was performed on waste rock samples that were collected from the Whistle Mine site. The Whistle Mine is an open-pit nickel/copper mine located approximately 20km north of Sudbury, Ontario. Waste rock from this site was collected in October, 1994 and December, 1995. The majority of the waste can be classified as **norite** which is the host rock for the ore and makes up approximately 70% of the waste rock dump. The balance of the waste rock is a pink granite material which is easily distinguishable from the **norite**. The primary sulphide mineral at this location is pyrrhotite (**FeS**) with small amounts of pentlandite ( $(\text{Fe, Ni})_9\text{S}_8$ ) and chalcopyrite (**FeCuS<sub>2</sub>**).

The **norite** material was further categorized according to sulphide content. The rocks were separated into low, medium, high and massive sulphide categories based on visual classification. Subsamples of each rock type were sent to Activation Laboratories Ltd. (Ancaster, ON) for total sulphur and carbonate analysis. Total sulphur, expressed as %S by mass, was determined using the **Leco** furnace technique. Previous test work on this material showed that total sulphur was equal to sulphide sulphur. Total carbonate was also determined by the **Leco** furnace method on some of the samples and is given as the mass percent of carbon dioxide evolved upon heating. The carbonate content has been converted into an equivalent mass of **CaCO<sub>3</sub>** per tonne of waste rock for reference. Whole rock chemical analysis of the waste rock samples collected from the Whistle Mine site are given in Table 3.1.

Table 3.1 Sulphide and carbonate content of Whistle waste rock samples

Description	Sulphur Content (%S)	Carbonate Content (%CO <sub>2</sub> )	Carbonate Content (kg CaCO <sub>3</sub> ·tonne <sup>-1</sup> )
low S norite	1.54	0.130	2.96
medium S norite	2.63	0.297	6.77
high S norite	<b>9.80</b>	0.084	1.91
massive sulphide	22.3	0.220	5.01
pink granite	0.137	0.183	4.16

### 3.1.2 Voisey's Bay Rock Samples

Following the development stage, an experimental programme was initiated using rock samples from the Voisey's Bay deposit. The Voisey's Bay deposit was recently discovered in northern Labrador and is being developed into a nickel/copper mine. Pyrrhotite is the main sulphide mineral in the waste and is associated with small amounts of pentlandite and chalcopyrite. Since the mine is not yet operational, actual waste rock samples could not be collected and drill core samples were used as analogs of the waste rock types to be produced. The drill cores were crushed and sieved into different size fractions. In order to provide a sufficient mass of sample, several drill cores from the same location were combined to make a representative composite of the material from that region. The composites were assumed to be relatively homogeneous samples with respect to mineralogy across a range of particle sizes.

Two sets of waste rock samples were produced from cores with specific objectives. One series was produced by classifying the samples according to location, host rock type and sulphide content. Composite samples were prepared from cores from the Eastern Deeps (ED), Western Extension (WE) and Ovoid regions. These samples were separated according to rock type and included the troctolite intrusive (TROC), orthogneiss (ORTHO), paragneiss (**PARA**), gneiss (GNEISS) and granite/syenite (GRAN) host rock. A second set of composite samples was created

to study the effects of particle size, temperature, sulphur content and bacterial inoculation on the oxygen consumption rate. Two high sulphur (3.5%) and two low sulphur (0.5%) samples were crushed and sieved to provide four different size fractions for each of the four composite samples. The nominal grain sizes for the 4 size fractions are; 8, 3, 1 and 0.3 mm corresponding to U.S. Standard sieve size intervals of -1/2 inch + 4 mesh, -4 mesh +10 mesh, -10 mesh +30 mesh and -30 mesh +100 mesh (see Table 3.4 for opening sizes in mm). Chemical analysis of whole rock samples was performed at Lakefield Research (Lakefield, ON) and these are summarized in Table 3.2 for the rock samples described above.

Table 3.2 Sulphide and carbonate content of Voisey's Bay rock samples

<b>Description</b>	<b>Average Sulphur Content (%S)</b>	<b>Carbonate Content (%CO<sub>2</sub>)</b>	<b>Carbonate Content (kg CaCO<sub>3</sub>·tonne<sup>-1</sup>)</b>
<b>ED-TROC-1</b>	0.505	0.30	6.83
<b>ED-TROC-2</b>	1.535	0.26	5.92
<b>ED-TROC-3</b>	3.08	0.30	6.83
<b>ED-TROC-4</b>	0.625	0.30	6.83
<b>ED-ORTHO-1</b>	0.63	0.22	5.01
<b>WE-TROC-5</b>	0.385	0.30	6.83
<b>WE-TROC-6</b>	1.57	0.26	5.92
<b>WE-TROC-7</b>	2.35	0.33	7.51
<b>WE-PARA-1</b>	0.35	0.56	12.74
<b>VB-GRAN-1</b>	0.20	0.22	5.01
<b>COMP1</b>	1.16	N/A*	N/A
<b>COMP2</b>	0.46	N/A	N/A
<b>COMP3</b>	4.63	N/A	N/A
<b>COMP4</b>	3.93	N/A	N/A

\* N/A = not available

### 3.1.3 Additional Rock Samples

This phase of the investigation entailed the study of a number of different rock types in order to construct a database of oxygen consumption rates for a variety of rock types. The rock samples were crushed and sieved into only two grain sizes with nominal diameters of 8 and 3 mm. Rock samples from six different locations were collected and examined. The rock types differ in terms of sulphide content, sulphide

mineral type (pyrite vs. pyrrhotite), host rock mineralogy and dissemination of sulphide in the host rock matrix. The total sulphur content (as mass %S) and carbonate content (given as equivalent kg  $\text{CaCO}_3 \cdot \text{tonne}^{-1}$ ) measured at Activation Laboratories (Ancaster, ON), as well as the sulphide minerals present in the rock types are given in Table 3.3. The source of the rock types is discussed briefly below.

Waste rock samples were collected from the Main Dump of the Grum pit at the Vangorda Plateau near Faro, Yukon Territory. This waste rock contained large amounts of pyrite with galena and sphalerite as accessories. The rock was classified as banded carbonaceous or graphitic quartzite with the sulphide well disseminated in the host matrix (Robertson Geoconsultants Inc, 1997). The bands were composed of dark grey to black, very fine grained carbonaceous phyllitic quartzite and white to light grey layers of quartz, the scale of foliation, was generally 2 mm to 2 cm. The sulphide minerals (pyrite, sphalerite and galena) occurred in the quartz containing bands.

La Mine Doyon is a gold mine which has been operating since 1978 in Abitibi, Quebec. Rock samples were collected from the south dump in 1994. The samples were stored under water in sealed plastic containers in an attempt to minimize the rate of oxidation. The rock samples used in this work were removed from the containers in 1996, washed with a strong solution of HCl (approximately 50%v/v), rinsed well with tap water and dried. The low pH (2.5 - 3) of the water and the presence of large amounts of ferric hydroxide in the storage bucket are evidence that would suggest that some oxidation had occurred during storage.

The selected waste rock was representative of the sericitic schists present in the South Dump of Mine Doyon. The host rock is very friable and weathers quickly. Sericitic schists make up approximately half of the wastes in the dump and are responsible for a significant portion of the acidic, metal-rich drainage at the site.

Fine-grained pyrite was distributed throughout the matrix with an average sulphide content of 7%S which occurs along schistosity planes making it easily accessible to oxygen and water (Gélinas et al., 1991; Choquette and Gélinas, 1994).

Core samples were received from the Kudz Ze **Kayah** (KZK) property in the Yukon Territory. Macroscopic observation of the drill core samples and mineralogic descriptions (Wheatherell, 1997) indicated that it contained small amounts of pyrite, and possibly pyrrhotite, which were widely disseminated as fine crystals (<0.5 mm diameter). Visual observations during the experimental work indicated that this rock type contained some carbonate material and this was supported by the results of whole rock chemical analysis (see Table 3.3). The host rock was classified as a carbonaceous phyllitic metasediment composed of quartz-feldspar-sericite schists with minor calcite, dolomite and iron carbonate.

Waste rock samples that originated from the **Pamour** Mine in Timmins, Ontario were

Table 3.3: Total sulphur and carbonate content for the additional rock samples

Location	Rock Type	Dominant Sulphide	Accessory (%S) Sulphides	Carbonate NP (kg CaCO <sub>3</sub> ·tonne <sup>-1</sup> )
<b>Mine Dovon</b>	sericite schist	Py	N/A 14.5	0.033
<b>Whistle Mine</b>	low S norite	PO	Cp, Pn 11.97	0.070
	high S norite	PO	Cp, Pn 3.83	0.070
<b>Faro</b>	carbonaceous quartzite	Py	Sp, Gal 18.9	0.051
<b>KZK</b>	quartz-feldspar-sericite schist	Py	Sp, Gal 0.87	1.79
<b>Pamour</b>	limestone/mudstone	Py	CP 0.73	4.14

note: Py=pyrite, Po=pyrrhotite, Cp=chalcoprite, Pn=pentlandite, Sp=sphalerite and Gal=galena, N/A=not applicable

collected from a tailings cover test-plot. The rock appeared to be a limestone/mudstone with large grains of pyrite (2-4 mm in diameter) which were

widely disseminated. The carbonate content of the waste rock is significantly higher than values in the other rock samples as seen in Table 3.3.

High and low sulphur **norites** from the Whistle Mine were also included for a total of six rock types examined in this phase of the investigation. This rock type is described in detail above.

### 3.2 Particle Size

Large rock fragments (10 cm size) collected from existing waste rock piles were broken mechanically using a sledge hammer or jaw crusher. The crushed material was then sieved using Standard US sieves into selected size fractions. The standard sieves used are given in Table 3.4. The particle diameter for a given size fraction was determined as the geometric mean of the mesh openings. For example, material passing through the 4 mesh sieve (4.75 mm), but not the 10 mesh sieve (2 mm), was estimated to have a mean particle diameter of 3 mm.

Table 3.4: Standard US Sieve Sizes (Boggs, 1987)

Standard US Sieve Mesh	Opening Diameter (mm)
-1 inch	25.4
-3/4 inch	19.3
-1/2 inch	12.7
-3/8 inch	9.5
-4 mesh	4.75
-10 mesh	2
-30 mesh	0.59
-100 mesh	0.149
-170 mesh	0.088
-230 mesh	0.0625

### 3.3 *Thiobacillus ferrooxidans* Cultures

The bacterial culture used in this investigation was isolated from acid mine drainage from the Elliot Lake, Ontario region. The culture has been serially transferred for more than 10 generations using pyrrhotite as the sole substrate. Rock samples were inoculated with active cultures of *T. ferrooxidans* and incubated in an effort to establish bacterial populations on the waste rock surface in order to study the effect

of bacteria on the rate of oxygen consumption. This species of bacteria and the biological catalysis of sulphide oxidation has been extensively studied although the role and relative importance of *T. ferrooxidans* in a waste rock scenario remains unclear.

Active cultures of the bacteria were maintained in growth medium containing 0.25 g·L<sup>-1</sup> (NH<sub>4</sub>)<sub>2</sub>SO<sub>4</sub>, 0.125 g·L<sup>-1</sup> KH<sub>2</sub>PO<sub>4</sub> and 0.04 g·L<sup>-1</sup> MgSO<sub>4</sub>·7H<sub>2</sub>O which was acidified to pH 3 with H<sub>2</sub>SO<sub>4</sub>. -The cultures were grown in shake flasks containing approximately 0.5 wt% pyrrhotite as substrate. The bacterial inoculum was harvested after two to three weeks when the culture was in the logarithmic growth phase. The pyrrhotite solids were allowed to settle to the bottom of the flask and the supernatant, containing about 10<sup>7</sup> - 10<sup>8</sup> cells/ml, was used to inoculate the waste rock samples.

Rock samples were placed in beakers and inoculated with 50 to 100 mL of bacterial culture in growth medium to cover approximately one quarter of the rock sample leaving three quarters unsaturated. The beakers were loosely covered with plastic film to allow adequate oxygenation without excessive evaporation of water. The beakers were rolled gently every day to oxygenate the medium and wet the rock surfaces. Periodically, the medium was decanted and the pH was measured and adjusted to a value of approximately 3 with H<sub>2</sub>SO<sub>4</sub>. The bacteria were acclimatized to the experimental temperature conditions by incubating the inoculated waste rock for at least two weeks at a particular temperature. The two week incubation period also allowed sufficient time for the bacteria to populate the surfaces of the rock sample. Within 24 hours of beginning the oxygen consumption test, the medium was decanted and the bacterial population in the liquid was enumerated. Bacterial density in the medium ranged from 1 ×10<sup>6</sup> to 1 ×10<sup>8</sup> cells·mL<sup>-1</sup>. The population density on the solid surface could not be enumerated, however the presence of bacteria in the liquid phase implied sufficient conditions for attached growth.

A scanning electron microscope (SEM) was used to observe the bacterial population on the surface of waste rock particles. Small fragments of waste rock that had previously been inoculated with *T. ferrooxidans* were collected at the completion of an oxygen consumption test. The bacteria were fixed to prevent the cell structure from disintegrating under high vacuum in the SEM. The rock samples were washed with a phosphate buffer solution (PBS) to remove the growth medium and buffer the pH. The PBS consisted of 8.18 g NaCl, 0.20 g KCl, 0.204 g KH<sub>2</sub>PO<sub>4</sub> and 1.15 g Na<sub>2</sub>HPO<sub>4</sub>. The cells were fixed by placing the rock fragments in a 2.5% gluteraldehyde solution for 3 hours. The gluteraldehyde solution was removed by rinsing the samples 3 times with fresh PBS over the course of one hour. After the final rinse with PBS the samples were dehydrated using acetone. To prevent the cells from bursting under strong osmotic pressure, water was sequentially substituted with acetone. The samples were washed with 20%(volume/volume) acetone for 5 minutes, 50% acetone for 5 minutes, 70% acetone for 10 minutes and finally, 100% acetone for 10 minutes. A final rinse with pure acetone was performed to ensure complete dehydration. The samples were air dried to remove residual acetone before preparing the samples for scanning electron microscopy.

The dry samples were mounted to an aluminum stud using conductive double-sided tape. Sample studs were coated with a 120 Å thick layer of gold using a Polaroid Gold Coater. The gold coating provided additional secondary electrons for better imaging. The samples were observed using a Hitachi S570 Scanning Electron Microscope.

### **3.4 Reactor Configurations**

The waste rock samples were subjected to oxygen consumption tests using a protocol that was adapted from the experimental work conducted on tailings (Elberling et al., 1994). The reactor system consisted of a sealed test chamber, oxygen sensor and data acquisition system. Three variations of this system are described below and each was designed to meet a specific objective.

### 3.4.1 Oxygen Sensor

The oxygen sensor was the central focus in all reactor systems. The sensor used for all reactor configurations was the **GC33-200** manufactured by GC Industries. The sensor is a galvanic electrochemical cell using the **Pb-PbOOH** half-cell to reduce oxygen. The emf produced is directly proportional to the partial pressure of oxygen in the gas phase. The voltage output from the sensor was measured by a multi-channel multimeter (Fluke 2620A data acquisition unit) which was then recorded by a data-logging computer. The multimeter had the capacity to measure as many as 21 channels simultaneously. Usually two channels were reserved for thermistors, one for measuring the water temperature surrounding the reactors and the other for measuring the temperature of the air adjacent to the oxygen sensors. A schematic representation of the system is illustrated in Figure 3.1.

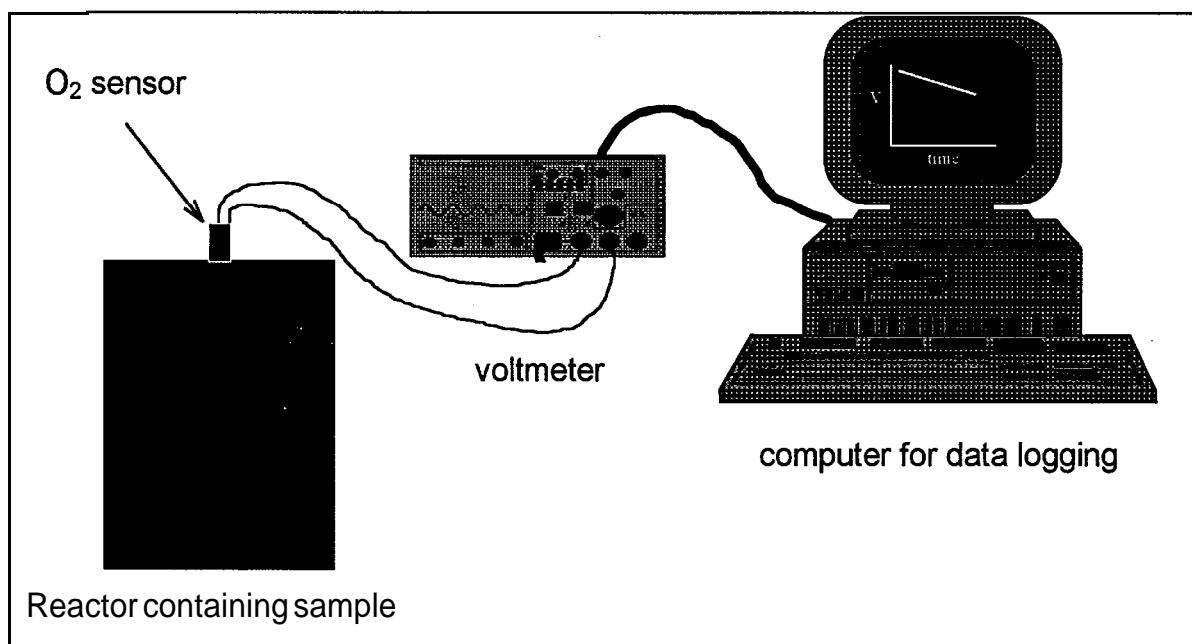


Figure 3.1 Schematic representation of oxygen consumption equipment

### 3.4.2 Acrylic Reactor

Initial tests were performed in a cylindrical acrylic reactor with an internal volume of approximately 355 mL. A scale drawing of the reactor is shown in Figure 3.2. Both the top and bottom of the reactor were secured by six  $\frac{3}{4}$  inch 4-40 stainless steel

bolts which were secured to flanges and were removable for cleaning. A gas-tight seal was maintained by means of rubber o-rings set into the top and bottom flanges. The oxygen sensor was mounted in the top of the reactor and was held in place initially with silicone sealant. A mounting collar was designed later to allow easy removal and replacement of the sensor and to provide a better seal. The mounting collar was held in place with 4 bolts and provided for an o-ring seal against both the side of the sensor and the top of the reactor. This reactor design was sufficient for initial investigations but high material costs and time-consuming construction lead to the abandonment of this design in favour of the 500mL glass reactor.

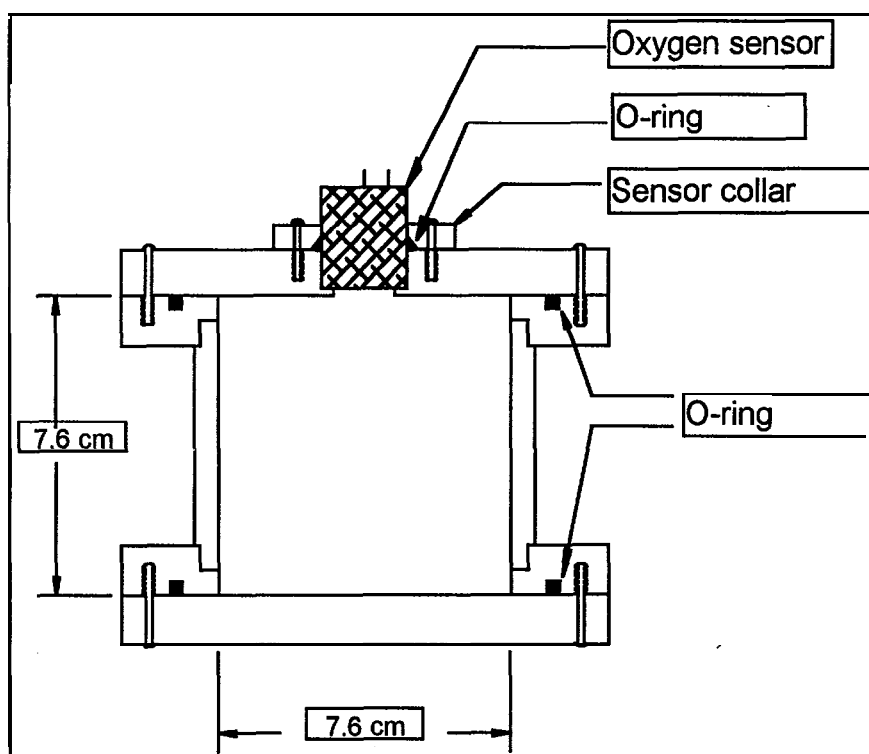


Figure 3.2 Scale drawing of acrylic reactor

### 3.4.3 Glass Reactor

The 500 mL glass reactor was adopted when the need arose to run numerous tests simultaneously. The internal volume varied from one reactor to another but was approximately 500 mL, on average. A scale drawing of the 500 mL glass reactor is shown in Figure 3.3. The lid design was based on the acrylic reactor with minor

modifications, such as the use of a retaining ring rather than bolts and flanges to secure the cap to the body of the reactor. A seal between the lid and reactor was accomplished by a rubber gasket which was lubricated with silicone high-vacuum grease.

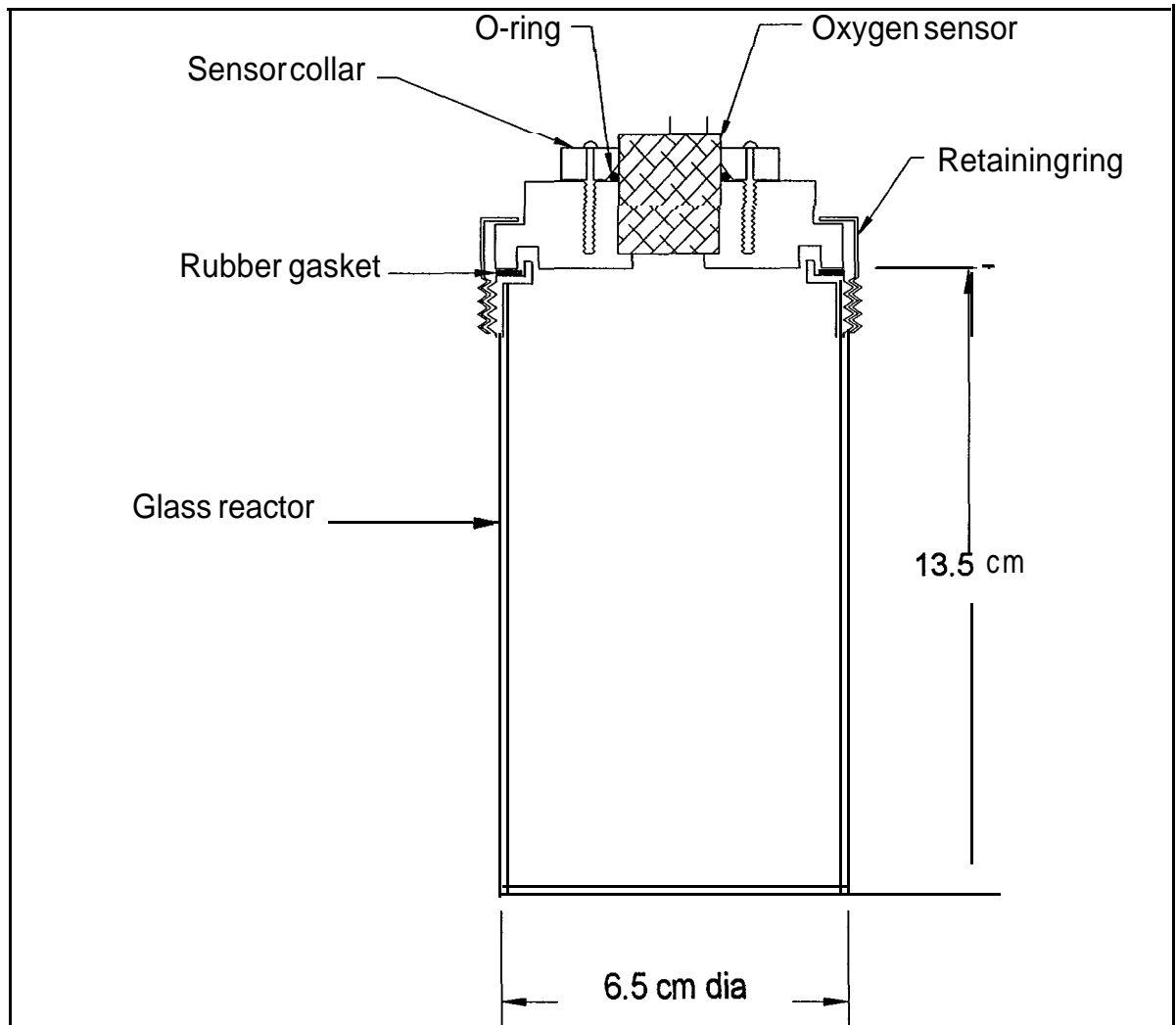


Figure 3.3 Scale drawing of glass reactor

#### 3.4.4 Large Volume Reactors

Experiments were also conducted in 17 L polyethelene (PE) reactors for large rock fragments (8 - 10 cm size). This required further modifications to the standard reactor configuration. Due to the length of the test (over two months), the reactors were designed to have removable sensors without significantly affecting the seal between the interior of the reactor and the atmosphere. In order to do this the

sensor was mounted in a polyvinyl chloride (PVC) block. The stem of a **Swagelok®** gas-tight Quick-Connect fitting was tapped into the other end of the block (see inset, Figure 3.4). The single end shut-off body of the fitting was attached to the lid of the 17L reactor to prevent the ingress of atmospheric oxygen into the reactor. Using this arrangement, the sensor could easily be connected and disconnected from the reactor. The amount of oxygen introduced into the reactor by connecting and disconnecting the sensor assembly was negligible compared to the volume of the reactor. A scale drawing of the 17L reactor system is shown in Figure 3.4.

Each sampling event consisted of measuring the full-scale output from the sensor under atmospheric conditions for approximately 10 to 15 minutes before connecting the sensor assembly to the reactor. The sensor was connected to the 17L reactor and allowed to come to equilibrium with the oxygen concentration in the reactor. The voltage reading given by the sensor exposed to the interior of the reactor was normalized with respect to the full-scale value measured under atmospheric partial pressure of oxygen. This was done to compensate for sensor drift over the course of the test. Oxygen sampling events were performed every week for 10 weeks.

The 17 L reactors were placed under water to moderate temperature changes and provide an extra oxygen barrier in the event of small leaks. The water temperature was monitored twice per week and was generally between 17 and 19°C.

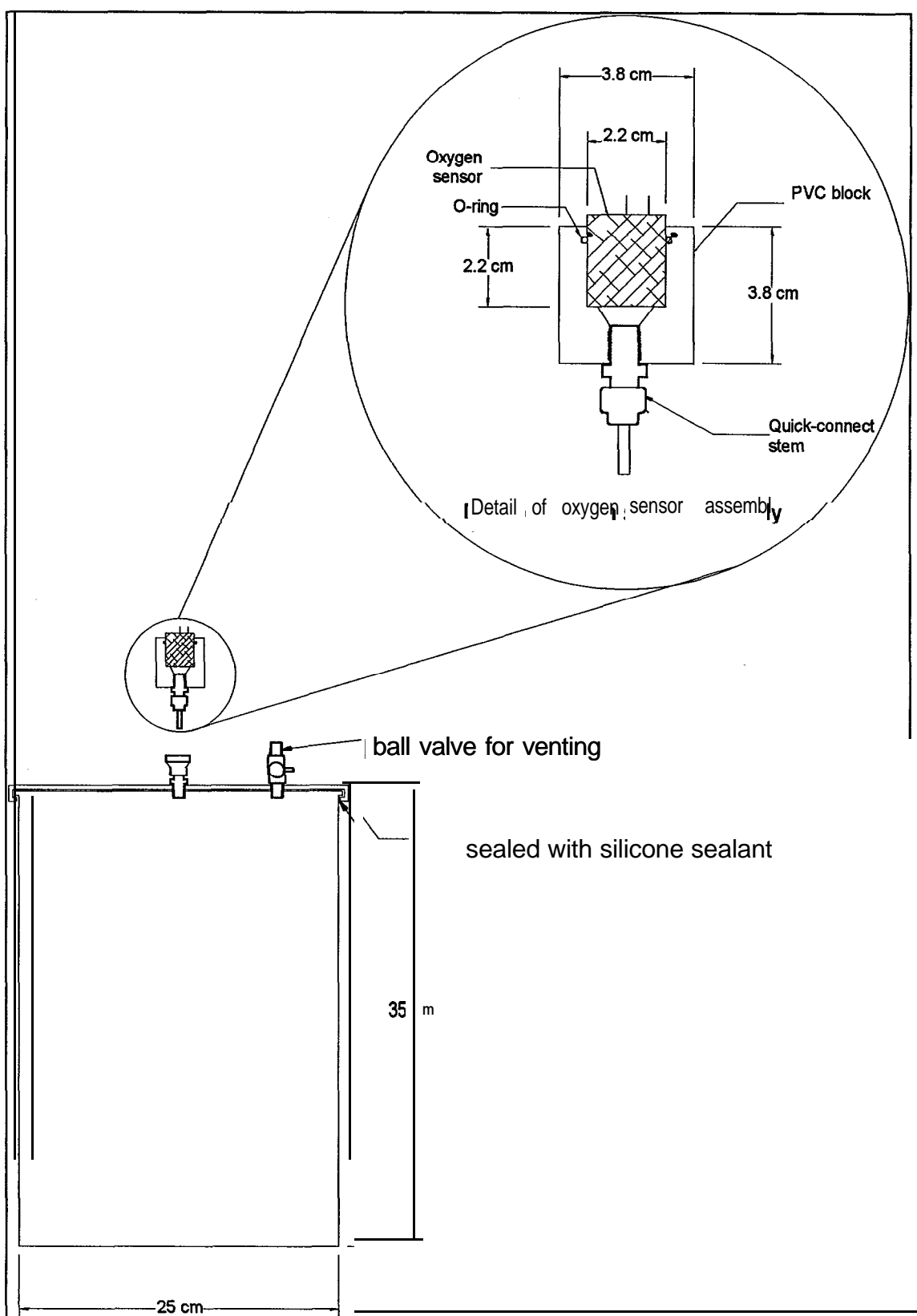


Figure 3.4 Scale drawing of 17L reactor

### **3.5 Oxygen Consumption Method for Waste Rock**

A standard procedure was developed and adopted for preparing the rock samples before each oxygen consumption test to assure comparability and reproducibility of the measurements. All rock samples were crushed and sieved to the appropriate size fraction.

Most of the rock samples were then washed with tap water to remove any fine particles produced by the crushing procedure. The rocks were then subjected to a solution of approximately 5 to 10% concentrated HCl in order to remove oxidation products or coatings that may have been formed. This step was particularly important when working with a sample that had been tested previously. Despite this, visual observations indicated that the oxide coatings were quite resilient and could not be completely removed by this HCl rinse. Following acid-treatment, the rocks were rinsed well with tap water and given a final rinse in deionized water. After decanting the deionized water, the reactor was sealed from the atmosphere, placed in a temperature controlled water bath and oxygen measurements begun. Oxygen concentration measurements were recorded automatically every 15 minutes for a period of 2 to 3 days. The oxygen concentration in the reactor decreased from atmospheric (ie. 21%) to a final value of no less than 17 %, by volume.

At the completion of the test the reactor was flooded with deionized water and allowed to stand for approximately 1 hour. The purpose of this step was to allow oxidation products, ie. sulphate and metal ions, to dissolve into the bulk water phase which was then collected and sampled. The volume of water was made up to a known volume, usually 250 mL, from which two 20 mL aliquots were taken. One aliquot was kept for sulphate analysis by HPLC and did not require any preservative treatment. The other aliquot was acidified with 10 drops of concentrated HCl and kept for ICP analysis of metals. Liquid samples were analyzed by Zenon Laboratories, Burlington according to the methods described in 'Standard Methods for the Examination of Water and Wastewater', Seventeenth Edition.

Knowing the concentration of sulphate (or a particular metal) in the rinse water and the volume to which it had been diluted, a mass loading rate could be calculated in terms of milligram of sulphate (or metal) per kilogram of waste rock over the length of time of the test. The rate of sulphate released could then be compared with the measured oxygen consumption for the stoichiometry of the assumed oxidation reaction.

Calculation of the oxygen consumption rate requires the determination of the volume of air and the mass of rock in the reactor. The mass of rock was determined by weighing. The volume of air in the pore spaces between rock particles was estimated by weighing the reactor and contents, filling the pore spaces with water and re-weighing the reactor. The mass of water required to fill the pore spaces can be converted into a volume by dividing by the density of water.

### **3.51 Detection Limit**

Being galvanic cells, the oxygen sensors consume oxygen at a low but measurable rate and this had to be accounted for in the oxygen consumption rate calculations. The detection limit of the test was established by the rate of oxygen consumption by the sensor and the volume of air in the reactor. The consumption rate of the sensor was assumed to be independent of the air volume in the reactor and therefore a larger volume of air was less significantly affected by the rate of oxygen consumption by the sensor and exhibited a lower detection limit than tests with smaller air volumes.

The oxygen consumption rate of each individual sensor was determined by performing blank controls (i.e. reactors without a reactive sample). The oxygen consumption measurements were conducted on small volumes of headspace with no sample present. The small volume was required to observe a response in a reasonable time. The rate of oxygen consumption by the individual sensors was determined at each of the temperatures investigated.

For an average test with 8 mm diameter particles the reactor contained about 600 g of rock and 220 mL of air. With an average sensor consumption rate of  $2.8 \times 10^{-10}$  mol  $O_2 \cdot s^{-1}$  at 30°C, the detection limit was  $4.7 \times 10^{-10}$  mol  $O_2 \cdot kg^{-1} \cdot s^{-1}$ . The detection limit was generally taken to be about  $5 \times 10^{-10}$  mol  $O_2 \cdot kg^{-1} \cdot s^{-1}$ , however this depends on the rate of oxygen consumption by the sensor. It was possible to measure rates lower than this by minimizing the consumption of oxygen by the sensor (by lowering the temperature, for example).

The detection limit of the 17L tests was determined in a different manner. In this case, the oxygen sensors consumed a minute amount of the total oxygen present in the reactor and the detection limit was determined by the ability to observe a coherent trend in the oxygen concentration in the reactor. A coherent trend was defined arbitrarily as a decrease in the oxygen partial pressure in the reactor by 5% over the timescale of the test. This translates to an observed 2 mV decrease over 70 days. The detection limit for the 17L reactor was calculated to be approximately  $3 \times 10^{-11}$  mol  $O_2 \cdot kg^{-1} \cdot s^{-1}$ .

### 3.5.2 Data Analysis

The oxidation reaction of iron sulphide minerals is generally believed to be zero-order with respect to oxygen at high concentrations, at least in a short time frame (Nicholson et al., 1988a; Ritchie, 1994). Coupling this with the assumption that diffusion does not limit the reaction, the system can be described as;

$$-\frac{dC}{dt} = k \quad \text{Equation 3.1}$$

where C is the gas phase concentration of oxygen, t is time and k is the apparent reaction rate constant. The experimental results support this model and the rate was easily calculated from a linear regression analysis of the oxygen sensor output over time. The oxygen consumption rate of a sample of Whistle medium sulphide norite is detailed below.

Figure 3.5 shows the measured output from an oxygen sensor and the linear regression line which best represents the data. Linear regression of the oxygen sensor output yields a slope in terms of volts per second. This was converted to a rate of change in oxygen concentration given in moles of oxygen per litre per second using a conversion factor which translates the sensor output from volts to partial pressure of oxygen and the ideal gas law. The rate in moles of oxygen per kilogram of rock per second was calculated by multiplying by the volume of air divided by the mass of rock in the reactor.

The rate of change in the oxygen concentration was corrected for the consumption of oxygen by the sensor using the measured sensor consumption rate (SCR). The observed rate of oxygen depletion (OCR) in the reactor was assumed to be the sum of the oxygen sensor consumption (SCR) and the consumption due to oxidation of the reactive sample (R).

The scaling factor (volume of air in blank reactor/volume of air in test reactor) is applied to the SCR to account for the fact that the rate of oxygen consumption of the sensor (in moles of oxygen per unit time) is constant but the apparent rate of change in the sensor output will depend on the volume of air that the oxygen sensor “sees”.

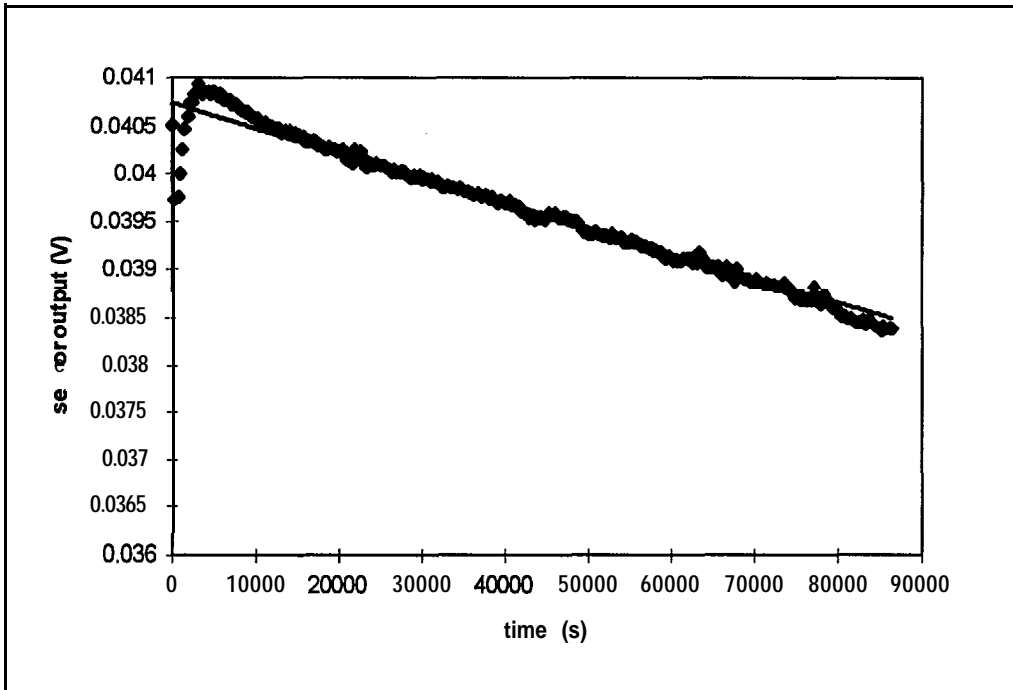


Figure 3.5 Sensor output for Whistle medium sulphide, 7 mm size fraction, T=30°C

### 3.5.3 Reproducibility and Precision

The reproducibility of the oxygen consumption rate measurement was determined by repeating the test procedure on samples of the 8 mm size fraction of waste rock from Faro. Approximately 1.6 kg of waste rock was split into two sub-samples. Each sub-sample was washed and prepared for testing according to the protocol outlined above. The tests were performed in parallel under identical temperature conditions. The oxygen consumption rates for each sub-sample were compared and the mean rate of the two populations were not statistically different at the 95% confidence level. The oxygen consumption rates were pooled in order to calculate the average oxygen consumption rate and standard deviation of the population.

#### 4. Results

Initial tests and method development were completed using waste rock from the Whistle Mine. Preliminary tests indicated that it was possible to obtain measurable oxygen consumption rates using the acrylic reactor and waste rock particles with diameters between 22 and 7 mm. Results from the first tests suggested that temperature control was necessary to prevent erratic sensor response due to small changes in the room temperature over the course of the test. From this point on all tests were carried out in a temperature controlled water bath equipped with a lid that effectively insulated the entire reactor and oxygen sensor from changes in ambient conditions. Oxygen consumption rates were measured on Whistle waste rock for selected size fractions from approximately 10 cm to 7 mm over a range of sulphur contents. The results of these tests suggested that attention should be focused on particle sizes smaller than about 2 cm since these particles tend to consume oxygen at a higher rate.

The second phase involved the characterization of rock samples from the Voisey's Bay mining project. The oxygen consumption method was employed to assess the effect of the particle size or surface area, temperature, sulphide content and the presence of *T. ferrooxidans* on the oxidation of sulphide minerals in the waste rock. The rate of oxygen consumption was expected to be positively correlated with decreasing particle size (increasing surface area), increasing temperature, increasing sulphide content and inoculation with *T. ferrooxidans*. The results presented below bore out these trends. During the second phase of investigation some anomalous results led to the discovery that the oxygen sensors were consuming oxygen at a measurable rate. The consumption of oxygen by each sensor was measured and this was accounted for in the oxygen consumption rate calculation. Previously measured rates were also corrected using this information.

The final phase encompassed the determination of oxygen consumption rates for six different rock types in order to compare and contrast the rates associated with

the miscellaneous types. The rock types examined differed in terms of the host rock type (ie. mafic compared to metasedimentary), the dominant sulphide mineral (i.e. pyrite vs. pyrrhotite), the presence and type of accessory sulphide mineralogy and the distribution of the sulphides in the rock matrix.

The oxygen consumption rates measured during the three phases covered a broad range of values from a lower limit of  $4.01 \times 10^{-4}$  mol  $O_2 \cdot kg^{-1} \cdot s^{-1}$  (Faro waste rock, 16 mm size, 10°C) to an upper value of  $1.8 \times 10^{-6}$  mol  $O_2 \cdot kg^{-1} \cdot s^{-1}$  (Whistle massive sulphide material, 0.074 mm size, 20°C). A summary of the oxygen consumption rates and test conditions are given in Tables A.1 to A.14 in Appendix A.

## **4.1 Particle Size**

### **4.1.1 Initial Tests on Whistle Mine Samples**

The theoretical model states that the oxidation rate should be inversely proportional to the particle diameter. The results of the Whistle Mine tests were consistent with this model given the experimental error inherent in the measurements. The oxygen consumption rate was a function of  $1/d^n$ , where n is equal to 0.97 for the massive sulphide material, 1.8 for high S norite and 1.6 for the medium S norite. Insufficient data were available to determine the size dependence of the low S norite material. The value of n was determined by linear regression of the logarithm of the oxygen consumption rate vs. the logarithm of the particle diameter. The regression plots for selected sulphur contents are shown in Figure 4.1, Figure 4.2 and Figure 4.3. The results of several experiments conducted at 20°C using the acrylic or glass reactors for the smaller rock fragments (less than 22 mm) and the 17L PE reactors for large particles (80-100 mm) are included in these figures.

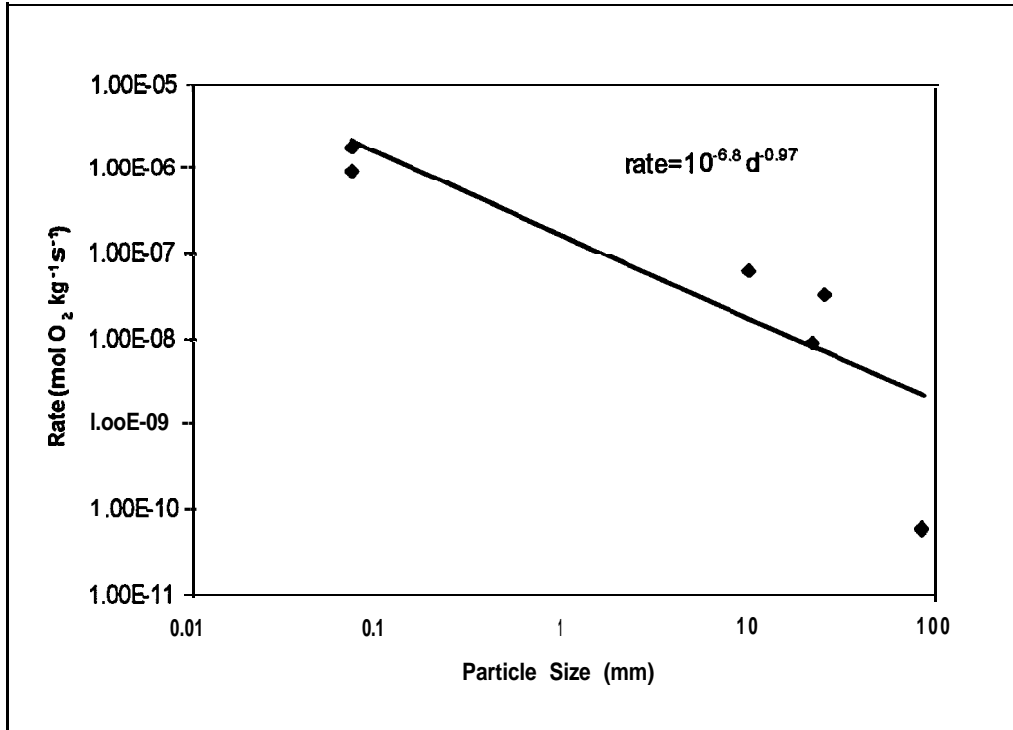


Figure 4.1 Oxygen consumption rate vs. size - Whistle massive sulphide at 20°C

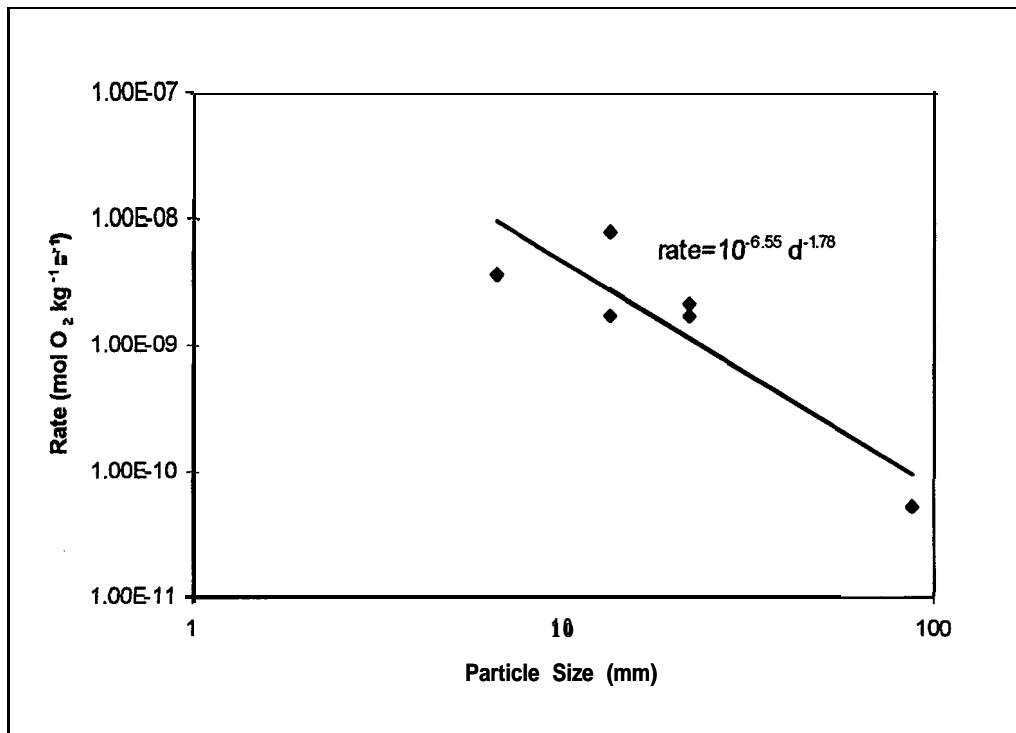


Figure 4.2 Oxygen consumption rate vs. size - Whistle high S norite at 20°C

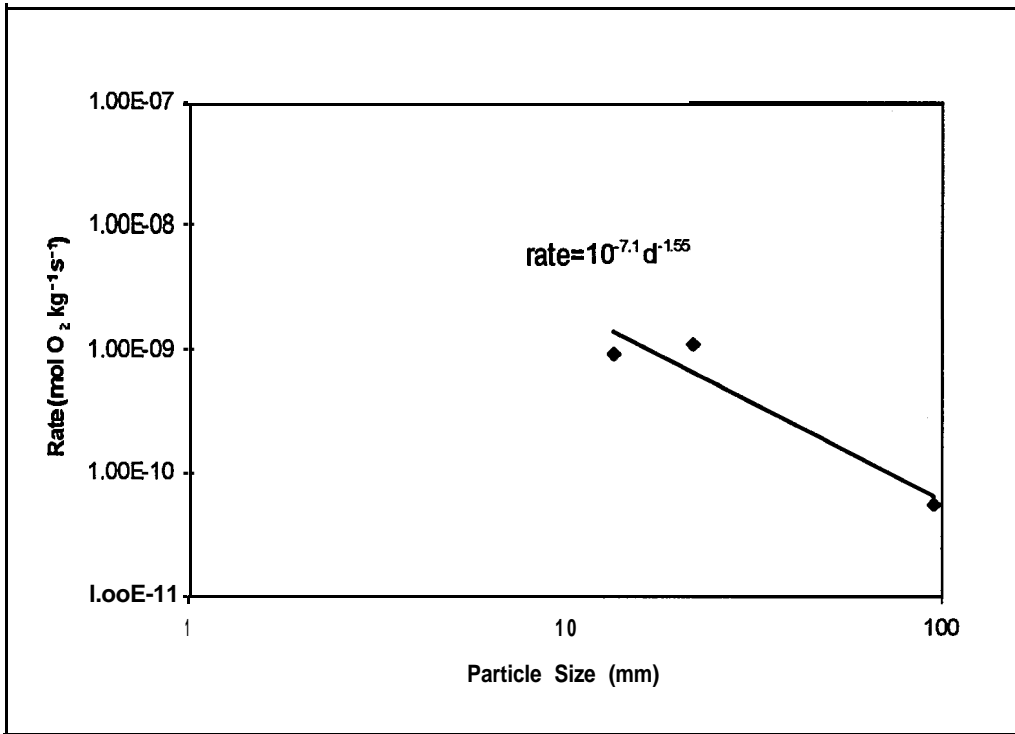


Figure 4.3 Oxygen consumption rate vs. size - Whistle medium *S norite* at 20°C

#### 4.1.2 Voisey's Bay Tests

Four composites of the Voisey's Bay material were created to investigate particle size effects over the range of 0.3 to 8 mm. Four samples, each with four size fractions, were tested at four different temperatures in the range of 4 to 30°C. The tests were repeated using waste rock samples that had been inoculated with an active culture of *T. ferrooxidans* at three temperatures; 4, 10 and 30°C. The dependence of rate on  $1/d^n$  was also used to describe these results. The values of  $n$  determined in these cases are summarized in Table 4.1 for the different composites at the given temperatures under inoculated and uninoculated conditions. The average values of  $n$  were also calculated, values based data from only two size fractions were not included in the calculation. The log-log plots of oxygen consumption rate vs. particle diameter from which these numbers were calculated can be found in Appendix B, Figures B.1 to B.16.

Three different size fractions of the Eastern Deeps (ED) and Western Extension (WE) composites were also tested at 30°C. The results are depicted in Figure 4.4.

#### 4.1.3 Tests on Additional Rock Samples

Data from tests using the six different rock types were used to make qualitative comparisons as only two size fractions of each rock type were examined. A third size fraction of Faro and Mine Doyon rock was later added, but these tests yielded

Table 4.1: Values of n for Voisey's Bay COMP samples

Composite	Temperature (°C)	Uninoculated (n)*	Inoculated (n)
COMP 1	30	0.88"	<b>0.59</b>
COMP 2	30	0.40	<b>0.50</b>
COMP 3	30	1.9"	1.1
COMP 4	30	<b>0.79</b>	0.74
COMP 1	20	1.8	N/A*
COMP 2	20	1.4	<b>N/A<sup>‡</sup></b>
COMP 3	20	1.5	N/A*
COMP 4	20	1.5	N/A*
COMP 1	10	1.1	0.64
COMP 2	10	1.6	0.73
COMP 3	10	1.3	0.56
COMP 4	10	0.62	0.063
COMP 1	4	1.3	0.66
COMP 2	4	2.2	0.27
COMP 3	4	1.3	0.19
COMP 4	4	1.5	0.27
<b>Average</b>		<b>1.3</b>	<b>0.53</b>

"from rate vs. particle size relationship,  $\text{Rate} \propto 1/d^n$

"based on data from only two size fractions

\*N/A = not available, tests were not performed at this temperature

ininterpretable sensor output, which may have been due to aging sensors. The tests were performed at three temperatures (10, 20 and 30°C) prior to inoculation and at 20°C after being inoculated with *T. ferrooxidans* (labelled 'w/T.f.' on graphs). Figures 4.5 to 4.10 depict the rates for each size fraction at a given temperature for each of the rock types.

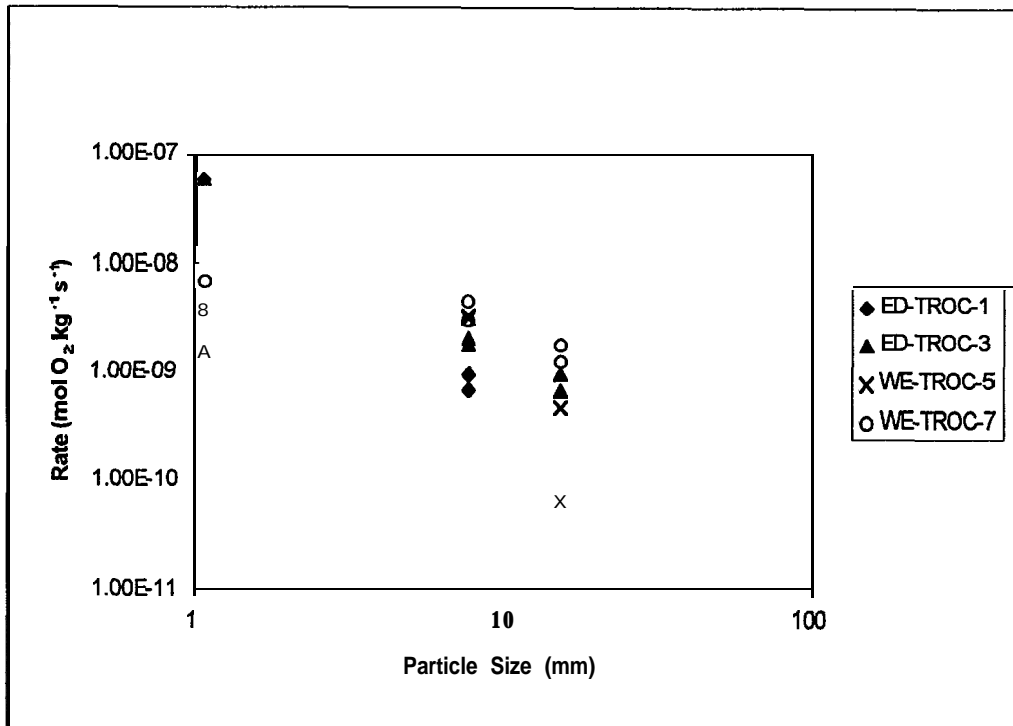


Figure 4.4 Oxygen consumption rate vs. size - ED and WE composites

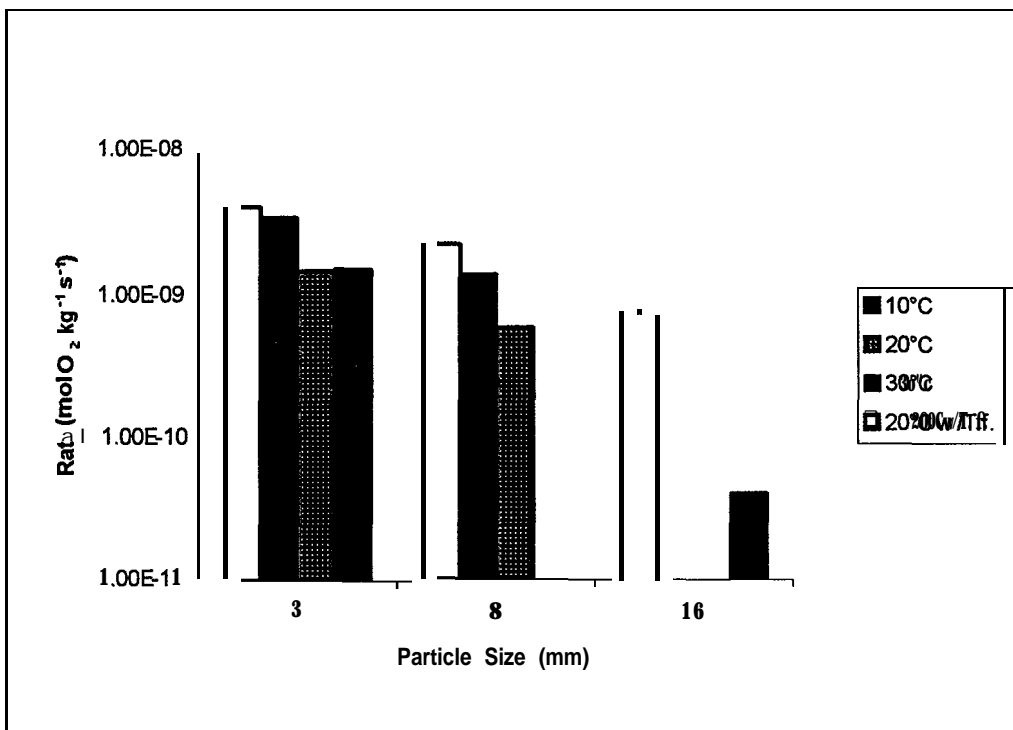


Figure 4.5 Oxygen consumption rate vs. size - Faro waste rock

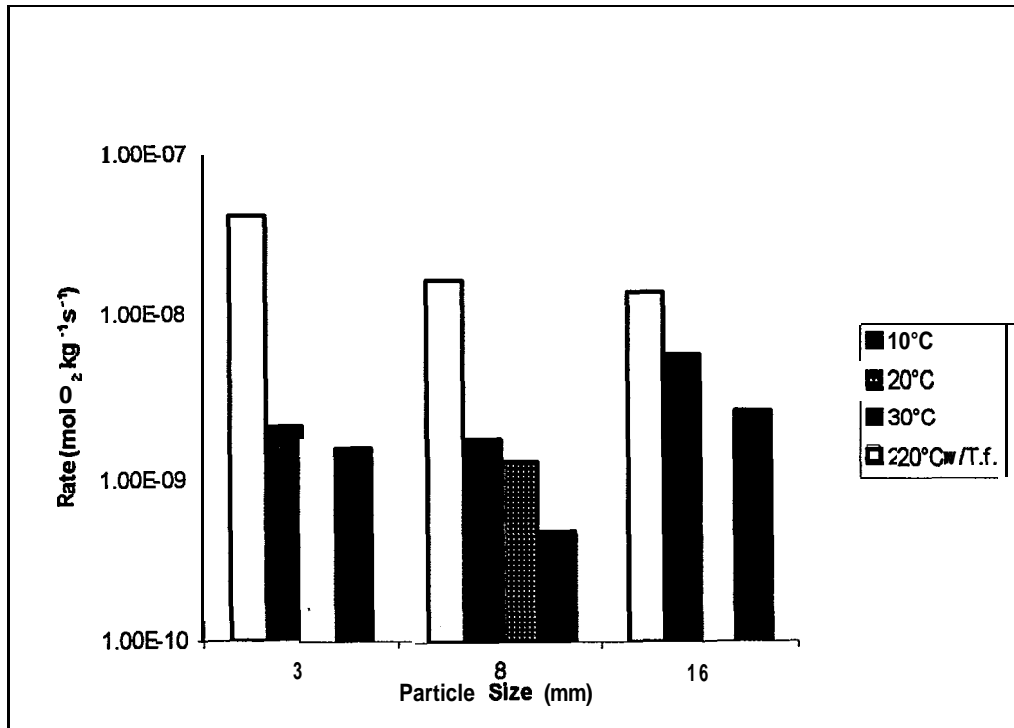


Figure 4.6 Oxygen consumption rate vs. size - Mine Doyon waste rock

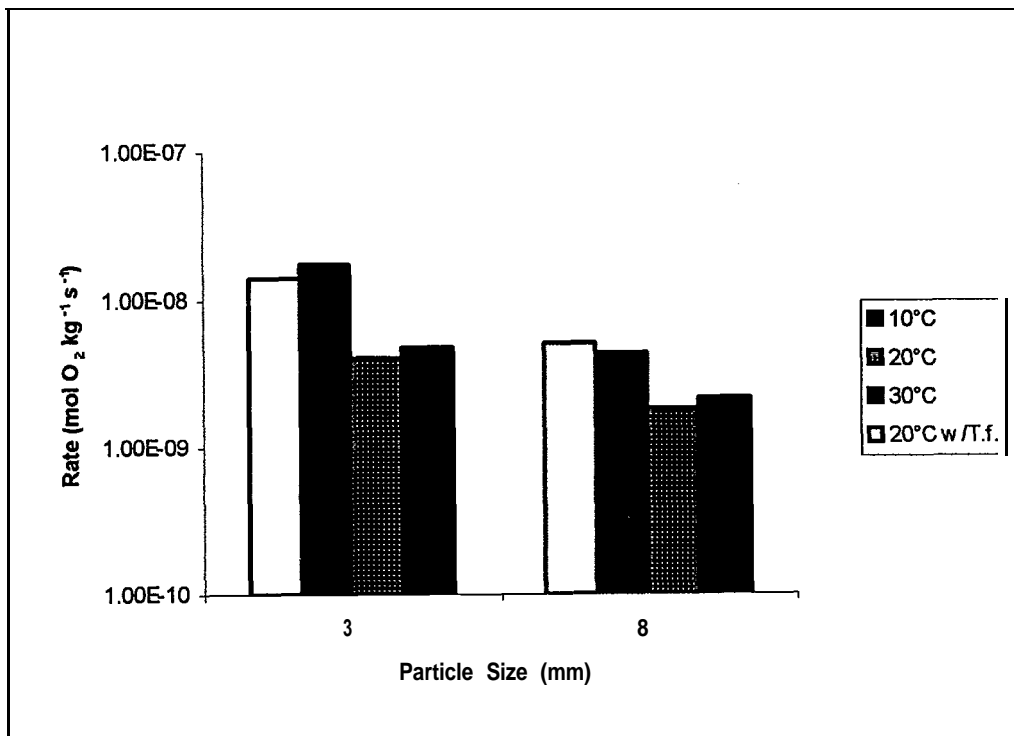


Figure 4.7 Oxygen consumption rate vs. size - Whistle high S norite

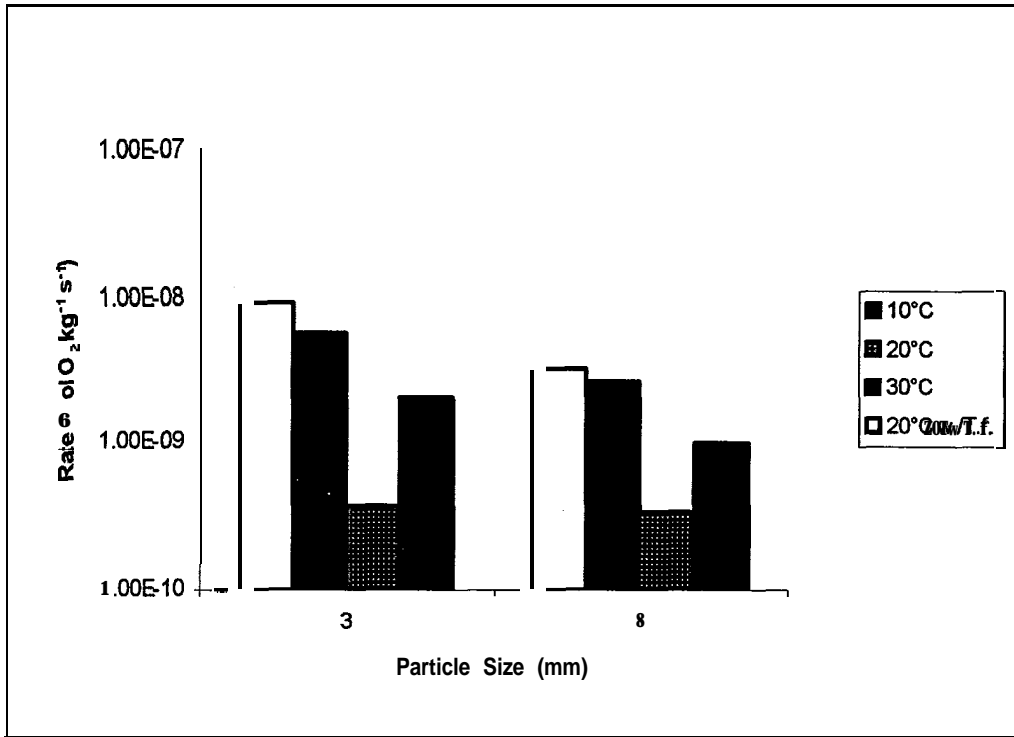


Figure 4.8 Oxygen consumption rate vs. size - Whistle low S norite

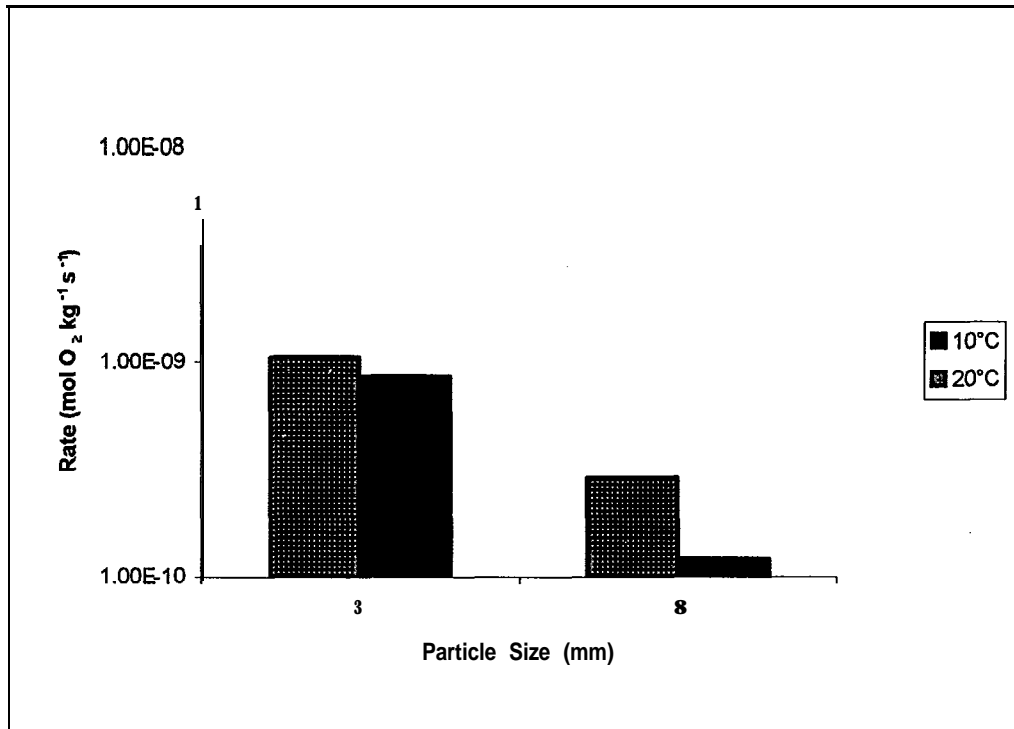


Figure 4.9 Oxygen consumption rate vs. size - Pamour waste rock

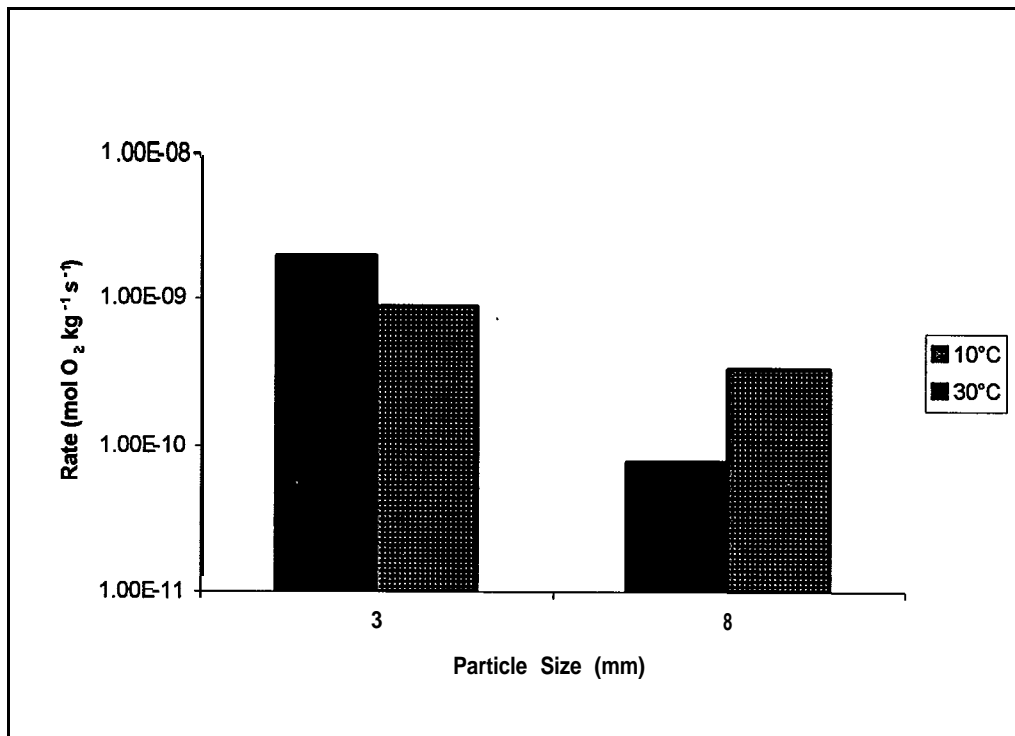


Figure 4.10 Oxygen consumption rate vs. size - KZK waste rock

## 4. 2 Temperature

### 4. 2. 1 Initial Tests on Whistle Mine Samples

Oxygen consumption rates were measured for the various Whistle Mine waste rock samples at three different temperatures; 10, 20, and 30°C. Activation energies were determined from linear regression analysis of the natural logarithm of the oxygen consumption rate ( $k$ ) as a function of the reciprocal temperature ( $1/T$ ) in degrees Kelvin. Plots of  $\ln(k)$  vs.  $1/T$  can be found in Appendix C, Figures C.1 to C.4. The calculated activation energies are summarized in Table 4.2.

Table 4.2 Activation energies for Whistle waste rock samples

<b>Rock Type</b>	<b>Activation Energy (kJ·mol<sup>-1</sup>)</b>
<b>Massive sulphide</b>	N/A*
<b>High S norite</b>	42.2
<b>Medium S norite</b>	65.0''
<b>Low S norite</b>	15.8*

\*N/A = insufficient data to calculate activation energy

\* based on only two data points

#### 4.2.2 Voisey's Bay Tests

The 16 size fraction composites from Voisey's Bay were examined at four temperatures ranging from 4 to 30°C. Testing with inoculated samples was conducted at 30, 10 and 4°C. An activation energy was calculated for each size fraction of each composite under inoculated and uninoculated conditions. These values are give in Table 4.3, Arrhenius plots are presented in Appendix C as Figures C.5 to C.8.

#### 4.2.3 Tests with Additional Rock Samples

Activation energies were calculated for the two size fractions of the six rock types based on measurements at temperatures of 10, 20 and 30°C. These values are compiled in Table 4.4. The Arrhenius plots from which the activation energies were derived are presented in Appendix C, Figures C.9 to C.14.

Table 4.3 Activation energies for Voisey's Bay waste rock samples

Description	Particle size (mm)	Uninoculated Activation Energy (kJ·mol <sup>-1</sup> )	Inoculated Activation Energy (kJ·mol <sup>-1</sup> )
COMP 1	8	29.9	33.4
COMP 2	8	108.4	64.9
COMP 3	8	36.5	N/A <sup>‡</sup>
COMP 4	8	19.4	N/A <sup>‡</sup>
COMP 1	3	64.0	N/A <sup>‡</sup>
COMP 2	3	N/A <sup>‡</sup>	40.7
COMP 3	3	45.3	42.8
COMP 4	3	50.4	42.5
COMP 1	1	104.9	20.9*
COMP 2	1	78.6*	206.1*
COMP 3	1	83.9*	44.2
COMP 4	1	86.2	11.7
COMP 1	0.3	96.1	27.4
COMP 2	0.3	N/A <sup>‡</sup>	44.0*
COMP 3	0.3	43.0	93.5
COMP 4	0.3	26.3	75.1
<b>Average</b>		<b>59.2</b>	<b>47.6</b>

\*N/A = insufficient data to calculate activation energy

\*based on only two data points

Table 4.4 Activation energies for different rock types

Rock Type	Particle Size (mm)	Activation energy (kJ·mol <sup>-1</sup> )
Faro	16	N/A*
Faro	a	67.3 <sup>‡</sup>
Faro	3	19.5
Mine Doyon	16	33.4*
Mine Doyon	a	a.9
Mine Doyon	3	13.0
Whistle high S norite	8	43.3
Whistle high S norite	3	60.2
Whistle low S norite	8	33.2
Whistle low S norite	3	36.1
Pamour	a	66.8 <sup>‡</sup>
Pamour	3	N/A*
KZK	a	N/A*
KZK	3	38.4

<sup>‡</sup>N/A = insufficient data to calculate activation energy

\*based on only two data points

### 4.3 Sulphide Content

#### 4.3.1 Initial Tests on Whistle Mine Samples

Oxygen consumption rates were determined for three size fractions of the four Whistle porite samples. The 22 mm and 14 mm size fractions were tested at 20°C and the 7 mm size fraction was tested at 30 and 10°C before inoculation. Samples of the 7 mm size fraction were inoculated with *T. ferrooxidans* and oxygen consumption rates measured at 30°C. The oxygen consumption rates of the three size fractions are plotted against sulphide content in Figure 4.11 to Figure 4.15.

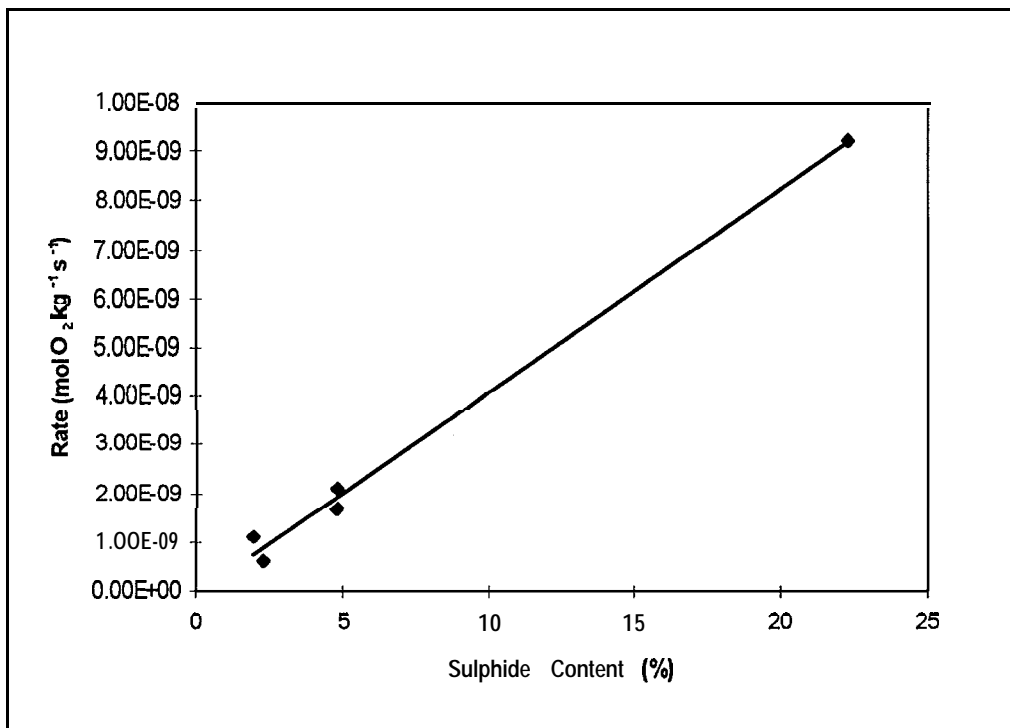


Figure 4.11 Oxygen consumption rate vs. sulphide content -Whistle waste rock, 22 mm size at 20°C

#### 4.3.2 Voisey's Bay Tests

Oxygen consumption rates were determined for the 16 composite samples at 4 different temperatures prior to inoculation and 3 temperatures after inoculation

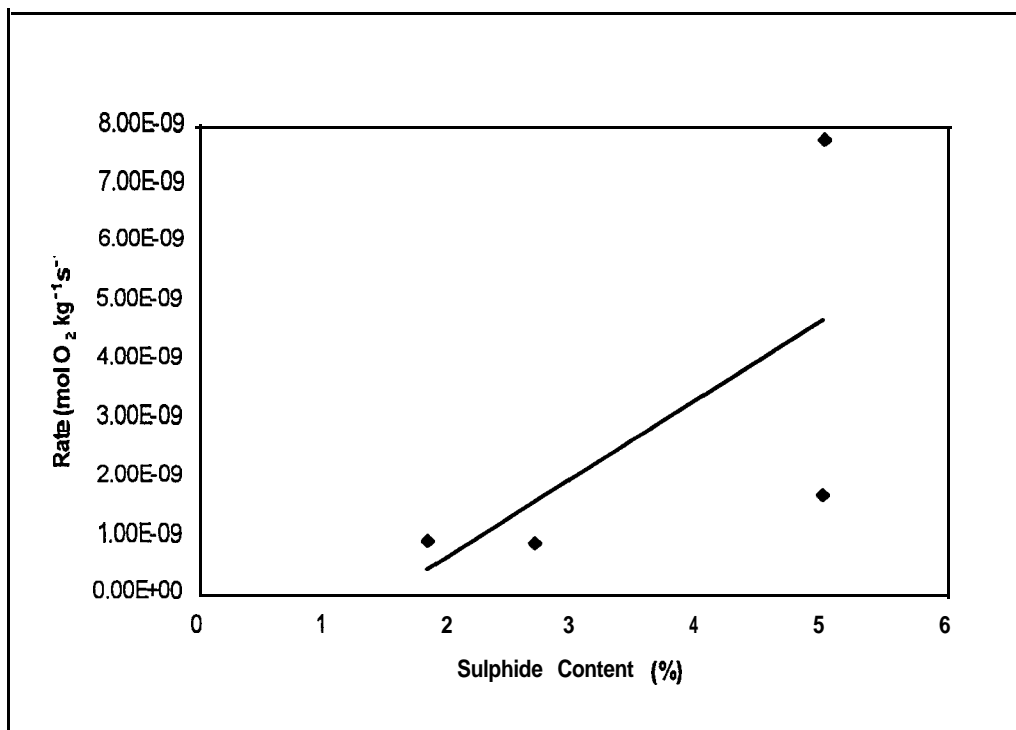


Figure 4.12 Oxygen consumption rate vs. sulphide content - Whistle waste rock, 14 mm size at 20°C

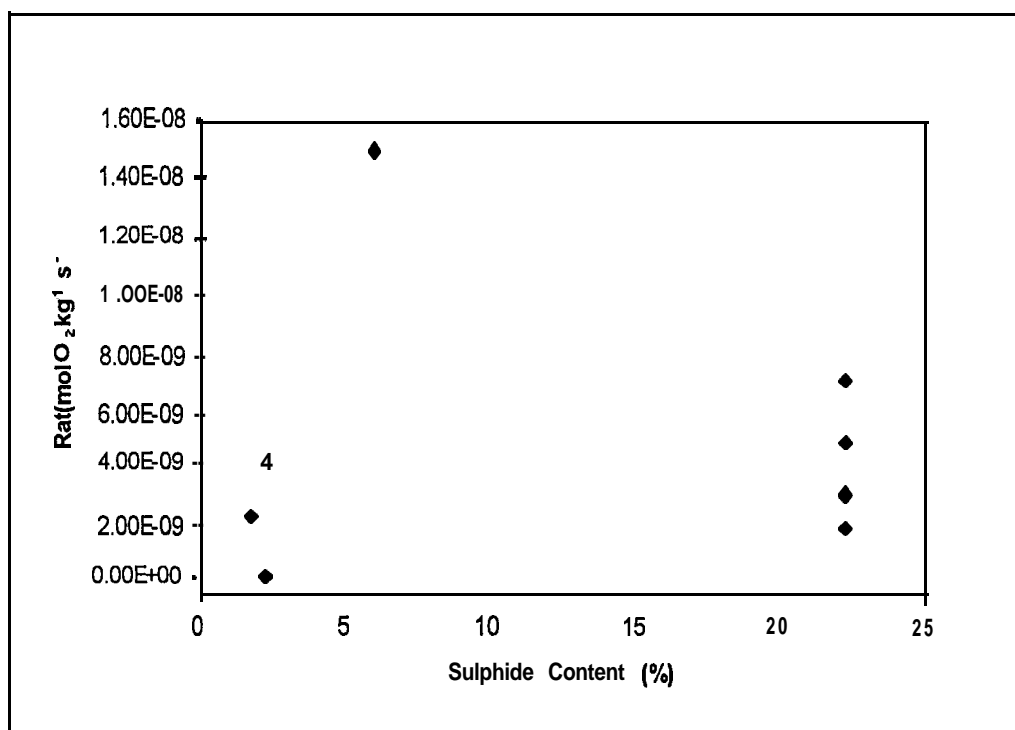


Figure 4.13 Oxygen consumption rate vs. sulphide content - Whistle waste rock, 7 mm size at 30°C

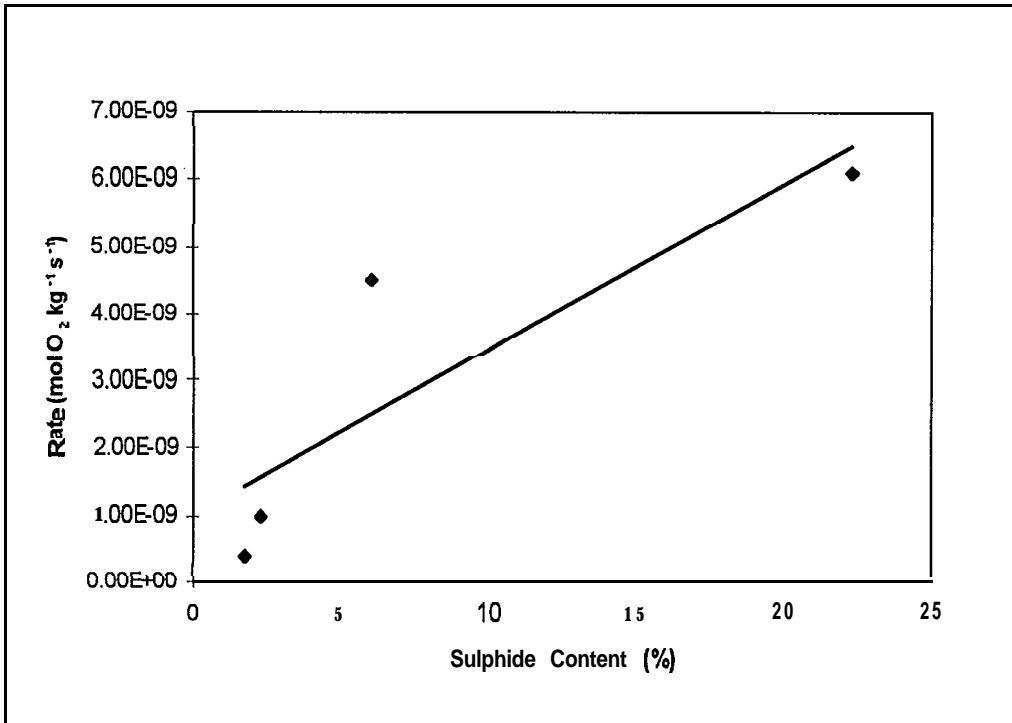


Figure 4.14 Oxygen consumption rate vs. sulphide content - Whistle waste rock, 7 mm size at 10°C

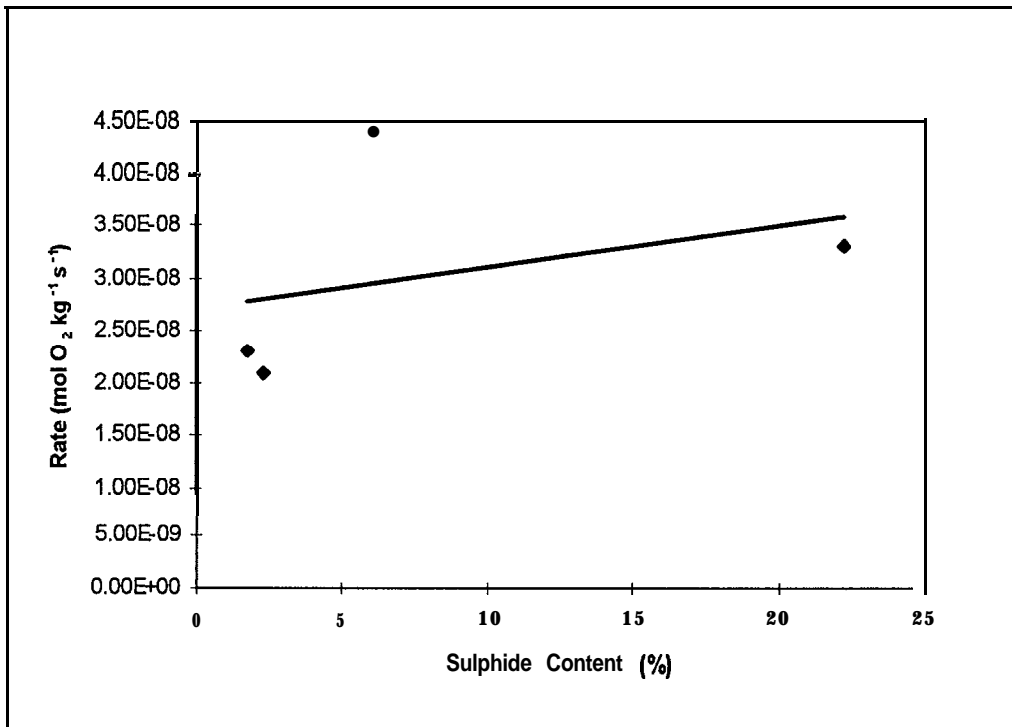


Figure 4.15 Oxygen consumption rate vs. sulphide content - Whistle waste rock, 7 mm size at 30°C inoculated with *T. ferrooxidans*

with *T. ferrooxidans*. Plots of the oxygen consumption rate as a function of the sulphide content are presented in Appendix D.

Similar plots are shown in Figure 4.16 and Figure 4.17 for the ED and WE composites and Ovoid samples under inoculated and uninoculated conditions. Figure 4.17b shows the same data as Figure 4.17a, except that the HC8 sample (containing 24% S) has been omitted and the axis scales have been scaled in order to clearly show the trends for the samples having less than 3% S.

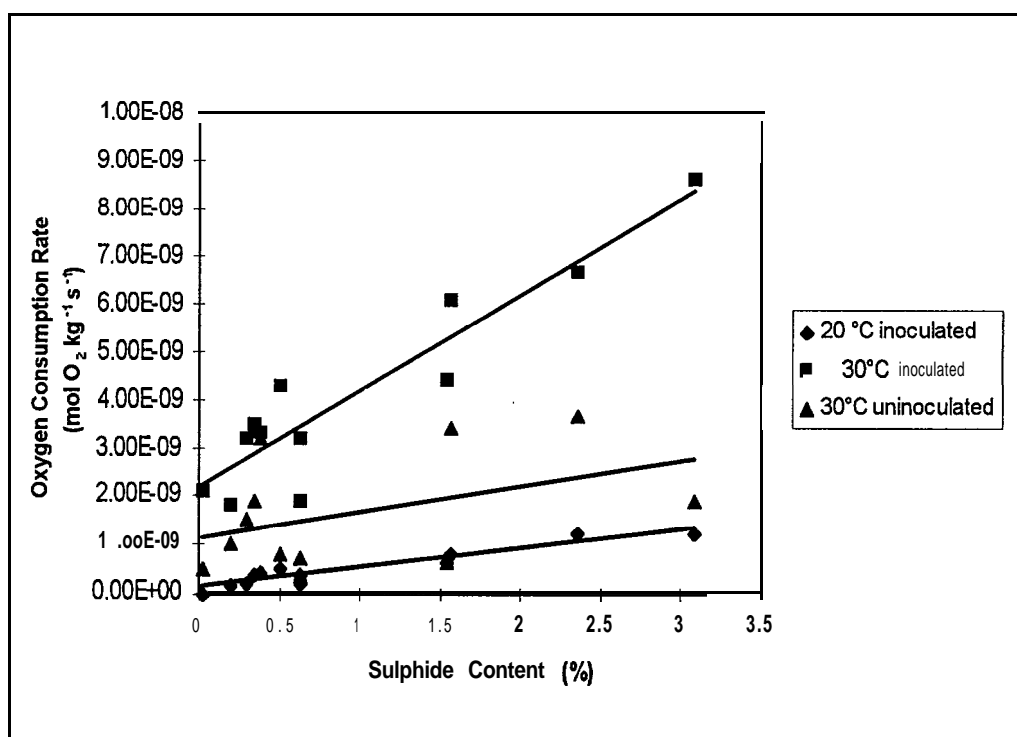


Figure 4.16 Oxygen consumption rate vs. sulphide content - ED and WE composites

### 4.3.3 Tests on Additional Rock Samples

The rates of oxygen consumption for the six rock types investigated are plotted against the sulphide content for inoculated and uninoculated rock samples at 20°C in Figure 4.18 and Figure 4.19. Figure 4.18 shows trends in oxygen consumption rate with total sulphur content for 8 mm size particles and Figure 4.19 depicts similar information for the 3 mm size fraction of the same materials.

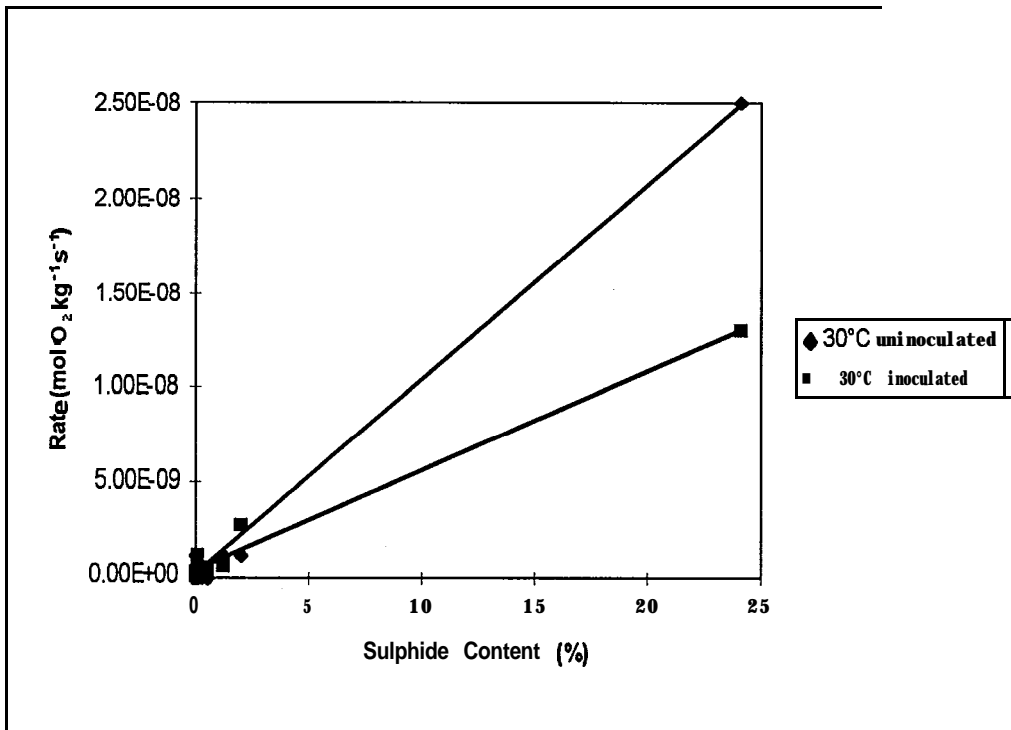


Figure 4.17a Oxygen consumption rate vs. sulphide content - Ovoid samples

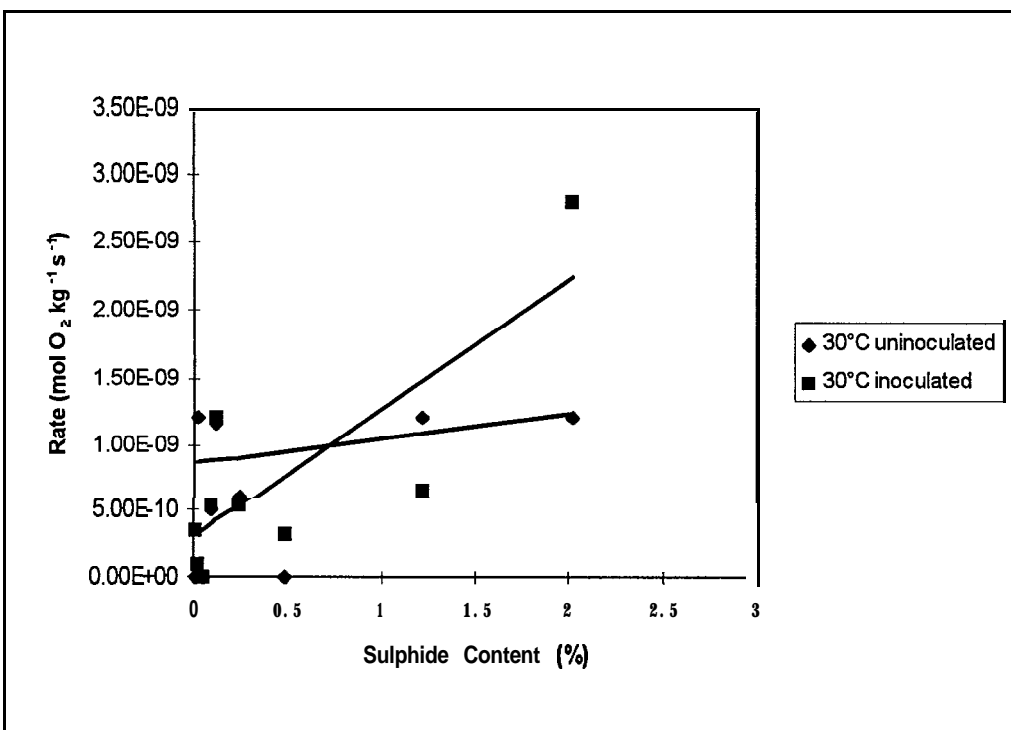


Figure 4.17b Oxygen consumption rate vs. sulphide content - Ovoid samples, excluding HC8 (24%S)

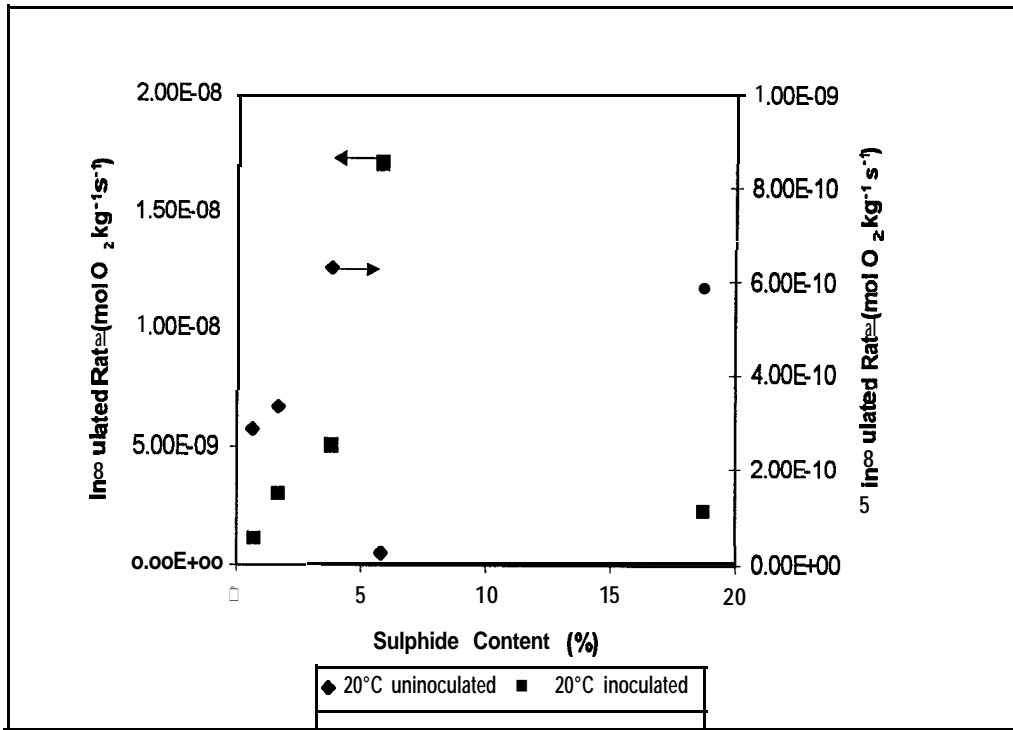


Figure 4.18 Oxygen consumption rate vs. sulphide content - 6 rock types, 8 mm size

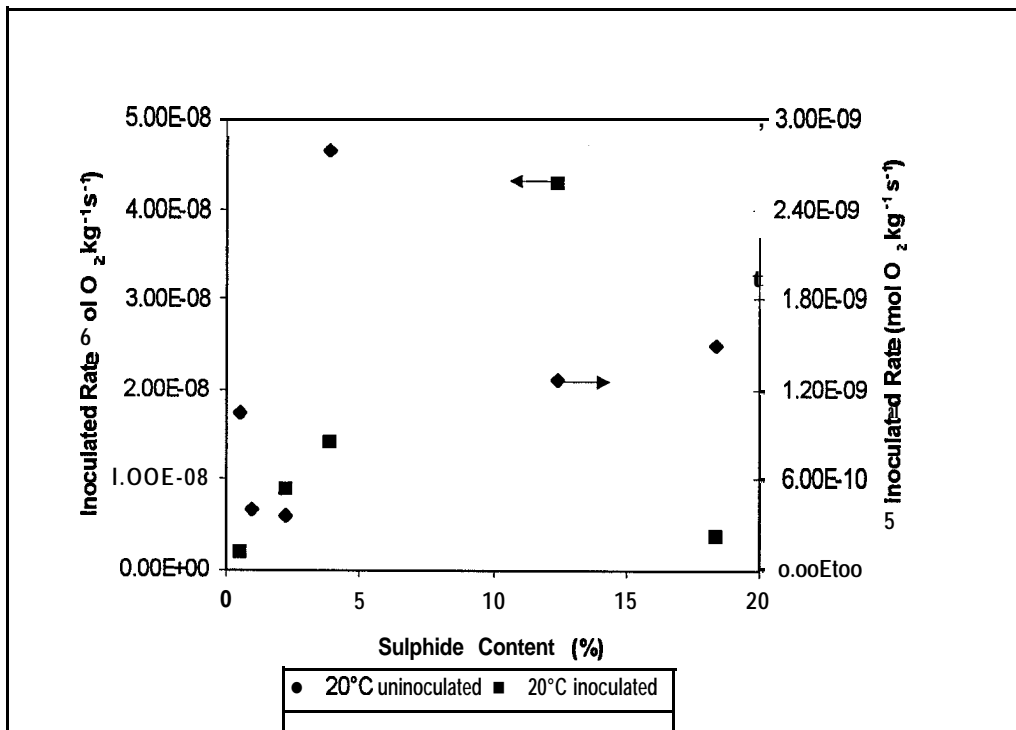


Figure 4.19 Oxygen consumption rate vs. sulphide content - 6 rock types, 3 mm size

#### **4.4 Inoculation with *Thiobacillus ferrooxidans***

Many of the rock samples were inoculated with an active culture of *T. ferrooxidans* after measuring the oxygen consumption rate under uninoculated conditions. Scanning electron microscopy was used to observe the bacterial growth and attachment on the surface of the Whistle massive sulphide material after one of the tests. Figure 4.20 shows the presence of the bacteria on the surface of the sulphide material. The scale of the micrograph is given in the lower right corner of the picture and indicates that the cells were approximately 1  $\mu\text{m}$  long and 0.2  $\mu\text{m}$  in diameter, which is consistent with *T. ferrooxidans*. The fibrous material present in the background is suspected to be an extracellular secretion which serves to anchor the bacteria to the mineral surface (Davis *et al.*, 1995).

##### **4.4.1 Initial Tests on Whistle Mine Samples**

Experiments were conducted at 30°C after inoculating the 8 mm waste rock samples with an active culture of *T. ferrooxidans*. The results are depicted in Figure 4.21 which shows the relative rate of reaction after inoculation plotted against the sulphide content of the sample. The relative rate is defined as the measured rate of the inoculated sample divided by the measured rate of the same material without inoculation. The rate of oxygen consumption increased by a factor of 2 to 9 after inoculation compared to the uninoculated rate for the Whistle waste rock samples.

##### **4.4.2 Voisey's Bay Tests**

Similar tests were performed using all size fractions of the COMP samples from Voisey's Bay and these results are summarized in Figure 4.22. The relative rate was generally greater than one, indicating an increase in the oxygen consumption rate, for rock samples inoculated and tested at 30°C reaching a maximum of approximately 5. The rate of oxygen consumption decreases in almost all cases where the rocks were inoculated at 10 and 4 °C.

The relative oxygen consumption rate of the ED and WE composites are depicted in Figure 4.23. In this case, the uninoculated samples were only run at 30°C and

these rates were used to calculate the relative rates at both 20 and 30°C. The relative rates at 20°C are all less than or equal to one indicating that the inoculated rates at 30°C are greater than or equal to the inoculated rates at 20°C for these rock samples.

#### **4.4.3 Tests on Additional Rock Samples**

Figure 4.24 shows the relative rate after inoculation for the two size fraction of the six rock types at 20°C. It should be noted that the 8 mm Mine Doyon sample was not included in this graph as it had a relative rate of 62, which is over three times higher than the next highest value. The majority of the other samples had relative rates ranging between 2 and 10.

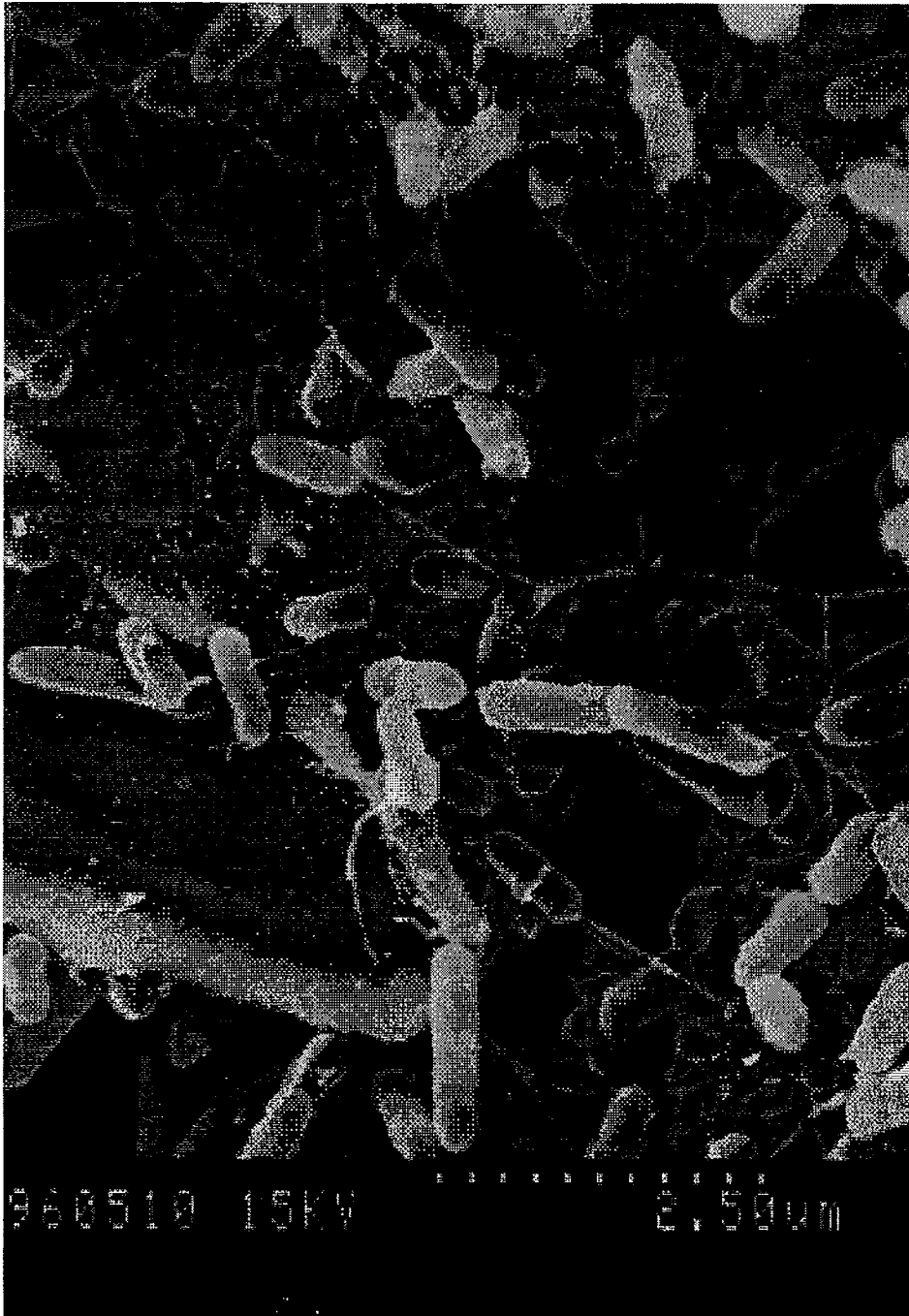


Figure 4.20 Scanning electron micrograph of *T. ferrooxidans* on Whistle massive sulphide material

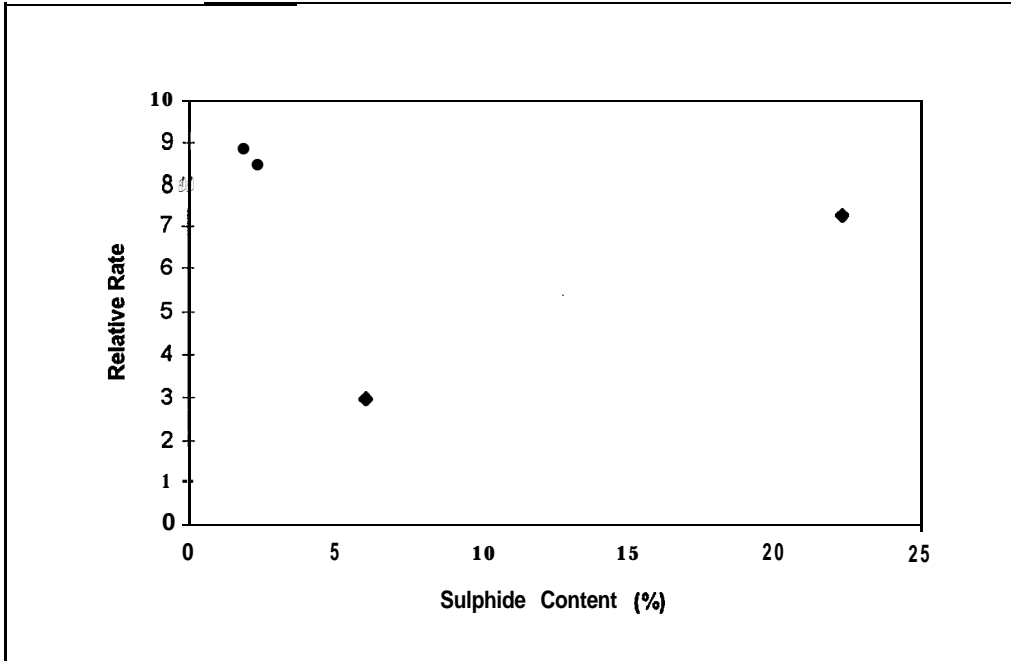


Figure 4.21 Relative rate of oxygen consumption after inoculation - Whistle waste rock, 30°C, 8 mm size fraction

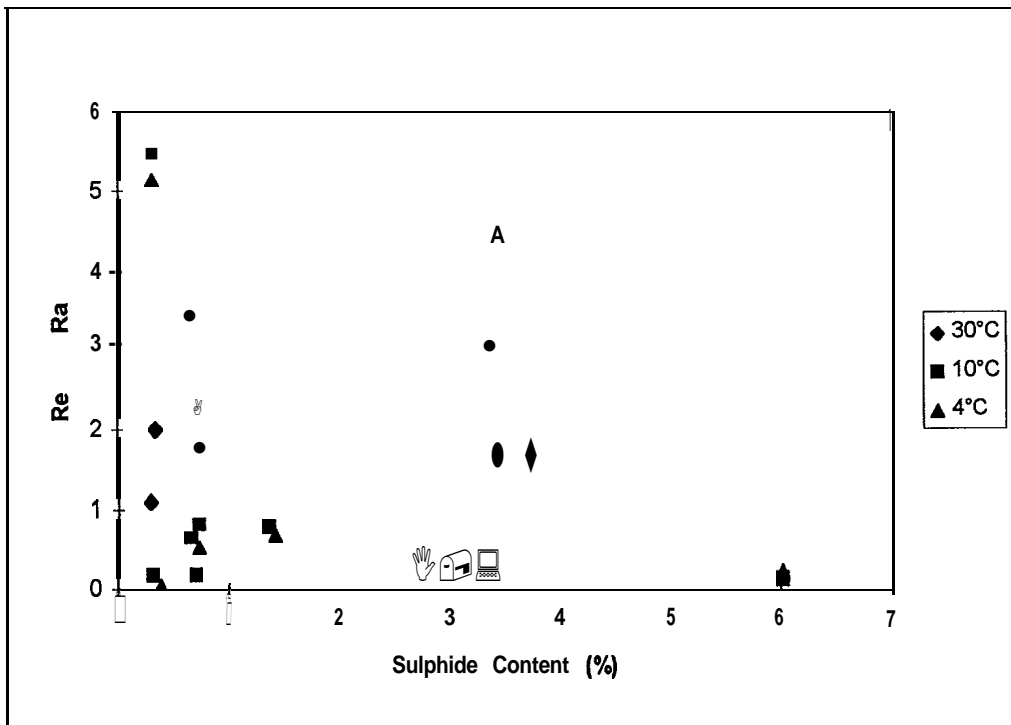


Figure 4.22 Relative rate of oxygen consumption after inoculation - Voisey's Bay COMPs, all size fractions

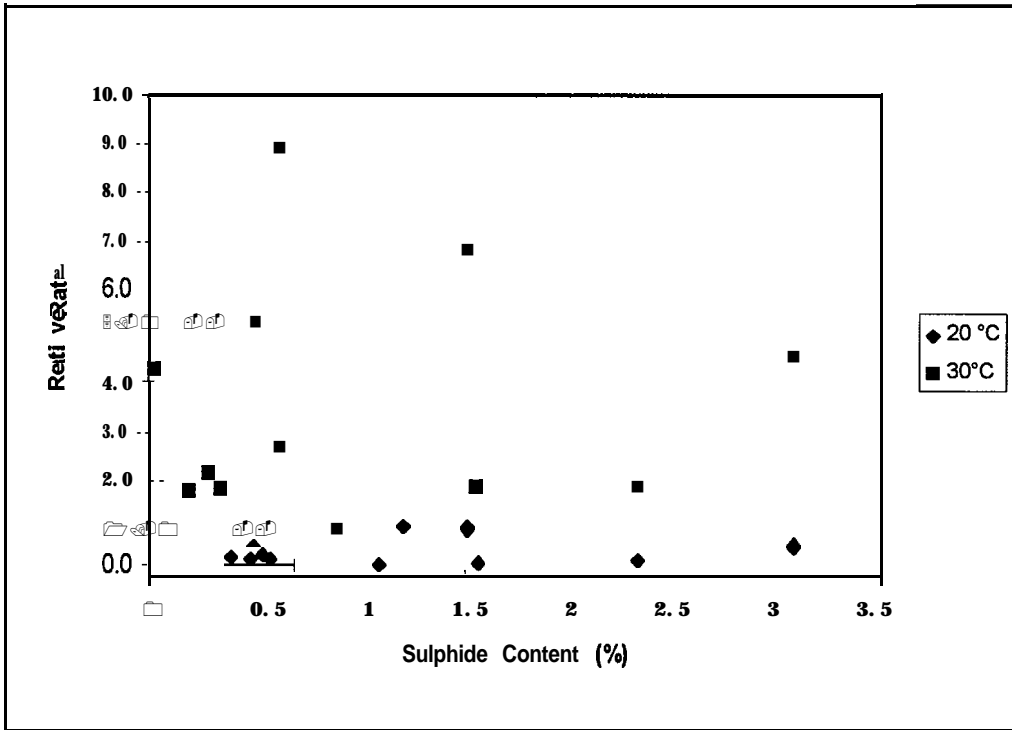


Figure 4.23 Relative rate of oxygen consumption after inoculation - ED and WE composites, 8 mm size fraction

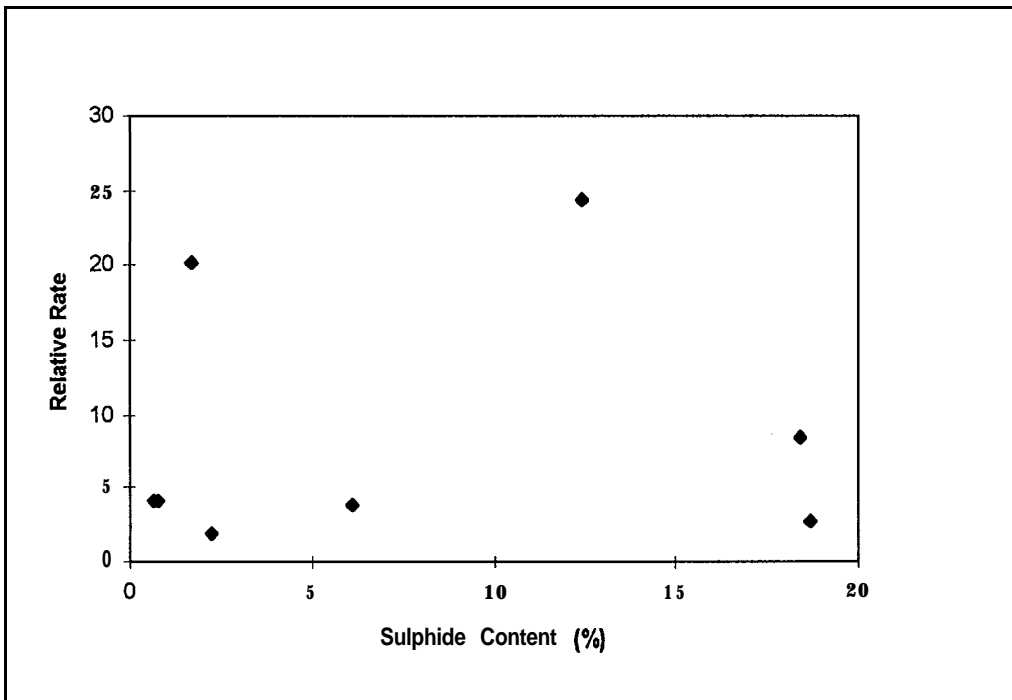


Figure 4.24 Relative rate of oxygen consumption after inoculation - 6 rock types, 8 mm and 3 mm size fractions

## **4.5 Measured Sulphate Release Rates**

### **4.5.1 Initial Tests on Whistle Mine Samples**

Figure 4.25 shows the measured oxygen consumption rate plotted against the measured sulphate release rate on a log-log scale. The sulphate release rate is a mass loading that was calculated from the concentration of sulphate collected in rinse water at the end of the test. The oxygen consumption rate was converted to an equivalent basis of  $\text{mg SO}_4 \cdot \text{kg}^{-1} \cdot \text{wk}^{-1}$  for comparison. The stoichiometry of pyrrhotite oxidation (from Equation 2.3b; 2.25 moles of  $\text{O}_2$  per mole of  $\text{SO}_4$ ) was used for the conversion. Also plotted on this graph is a line showing the 1:1 correspondence of oxygen consumption to sulphate release rate.

### **4.5.2 Voisey's Bay Tests**

Comparable results were obtained from the Voisey's Bay COMP, ED, WE and Ovoid composites, as depicted in Figures 4.26 and 4.27. It should be noted that the data have been plotted on a logarithmic scale due to the wide range of rates encountered and that a line with a slope of 1 has been added for reference.

Concurrent humidity cell tests were performed on sub-samples of the ED and WE composite materials. The crushed rock used in the humidity cells had an average particle size of 16 mm and the cells were operated at room temperature (ie. 17-20%). The humidity cell rates are based on average sulphate release rates over a 20 week period. The rates of oxygen consumption of 8 mm size, inoculated samples measured at 20°C were plotted against the measured sulphate loading rates from the humidity cells, as shown in Figure 4.28. Linear regression was performed and the equation that best represents the data is also given in Figure 4.28. A regression coefficient of 0.76 indicates a good correlation between the rate of oxygen consumption and sulphate release rate from the humidity cell tests.

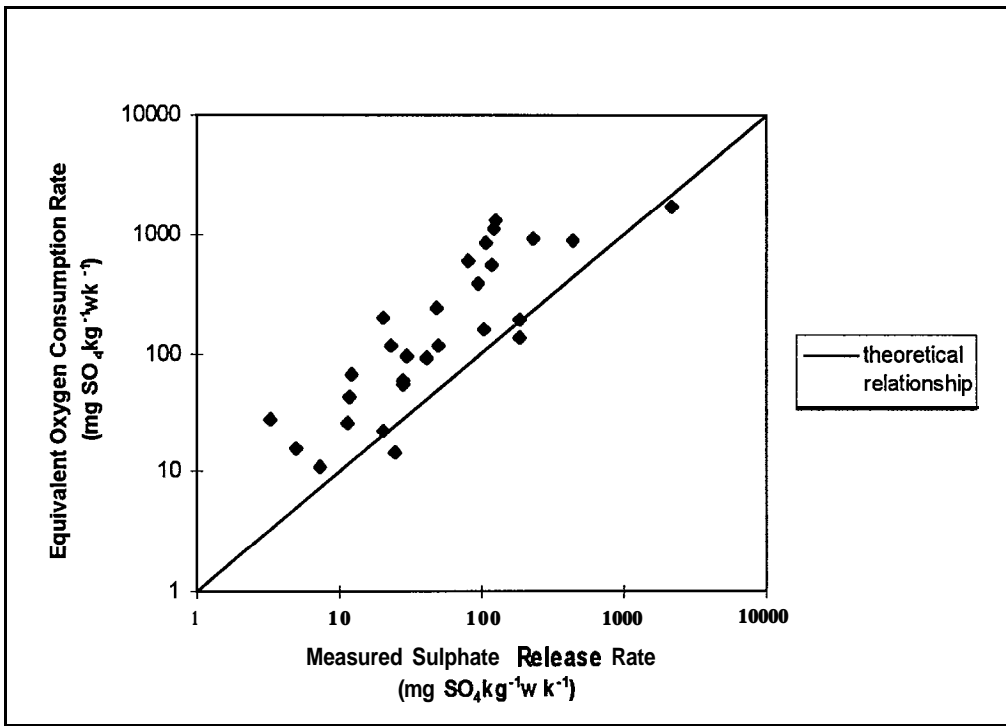


Figure 4.25 Oxygen consumption rate vs. sulphate release rate - initial Whistle tests

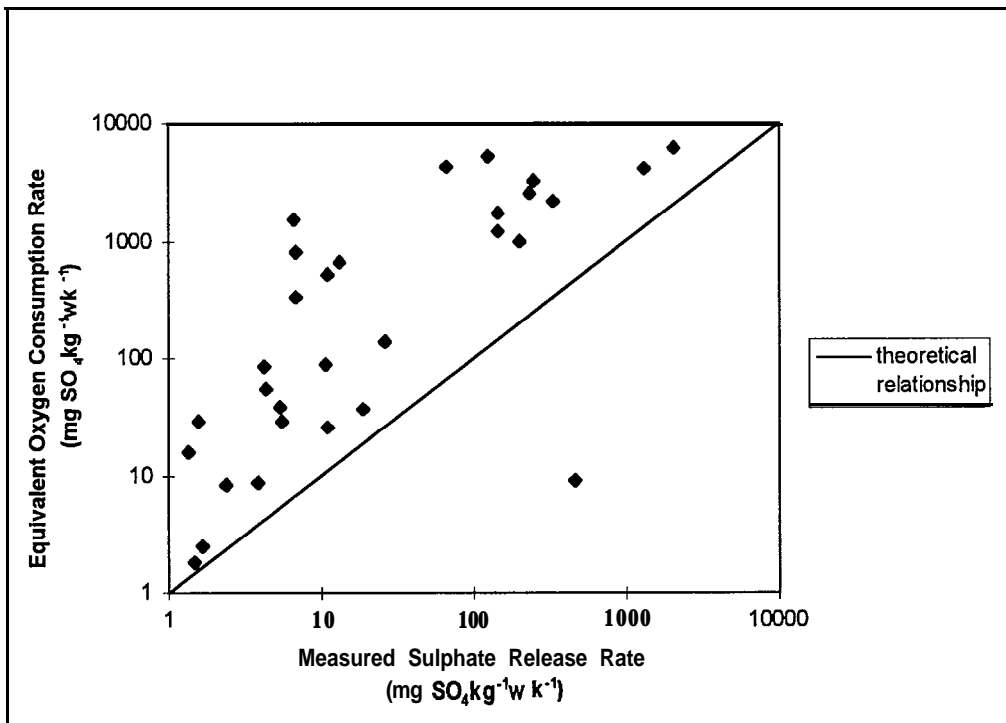


Figure 4.26 Oxygen consumption rate vs. sulphate release rate - Voisey's Bay COMPs

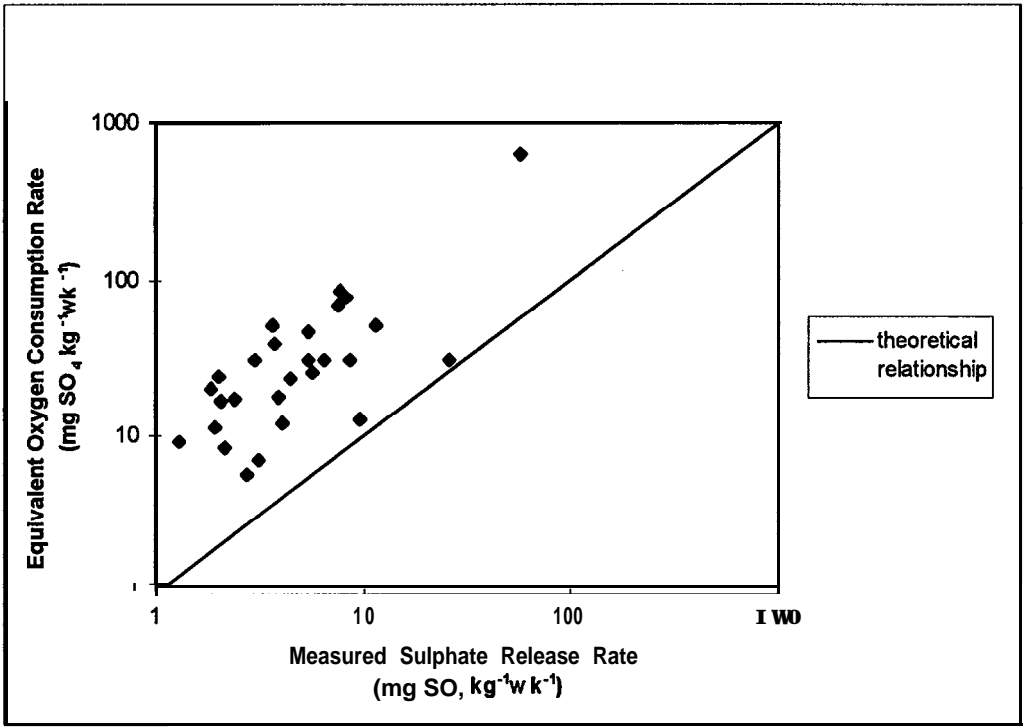


Figure 4.27 Oxygen consumption rate vs. sulphate release rate - Voisey's Bay ED, WE and Ovoid samples

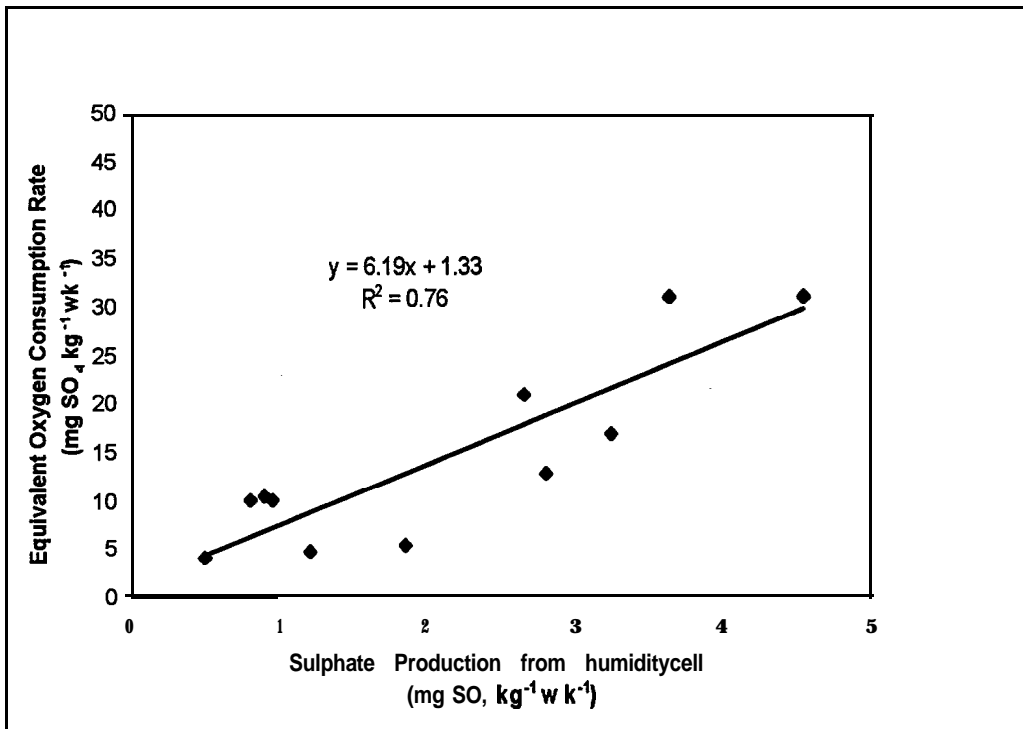


Figure 4.28 Oxygen consumption rate vs. sulphate release rate from humidity cells - ED and WE composites @ 20°C

### 4.5.3 Tests on Additional Rock Samples

Figure 4.29 depicts the oxygen consumption rate vs. sulphate release rate for the six rock types under a variety of experimental conditions plotted on a log-log scale. The plot includes the results of tests conducted at 10, 20 and 30°C without inoculation and at 20°C after inoculation. It should be noted that the results from samples containing pyrite were converted to an equivalent rate of sulphate production using the stoichiometry of pyrite oxidation, i.e. 3.5 mole of  $O_2$  per 2 moles of  $SO_4$ .

Figures 4.30 and 4.31 show the same data in greater detail on linear scales for samples containing pyrrhotite and pyrite, respectively. The data were separated to accentuate the apparent differences between samples containing pyrite and those containing pyrrhotite. Linear regression analysis was performed on the two data sets and the line of best fit was plotted on each graph.

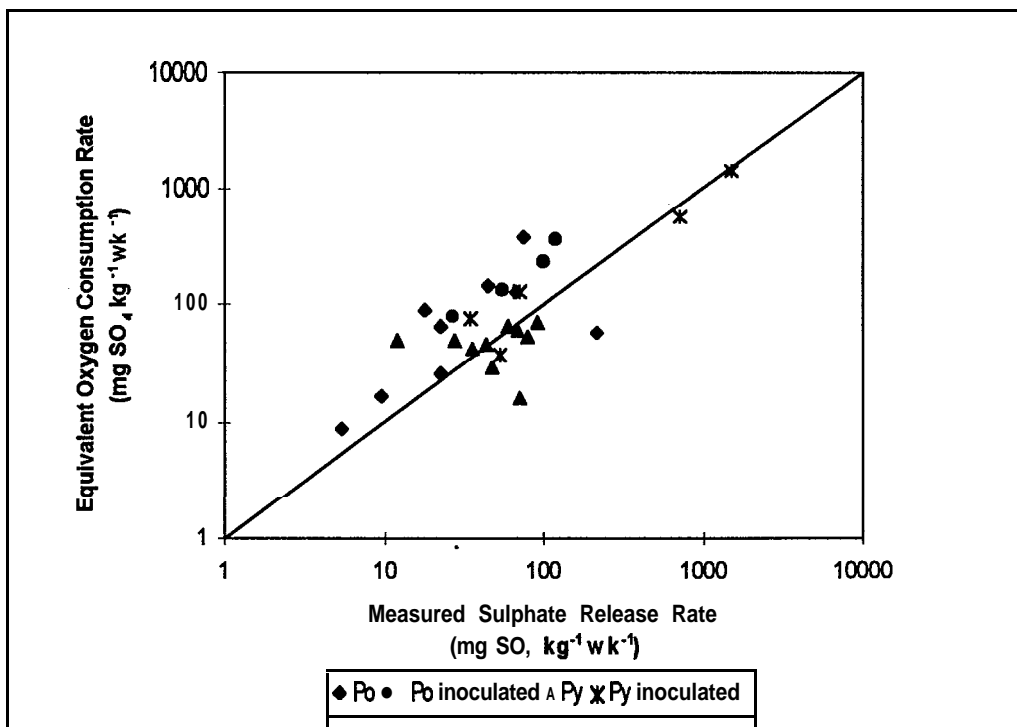


Figure 4.29 Oxygen consumption rate vs. sulphate release rate - 6 rock types

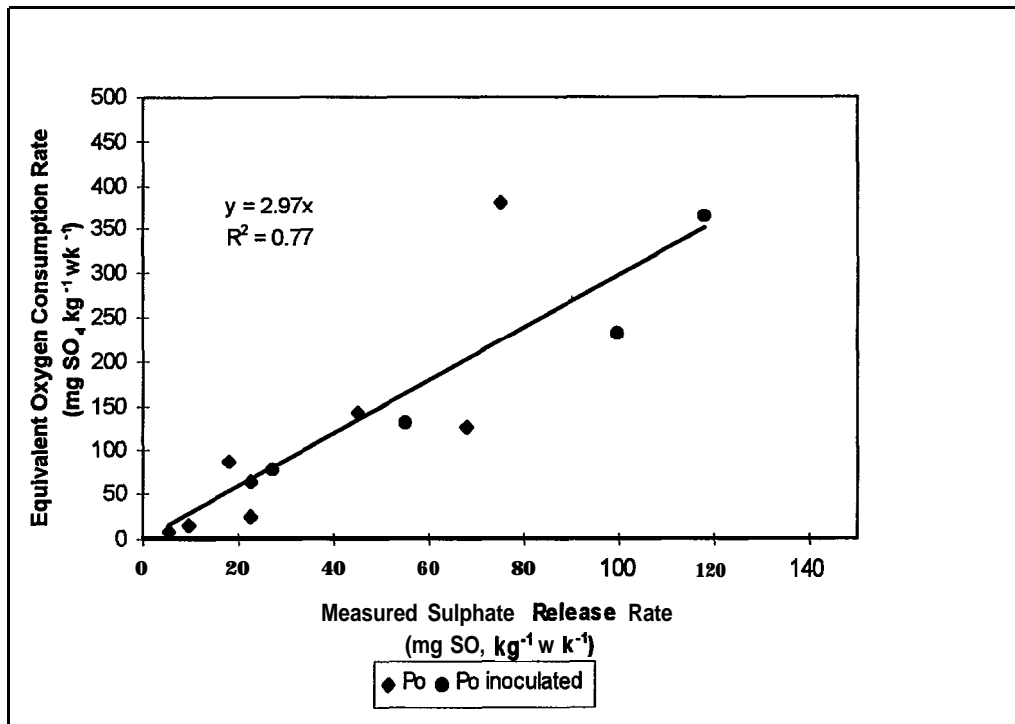


Figure 4.30 Oxygen consumption rate vs. sulphate release rate - pyrrhotite samples only

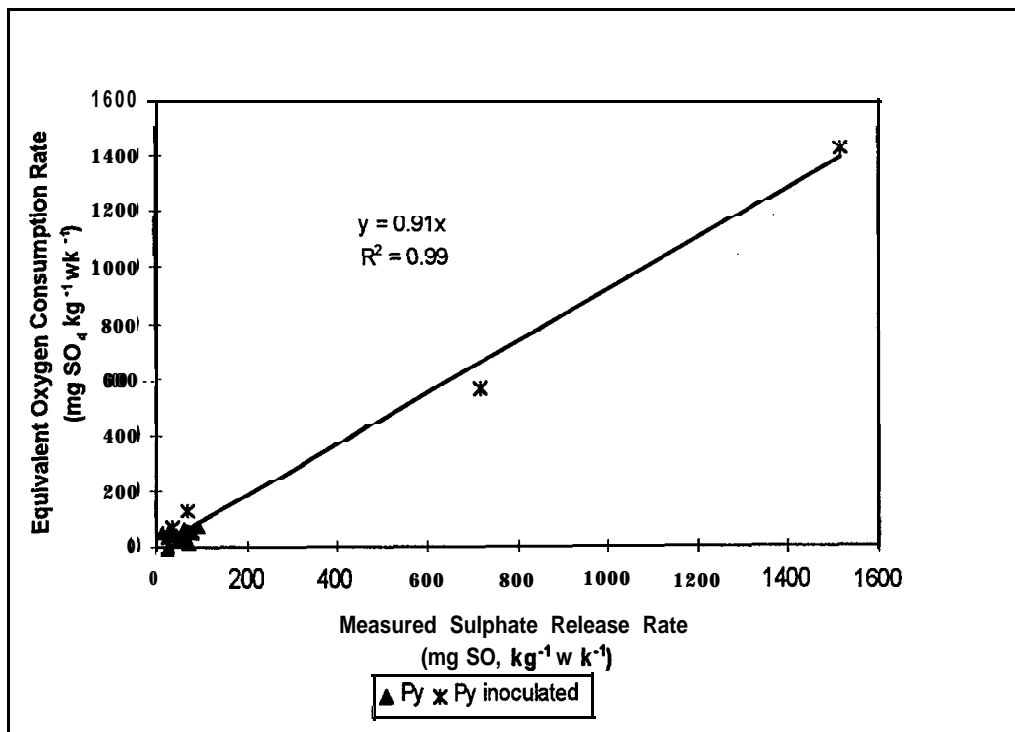


Figure 4.31 Oxygen consumption rate vs. sulphate release rate - pyrite samples only

## 5. Discussion

The observed effects generally followed expected trends; the oxygen consumption rate increased with decreasing particle size, increasing temperature, higher sulphur content and after inoculation with *T. ferrooxidans*. A multivariable linear regression model was constructed for the 16 Voisey's Bay composites and the utility of this model can be demonstrated. An attempt was made to use sulphate as a secondary indicator of the oxidation reaction. An overview of the sources of error inherent in the measurement technique is required in order to put the results in perspective.

### 5.1 Error Analysis

The rate of oxygen consumption was calculated from the measured decrease in oxygen partial pressure (expressed as  $V \cdot s^{-1}$ ), the full-scale output from the sensor in contact with atmospheric oxygen and the volume of air, the mass of rock and the temperature in the reactor. An example calculation is shown in Section 3.5.2. The random measurement error associated with each parameter is listed in Table 5.1. The precision of the slope of sensor output vs. time was estimated from the 95% confidence interval of the linear regression estimate. The 95% confidence limits were usually within 10% of the linear regression estimate of the slope. For example, linear regression analysis of a typical test gave a slope of  $1.0 \times 10^{-8} V \cdot s^{-1}$  with a 95% confidence interval of  $0.9 \times 10^{-8}$  to  $1.1 \times 10^{-8} V \cdot s^{-1}$ . It should be noted, however, that the error in this parameter increases as the magnitude of the slope decreases and could become relatively large near the detection limit. Measurement errors associated with the full-scale output from the sensor and the volume of air in the reactor were estimated from empirical observations of the reproducibility of these values. The mass of rock and temperature measurements can be measured very precisely and the error in these values was due mainly to instrument error.

Table 5.1 Estimated random error of measurements

Measurement	Error
slope of V vs. time ( $V \cdot s^{-1}$ )	$\pm 10\%$
full-scale output of sensor (V)	$\pm 5\%$
volume of air (mL)	$\pm 2\%$
mass of rock (kg)	$\pm 0.05\%$
temperature (K)	$\pm 0.5\%$

Based on these values, the inherent random error in the rate of oxygen consumption is approximately  $\pm 20\%$ .

The largest single source of systematic error in the calculation is introduced by the sensor. The electrochemical nature of the sensor leads to consumption of oxygen at a measurable rate over the course of the experiment. It has been assumed that the oxygen consumption rate of the sensor was constant over time and therefore could be accounted for in the rate calculation. However, this limits the lower limit of oxygen consumption rates that can be detected with any degree of accuracy. Unfortunately, this was not realized until late in the experimental programme and resulted in the rejection of a large number of experimental results. The detection limit can be lowered by increasing the volume of air in the reactor while maintaining the gas volume to rock mass ratio. This would involve using a larger reactor and filling it with a proportional amount of waste rock. In this manner the amount of oxygen consumed by the sensor becomes less significant in comparison to the amount of oxygen consumed by the waste rock.

The reproducibility of the measurement was quantified using the 8 mm size material from Faro. Approximately 1.6 kg of material was split into two sub-samples and each split was tested in parallel experiments. The results showed that the mean rates of each population (i.e. each sub-sample) were not statistically different at the

95% level. All 8 rate measurements were therefore pooled to give an average oxygen consumption rate of  $4.1 \times 10^{-9} \text{ mol O}_2 \cdot \text{kg}^{-1} \cdot \text{s}^{-1}$  with a standard deviation of  $1.1 \times 10^{-9} \text{ mol O}_2 \cdot \text{kg}^{-1} \cdot \text{s}^{-1}$  or 27% of the mean.

The results of early tests using a sample of 22 mm size particles composed of Whistle massive sulphide material gave slightly different results. The rates calculated from four sequential tests using a single sample indicate that the rate decreased over a period of 7 days from a high value of  $7.3 \times 10^{-9} \text{ mol O}_2 \cdot \text{kg}^{-1} \cdot \text{s}^{-1}$  to a low of  $2.3 \times 10^{-9} \text{ mol O}_2 \cdot \text{kg}^{-1} \cdot \text{s}^{-1}$ . The average rate was  $4.6 \times 10^{-9} \text{ mol O}_2 \cdot \text{kg}^{-1} \cdot \text{s}^{-1}$  with a standard deviation of  $2.2 \times 10^{-9} \text{ mol O}_2 \cdot \text{kg}^{-1} \cdot \text{s}^{-1}$  or 48% of the mean rate. In this case discolouration of the surface of the sulphide mineral was evident. This staining was very resilient to removal even after treatment with a 10% HCl solution for 15 minutes. It is possible that the accumulation of oxidation products on the sulphide mineral surface was presenting a significant diffusion barrier to the transport of oxygen to the reactive surface as shown below.

The material causing the staining was not analysed but is suspected to be composed of ferric oxides and hydroxides (such as goethite or ferrihydrite) and possibly jarosite, depending on the availability of sulphate and local pH conditions. Coating of the reactive surface by these secondary minerals can produce a diffusive barrier to oxygen on the surface of the sulphide mineral and cause an apparent decrease in the oxidation rate as noted by Nicholson *et al.* (1988b). The rapid formation of oxidation product layers was particularly notable in samples containing pyrrhotite, those which contained pyrite as the dominant sulphide mineral did not exhibit noticeable staining.

Nicholson *et al.* (1990) estimated the diffusion coefficient of oxygen through an oxide coating on pyrite crystals which yielded a value of  $3 \times 10^{-16} \text{ m}^2 \cdot \text{s}^{-1}$ . This value can be used to estimate the flux of oxygen across the surface of the rock particles to the reactive surface of sulphide minerals if the concentration gradient across the

oxide layer can be calculated. This analysis assumes that oxygen is transported from the bulk gas phase through the oxide layer by diffusion according to Fick's law (see Equation 2.7). If the system is limited by the diffusion of oxygen through the oxide layer then the oxygen concentration at the reactive surface will be zero and the gradient across the oxide layer will be equal to the concentration of oxygen in the bulk gas phase (at 0.21 atm O<sub>2</sub>, [O<sub>2</sub>]=8.6 mol O<sub>2</sub>·m<sup>-3</sup> at 25°C). The thickness of the oxide coating on the surface of the particle can be estimated by assuming that iron is released during the oxidation of pyrrhotite and precipitates on the surface of the particle as a secondary mineral such as Fe(OH)<sub>3</sub>. The stoichiometry of Equations 2.2 and 2.3 dictates that 2.25 mole of oxygen is consumed for every mole of iron that precipitates as Fe(OH)<sub>3</sub>. From the data presented above for Whistle massive sulphide material, oxygen was consumed at a maximum rate of 7.3~10<sup>9</sup> mol O<sub>2</sub>·kg<sup>-1</sup>·s<sup>-1</sup>, this translates into an iron oxide production rate of 3.2×10<sup>-9</sup> mol Fe(OH)<sub>3</sub>·kg<sup>-1</sup>·s<sup>-1</sup>. If the oxide coats the particles uniformly and the particles are assumed to be spheres, a 0.54 μm layer could accumulate in a period of 7 days. The flux of oxygen across this layer would be 4.7×10<sup>-9</sup> mol O<sub>2</sub>·m<sup>-2</sup>·s<sup>-1</sup>, or 1.1 ×10<sup>-9</sup> mol O<sub>2</sub>·kg<sup>-1</sup>·s<sup>-1</sup> for 22 mm diameter particles having a solid density of 3700 kg·m<sup>-3</sup>. Comparing this value to the measured rate of 2. 3x10<sup>9</sup> mol O<sub>2</sub>·kg<sup>-1</sup>·s<sup>-1</sup>, the diffusive flux of oxygen in this "worst case" scenario is lower than the oxygen consumption rate measured after 7 days of oxidation. Although the analysis presented above is simplistic, and a number of assumptions were made, the results indicate that the accumulation of oxide coatings on the surface of sulphide minerals could explain the decrease in measured oxygen consumption rate over the 7 day test period.

## 5.2 Multivariable Linear Regression

Data from the Voisey's Bay composites were compiled and used to fit a multivariable regression model with the following form:

$$R = a_1 d^{a_2} S^{a_3} e^{\frac{a_4}{T}} \quad \text{Equation 5.1}$$

where R is the oxygen consumption rate in mol O<sub>2</sub>·kg<sup>-1</sup>·s<sup>-1</sup>, d is the particle size in mm, S is the sulphide content in % and T is the temperature in K. The experimental

data used to fit the model are found in Tables A.3 to A.6 in Appendix A. More than 50 independent measurements were used with averages calculated for replicate measurements. Linear regression analysis was performed by taking the natural logarithm of Equation 5.1 to give;

$$\ln(R) = a_1 + a_2 \ln(d) + a_3 \ln(S) + \frac{a_4}{T} \quad \text{Equation 5.2}$$

Linear regression of the  $\ln(R)$  vs.  $\ln(d)$ ,  $\ln(S)$  and  $1/T$  gave the least squares estimates of the parameters in Equation 5.2. The  $r^2$  value for this regression was 0.74 which is good considering the large population size and the number of parameters in the regression model. Taking the inverse natural logarithm of Equation 5.2 will yield the values of  $a_i$  in Equation 5.1. These values are summarized in Table 5.2 along with the upper and lower bounds of the 95% confidence interval for the estimates.

Table 5.2 Estimates of parameters in Equation 5.1

Parameter	Upper 95%	Lower 95%	Least Squares Estimate
<b>a<sub>1</sub></b>	42.44	<b>4.6×10<sup>-6</sup></b>	0.0135
a <sub>2</sub>	-1.11	-1.50	-1.31
<b>a<sub>3</sub></b>	0.55	0.07	0.31
<b>a<sub>4</sub></b>	-1654.6	-6309.3	-3981.9

Substituting the values in Table 5.2 into Equation 5.1 and rearranging the exponential term by multiplying  $a_4$  by the gas constant ( $R=8.314 \text{ J}\cdot\text{mol}^{-1}\cdot\text{K}^{-1}$ ) gives;

$$R = 0.0135d^{-1.31}S^{0.31}e^{\frac{-33106}{RT}} \quad \text{Equation 5.3}$$

The temperature term in the equation above has been reorganized such that it gives the familiar Arrhenius dependence on temperature. A summary of the SYSTAT<sup>®</sup> output file for this regression is given in Appendix F.

A method of sequential parameter selection was used to determine which parameters were significant. This method indicated that the particle size had the

most significant effect on the rate of oxygen consumption for this data set. Total sulphur content and temperature effects were minor when compared individually to the particle size effects. The effects of sulphur content and temperature are significant in the model presented above but only when they are considered in the context of particle size. This has implications for modelling sulphide oxidation in waste rock piles, collection of field data and laboratory measurement of sulphide oxidation rates.

A similar linear regression analysis was performed on oxygen consumption rates of inoculated samples from the Voisey’s Bay COMP samples. A total of 37 independent rate measurements were used to fit the parameters. The least squares estimates of the parameters in Equation 5.1 and the 95% confidence intervals for these estimates are given in Table 5.3. The regression coefficient for the inoculated rates was 0.75. Substituting these values into the regression equation yields the relationship given in Equation 5.4. A summary of the SYSTAT® output file for this regression can be found in Appendix F.

Table 5.3 Estimates of parameters in Equation 5.1 for inoculated rates

Parameter	Upper 95%	Lower 95%	Least Squares Estimate
<b>a<sub>1</sub></b>	2199.5	7.5×10 <sup>-3</sup>	4.08
<b>a<sub>2</sub></b>	-0.36	-0.78	-0.57
<b>a<sub>3</sub></b>	0.67	0.18	0.42
<b>a<sub>4</sub></b>	-4021 .0	-7631.0	-5826.0

$$R = 4.08d^{-0.57}S^{0.42}e^{\frac{-48437}{RT}} \quad \text{Equation 5.4}$$

The sequential parameter estimation routine was also used in this case and showed the same general trends, however the particle size did not have the same overwhelming effect on the oxygen consumption rate for inoculated samples. In the case of inoculated samples, the particle size, sulphur content and temperature had

equally significant effects on the rate of oxygen consumption. The method indicated that the three parameter model described the data significantly better than a one or two parameter model.

The regression models given above can be used to approximate an integrated oxygen consumption rate for an entire rock pile if something is known about the particle size distribution of waste rock in the pile, the sulphur content of the waste rock and the ambient temperature conditions. This becomes particularly important when attempting to make predictions about the rate of pollution production from waste rock piles.

Modelling of the oxidation of sulphide-bearing waste rock may be the only way to predict the long-term production and release of oxidation products, such as acidity, sulphate and dissolved metal species in some piles. In order to accurately assess the future behaviour of a waste rock pile, information about the intrinsic oxidation rate of the waste must be known. From the information presented above, the intrinsic oxidation rate was found to be strongly influenced by the particle size and, to a lesser extent, the total sulphur content and temperature. These factors have to be taken into account in a comprehensive model of waste rock oxidation. This is intricately linked to the collection of field and laboratory data because a predictive model cannot give reliable results without reasonable input data. Time, money and effort are best spent characterizing the particle size distribution of waste rock in piles and investigating waste rock fractions smaller than 2 cm, given the dependence of the oxygen consumption rate on particle size.

### **5.2.1 Comparison to Field Data**

Comprehensive field monitoring of the waste rock pile at the Whistle mine site has been carried out by Golder Associates (1996). Using the particle size distribution given by Golder Associates (1996) a bulk oxygen consumption rate was calculated using the rate-to-size relationship given in Figure 4.3 for the Whistle medium sulphur norite rock. The medium norite material was chosen to be representative of

the waste rock in the dump according to the average sulphur content of the pile given in Golder Associates (1996). The bulk oxygen consumption rate based on the results of laboratory measurements was  $4.5 \times 10^{-11} \text{ mol O}_2 \cdot \text{kg}^{-1} \cdot \text{s}^{-1}$  which is equivalent to  $1.3 \text{ mg SO}_4 \cdot \text{kg}^{-1} \cdot \text{wk}^{-1}$ . Sulphate loading from the pile was determined by measuring the flow of **leachate** in the collection drains and analyzing water samples for sulphate. The measured sulphate loading from the pile was  $0.77\text{--}1.3 \text{ mg SO}_4 \cdot \text{kg}^{-1} \cdot \text{wk}^{-1}$  (Golder Associates, 1997). The measured rate of sulphate released from the waste rock pile correlates very well with the estimated rate of sulphate production based on oxygen consumption measurements for this material. This type of simple analysis worked for the waste rock pile at Whistle but may not be applicable to all sites. In the case of the Whistle waste rock dump the diffusion of oxygen was not limiting the oxidation reaction. Field measurement of oxygen profiles within the rock pile indicated that the pore gas contained atmospheric levels of oxygen throughout the pile (Golder Associates, 1997). Numerous cases have been documented where the oxygen concentration measured inside waste rock dumps was significantly lower than atmospheric (Ritchie, 1994; Bennett et al., 1994; Gélinas et al., 1991). In a case where the transport of oxygen becomes limiting, the oxygen consumption rates could be used as input values for intrinsic oxidation rates in a more complicated modelling exercise that would be required to account for the diffusive and, perhaps, **advective** transport of oxygen in such a waste rock pile.

### **5.3 Particle Size**

Analysis of the plots in Chapter 4.1 clearly indicate that the rate of oxygen consumption decreases with increasing particle diameter. If the particles are assumed to be regular geometric solids with a uniform reactive surface area, the rate of oxygen consumption would be expected to vary inversely with the particle diameter, ie. the rate should be inversely proportional to  $d$ . The results are consistent with the model which states the oxygen consumption rate is proportional to  $1/d^n$ . The values of  $n$  in all of the cases examined are not statistically different from 1 at the 95% confidence level.

The plots of oxygen consumption rate vs. particle size for Whistle high S, medium S and massive sulphide shown in Figures 4.1, 4.2 and 4.3 show a very distinct increase in the oxygen consumption rate as the particle size decreased. The value of  $n$  varies from 0.97 to 1.78, equating to an increase in the rate by a factor of 3 to 8 with a change in particle size from 22 to 7 mm. The data are strongly biased by the results of the 17L tests and these results were considered to have a lower accuracy. The raw data used to calculate the rate of oxygen consumption had a large degree of scatter as depicted in Figures E.1 to E.4 in Appendix E. Consequently, the 17L tests yielded approximately the same rates for all of the Whistle samples. The main reason for the large random error is most likely due to the sensitivity of the sensor to changes in temperature. The temperature changed by as much as 4 to 5°C over the course of the measurement period. Insufficient temperature data were collected to account for this temperature variation to correct the oxygen consumption rate. The results of early tests with Whistle waste rock, including the 17L tests, suggested that experimental investigations should be focused on particles smaller than 20 mm since these particles tend to consume oxygen at much higher rates.

Testing of the waste rock analog samples from Voisey's Bay was conducted to further elucidate the relationship between oxygen consumption rate and particle size using the COMP samples. Graphs showing the oxygen consumption rate as a function of particle size under inoculated and uninoculated conditions are located in Appendix B. Table 4.1 summarizes the values of  $n$  calculated under various experimental conditions. The maximum absolute value of  $n$  for uninoculated samples was found to be 2.2, the minimum was 0.4. On average, the value of  $n$  was 1.32 for uninoculated rock samples. Based on these results, the rate of oxygen consumption would be expected to increase by a factor of 3.6 for a decrease in particle size from 8 to 3 mm. The linear regression model presented above for this data also indicated that particle size was a predominant factor in determining the oxygen consumption rate.

The results of oxygen consumption tests using three size fractions of rock samples from the Eastern Deeps (ED) and Western Extension (WE) are depicted in Figure 4.4. Linear regression analysis was not performed on these data, however the graph shows qualitatively that the rate of oxygen consumption decreases by approximately an order of magnitude over the range of particle size from 1 to 16 mm.

Similar qualitative trends can be seen in Figures 4.5 to 4.10 for the six rock types. The rate, in general, increases with particle size under similar temperature conditions. The only exception to this trend is the 15 mm size sample of waste rock from Mine Doyon. This sample appears to exhibit higher oxygen consumption rates than the two smaller size fractions at 10 and 30°C.

The oxygen consumption rate vs. size data discussed above yield values of  $n$  in the range of 0.06 to 2.2, this could be due to a number of reasons. First, each rate calculation has some degree of error associated with it as discussed in Chapter 5.1. A second factor which may contribute to this is the variation of sulphide content from one size fraction to another. This is clearly evident by examination of the total sulphur analysis of the Voisey's Bay COMP samples in Appendix G. In some cases the sulphide content differs by as much as a factor of 2 or more for different size fractions of a particular composite. No attempt was made to account for the difference in sulphide content between size fractions during the calculation of  $n$ . As discussed below, the sulphide content can have an effect on the oxygen consumption rate.

The difference in sulphide content among size fractions produced from a composite sample is related to the distribution of sulphide in the host rock as a whole. In order for the theoretical dependence of rate on particle size to hold, the spatial distribution of sulphide in the waste rock must be assumed to be homogeneous. The assumption of homogeneity may not be applicable in the range of particle sizes

under investigation in this work, especially as it relates to the Whistle waste rock and Voisey's Bay samples. In these cases the sulphide mineral phase is distributed in large blebs approximately 1 - 2 cm in diameter and may not be homogeneously distributed over the range of particle sizes examined. In contrast, waste rock samples from Faro and Mine Doyon are relatively homogeneous in terms of sulphide distribution with small grains (<0.5 mm in diameter) of pyrite having an apparent even distribution throughout the host rock matrix in rock particles larger than 3 mm. Despite these complications, the influence of particle size on the rate of oxygen consumption cannot be denied and should be the focus of future investigation and consideration.

#### **5.4 Temperature**

The activation energies given in Tables 4.2.1, 4.2.2 and 4.2.3 are consistent with the theory that the reaction rate increases with increasing temperature. Closer inspection of the Arrhenius plots in Appendix C suggests that in most cases however, the apparent rate of oxygen consumption at 10°C was higher than the rate at 20°C. The only exceptions to this were the results from the Voisey's Bay COMP tests with 1 and 0.3 mm size materials, the 8 mm size fraction of Mine Doyon rock and the 3 and 8 mm size fractions of Pamour waste rock. This effect may be due to some property of the sensor that affects the response at 10°C. Qualitative observations of the sensors' behaviour at lower temperatures (i.e. less than 20°C) indicate that the sensors are less sensitive to temperature perturbations in this range. This implies some fundamental change in the functionality of the sensor at lower temperatures. The oxygen sensor response to oxygen concentration was studied by Williams (1993) and was found to be linear with partial pressure of oxygen at ambient temperature conditions around 20°C. For the purposes of this study, a one point calibration of the oxygen sensor was assumed to be sufficient and this assumption was verified at room temperature, i.e. the sensor output decreases monotonically to zero with oxygen concentration. This relationship was not examined over the range of temperature conditions experienced during this experimental programme. It is possible that the sensor response is not linear or

requires a multi-point calibration at lower temperatures. This could provide an explanation for the unexpected behaviour of the oxygen sensors at 10°C, although this hypothesis has not been investigated. Given the nature of this observed anomaly, the Arrhenius relationship between oxygen consumption rate and temperature may not be the most appropriate method to calculate activation energy.

The calculated activation energies range from 9 to 108 kJ·mol<sup>-1</sup>, but in general the values were greater than 20 kJ·mol<sup>-1</sup> which suggests that the reaction system was not controlled by diffusion. Lasaga (1981) stated that diffusion controlled reactions should exhibit an activation energy of about 20 kJ·mol<sup>-1</sup>. The majority of rock types that have activation energies of approximately 20 kJ·mol<sup>-1</sup> are those with relatively large sulphide contents and small particle sizes. This is consistent with the theory that the reaction rate is a function of the reactive surface area which will depend on both the sulphide content and particle size. Diffusion of the reactants to the reaction site becomes increasingly important as the surficial reaction rate increases. This is compounded by the possibility that the 1 and 0.3 mm samples may have been inadvertently saturated with water at the beginning of the test. In order to supply the necessary water for sulphide oxidation, water was added to the granulated rock sample. In some cases enough water was added to theoretically fill all of the void spaces and completely saturate the samples that had a particle size similar to coarse sand. Given this condition, it is conceivable that the diffusion of oxygen to the sulphide mineral surface could have become the rate limiting step for 0.3 and 1 mm size particles and this would explain the apparent diffusion-based activation energy values for those samples.

### **5.5 Sulphide Content**

In general, the rate of oxygen consumption increased with the total sulphur content of a given rock type. However, the relationship was not well defined in some instances and may have been influenced by several factors, including the distribution of the sulphide mineral within the matrix and possible galvanic interactions between sulphide minerals. Inoculation with *T. ferrooxidans* seems to

give rise to an increase in the dependence of the oxygen consumption rate on the total sulphur content implying direct oxidation of sulphide-sulphur by the bacteria.

Figures 4.11 and 4.14 show the effect of total sulphur content on the oxygen consumption rate of waste rock samples from the Whistle Mine site. These graphs show a coherent increasing trend in oxygen consumption rate as the total sulphur content of the sample increases from approximately 2 to 22 %S. In both cases, the oxygen consumption rate increases by a factor of roughly 10 for a 10-fold increase in sulphur content. Figures 4.12, 4.13 and 4.15 do not appear to follow the same trend for similar materials under different experimental conditions. In these three cases, the rates for the high sulphur **norite** (approximately 5% S) does not appear to fit the anticipated trend. The rates of oxygen consumption of 7 mm size particles of high sulphur **norite** at 10°C and 30°C, both before and after inoculation, were much higher than expected given the linear increase in rate with total sulphur content observed previously in Figures 4.11 and 4.14. The reason for this behaviour is unknown at this time.

Similar trends in the rate of oxygen consumption were noticed for composite samples of the ED and WE rock from Voisey's Bay. This is depicted in Figure 4.16 for different temperature and inoculation conditions. Linear regression of the rates determined at 30°C for uninoculated samples gives a correlation coefficient ( $r^2$ ) of 0.19 indicating little or no correlation between oxygen consumption rate and sulphur content. Similar analysis of the rates measured at 20 and 30°C using inoculated samples yielded  $r^2$  values of 0.90 and 0.87, respectively. Comparison of the  $r^2$  values suggests that the relationship between oxygen consumption rate and total sulphur content was much stronger after inoculation with *T. ferrooxidans*

Oxygen consumption rate vs. total sulphur content for Voisey's Bay Ovoid samples are shown in Figure 4.17. The rate increases with the total sulphur content, however Figure 4.17 must be interpreted cautiously. Any linear regression would

be strongly biased by the rate of oxygen consumption of the sample containing 24 %S for both inoculated and uninoculated samples. Linear regression of the data, excluding the 24 %S sample, indicated that rate was not strongly dependent on the total sulphur content for both inoculated and uninoculated samples. The  $r^2$  values for the two populations were 0.11 and 0.64 for uninoculated and inoculated samples respectively which indicates that the inoculated samples show more dependence on total sulphur content than uninoculated ones.

The rate of oxygen consumption of the six rock types increased with the total sulphur content as shown in Figures 4.18 and 4.19 for 8 and 3 mm size rock fragments, respectively. Waste rock from Faro did not fit the expected trends. This is discussed in further detail below. The data from tests performed on 3 mm size particles support earlier findings that the oxygen consumption rate is much more dependent on the total sulphur content after inoculation with *T. ferrooxidans* and this can be seen in Figure 4.19. Linear regression of the results of these tests, excluding Faro waste rock, yields  $r^2$  values of 0.06 for uninoculated samples and 0.999 after inoculation.

The sulphur content of a given rock sample was found to be positively correlated to the rate of oxygen consumption, in most cases. Possible reasons for the lack of a strong trend include the heterogeneous distribution of the reactive sulphide mineral in the rock particles and possible galvanic interactions between adjacent sulphide minerals with different rest potentials.

One of the factors that might confound the relationship between oxygen consumption rate and sulphide content is the heterogeneous distribution of sulphide in the host rock. A fundamental assumption, if one were to expect a linear relationship between sulphide content and oxygen consumption rate, would be the homogeneous spatial distribution of the sulphide mineral within the unreactive matrix. Essentially this argument reduces to the assumption that the ratio of

reactive surface area to total surface area is proportional to the sulphide content. As mentioned previously, the homogeneous distribution of sulphide minerals may not hold for some of the rock types under investigation in the range of particle sizes considered.

Another factor which has been shown to influence the rate of oxidation of sulphide minerals is galvanic interactions between adjacent sulphide phases (Kwong, 1995b; Natarajan, 1990). When two sulphide minerals come into electrical contact in an oxidizing environment a galvanic couple is established. The mineral with the lowest rest potential will preferentially dissolve while the other will be cathodically protected. According to the galvanic series given by Natarajan (1990), the base-metal sulphides can be arranged as follows;

pyrite < chalcopyrite < pentlandite < galena < pyrrhotite < sphalerite

with pyrite being the most noble and sphalerite, the most active. Evidence of galvanic interaction was noticed during the oxidation of waste rock from Faro which contained about 1.5 wt% sphalerite and 1.5 wt% galena.

Water samples collected after oxygen consumption tests using 3 mm size waste rock from Faro showed elevated concentrations of lead and zinc with relatively little iron. Speciation calculations indicate that iron was not saturated with respect to ferric hydroxide and no **visible staining** or signs of oxidation product formation were noted on these samples. This is consistent with the galvanic series which suggests that pyrite is the most noble sulphide while galena and sphalerite are more reactive when coupled with pyrite. The concentration of iron, lead, zinc and sulphate in these water samples are summarized in Table 5.4. Also shown in this table is the molar ratio of metal to sulphate for each test which was calculated from the aqueous concentration data and corrected for the stoichiometry of pyrite oxidation. The ratio of metal to sulphate should be unity if oxidative dissolution of the sulphide minerals was congruent. From Table 5.4, the metal to sulphate ratios are fairly close to one

Table 5.4 Dissolved metals and sulphate in leachate from Faro waste rock

Experimental Conditions	Sulphate (mg·L <sup>-1</sup> )	Iron (mg·L <sup>-1</sup> )	Lead (mg·L <sup>-1</sup> )	Zinc (mg·L <sup>-1</sup> )	(0.5 mol Fe+mol Pb+mol Zn) mol SO <sub>4</sub>
10°C	13	0.11	71	7.7	3.41
20°C	20	n/d*	3.4	8.8	0.73
30°C	21	0.12	35	11	1.50
20°C inoculated	140	3.1	4.7	36	0.90**

\*n/d = below detection

\*\*includes copper which was found in significant amounts in this sample.

in most of the cases. The test conducted at 10°C is skewed by an unusually high concentration of lead, the reason for this is unknown. Copper was included in the calculation of the total metal to sulphate ratio for the inoculated sample. The ratios given above are roughly equal to one and would suggest that the majority of metal and sulphate present after the oxygen consumption test was the result of sphalerite and galena oxidation. Relatively little iron was released into solution during oxidation which agrees with the cathodic protection of pyrite at the expense of less noble sulphides such as sphalerite.

Galvanic dissolution theory may also explain why the rate of oxygen consumption by Faro waste rock is much lower than expected; Figure 5.1 shows the rate of oxygen consumption of Faro and Mine Doyon waste rock samples at three different temperatures for 3 mm size rock particles. Despite the fact that Faro waste rock contains almost three times more sulphide material, rock samples from Mine Doyon consume oxygen at roughly the same rate. This could be due to the galvanic interaction of sphalerite and galena in contact with pyrite in the Faro waste rock sample. According to Natarajan (1990) the rate of oxidation depends strongly on the current flowing between the galvanic couple and that cells containing sphalerite have low galvanic currents due to its poor conductivity. Natarajan (1990) also states that elemental sulphur tends to accumulate on the reactive surface during galvanic dissolution and that this will create a diffusive barrier which can slow the

rate of oxidation. These factors taken together could explain the observed slow rate of oxygen consumption exhibited by waste rock samples from Faro.

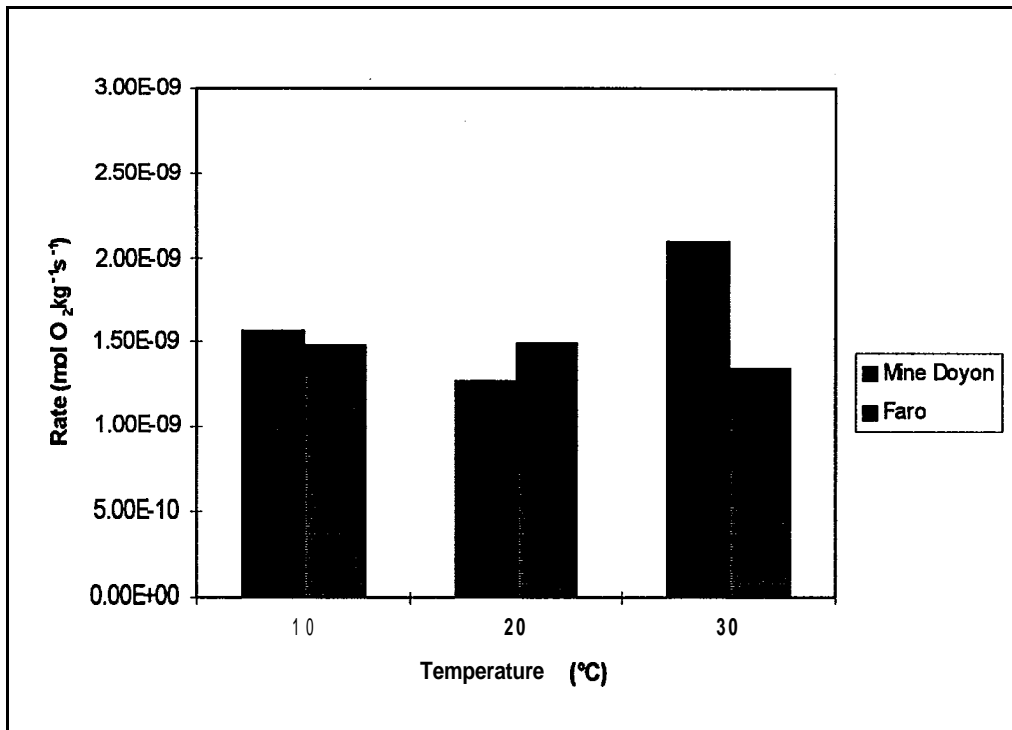


Figure 5.1 Comparison of rate for 3mm size rock from Mine Doyon and Faro

### 5.6 Inoculation with *Thiobacillus ferrooxidans*

A large number of tests were conducted on samples that had been inoculated with *T. ferrooxidans* with variable results. The bacterial cultures on the surface of Whistle massive sulphide material were observed by scanning electron microscopy. Figure 4.11 is a micrograph showing a bacterial colony growing on the sulphide mineral surface. The scale of the micrograph is given in the lower right corner of the picture and indicates that the cells are approximately 1  $\mu\text{m}$  long. The fibrous material present in the background is suspected to be an extracellular secretion which serves to anchor the bacteria to the mineral surface.

The bacteria appeared to grow well on Whistle Mine waste rock and this was indicated by an increase in the oxygen consumption rate by a factor of 3 to 9 as shown in Figure 4.21. Figures 4.22, 4.23 and 4.24 indicate that similar results were

obtained for Voisey's Bay ED and WE composites and the six rock types. Rates of oxygen consumption after inoculation with *T. ferrooxidans* at 20 and 30°C generally fell in a range between 2 to 10 times higher than the rate under similar experimental conditions before inoculation. Enhancement of the rate of oxygen consumption after bacterial inoculation was not noticeable at temperatures below 20°C. The rate of oxygen consumption after inoculation at 10 and 4°C was generally the same or lower than the uninoculated rate as seen in Figure 4.22. This can be explained by the decreased activity of the bacteria at lower temperatures. The bacterial culture of *T. ferrooxidans* used in these experiments has been growing and transferred serially at room temperature (approximately 20°C) for more than 2 years. Lower rates may have been due to the accumulation of oxidation products on the surface of the rock particles. Significant staining of the surface was noticeable after the inoculation step at all temperatures.

The range of relative rates observed for the different samples can be explained by the heterogeneous distribution of cells on the sulphide mineral surface. Observation of the surfaces of Whistle massive sulphide material by scanning electron microscopy indicated that the bacterial population was not evenly distributed over the rock surface. The bacteria tended to form dense colonies in selected areas and grew very sparsely in others. This could be due to the formation of microenvironments on the surface where the conditions were more favorable for growth. For example, a sulphide grain proximal to a calcite grain would not likely support growth owing to the high local pH conditions due to dissolution of the calcite but other sulphide surfaces with little buffer material nearby may support locally low pH conditions more conducive to *T. ferrooxidans* activity. Given the heterogeneous coverage of the sulphide surface by *T. ferrooxidans*, the catalytic effect of the bacteria on the oxygen consumption rate would not be expected to be the same for different rock samples and hence, the range of relative rates from 2 to 10.

Bacterial populations did not fare as well growing on the Voisey's Bay COMP and Ovoid samples. In many cases, the oxygen consumption rate actually decreased after inoculation. A difference was noted in the values of  $n$  for the Voisey's Bay COMP samples under inoculated and uninoculated conditions as seen in Table 4.1. The average value of  $n$  for uninoculated samples was -1.32 and the average  $n$  was -0.53 for samples inoculated with *T. ferrooxidans*. Statistical analysis of the averages of the two populations using a paired two sample Students t-test suggested that the two populations were statistically different. In general, the rate of oxygen consumption after inoculation with *T. ferrooxidans* is less sensitive to changes in the particle diameter, that is the value of  $n$  is less than 1. Upon closer inspection however, it is more likely that this observation is an artifact rather than a legitimate effect of bacterial inoculation. The reasons for this were likely two-fold.

First, inoculated rock samples with diameters of 1 and 0.3 mm experienced high saturation conditions. The rock samples were placed in a shake-flasks and completely submerged in the bacterial inoculum during the inoculation stage. The inoculum was drained off and the rocks rinsed to remove the growth medium at the beginning of the test but the samples remained highly saturated due to the capillarity of the small particles. The reaction rate of the 1 and 0.3 mm inoculated samples would be hindered in this case by the slow diffusion of oxygen through the water-filled pores to the reaction site. The resistance to oxygen transport could also be increased by the formation of oxidation reaction product layers on the surface of the sulphide. The formation of oxidation product layers is discussed in greater detail in Section 5.1. Evidence for diffusion limitation comes from the observation that the oxygen consumption rate decreased in almost all cases after inoculation for particle sizes of 1 and 0.3 mm. This can be seen in Figures B.1 to B.16 in Appendix B.

The second reason is the sub-optimal growth conditions resulting from the dissolution of buffering minerals in the host rock. Optimal growth of *T. ferrooxidans*

occurs under acidic conditions, when the pH is between 2 and 3, consequently growth is not expected to be significant above pH 4.5. Dissolution of buffering minerals, such as calcite, maintained the growth medium pH at values above 4 and as high as 5 or 6 in some cases.

The lower rates of oxygen consumption after inoculation can also be explained in terms of the formation of oxidation product layers. The rock samples were maintained in a wet, well oxygenated environment to facilitate bacterial growth and attachment to the sulphide surfaces. Under these conditions, chemical oxidation proceeds and can produce ferric iron which will precipitate from solution as a ferric hydroxide coating on the particle surface. This was visually observed as a rusty orange-brown coating which developed on the sulphide surface over the incubation period. No attempt was made to remove these coatings because doing so would jeopardize the bacterial colony inhabiting the sulphide mineral surfaces. Oxidation product coatings have been previously noted and documented under similar conditions (Kwong, 1995). Kwong (1995) used SEM to observe the surface of pyrrhotite after oxidation in the presence of *T. ferrooxidans* at pH 2 and 22°C. An oxidation product layer was evident after inoculation as well as an even distribution of small blebs which were thought to be elemental sulphur.

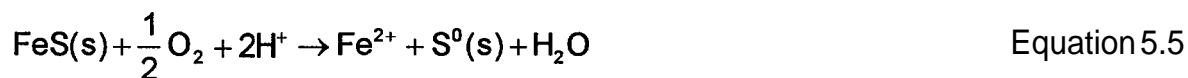
### **5.7 Measured Sulphate Release**

Figures 4.25 to 4.29 indicate that the oxygen consumption method consistently over-predicts the amount of sulphate that is released from samples containing pyrrhotite. This behaviour has been observed by other researchers (Elberling et al., 1994) and could be due to a number of factors.

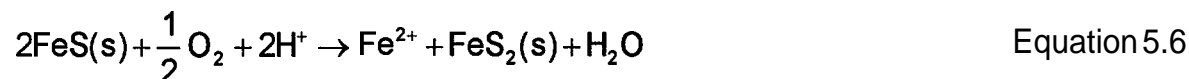
Other researchers have found that the rate of sulphate production often lags behind the rate of other reaction progress variables, such as iron, for the oxidation of pyrrhotite (Nicholson and Scharer, 1994; Kwong, 1995; Janzen, 1996). Kwong (1995) found that the release of sulphate was not congruent with the release of iron during the oxidation of pyrrhotite in aqueous experiments and that the molar ratio of

sulphate to iron changed depending on the reaction conditions. **Janzen (1996)** found that the oxidation of sulphide sulphur to sulphate was only 5 to 18% complete for the oxidation of pyrrhotite by ferric iron. The authors point to the partial oxidation of the sulphide moiety to form a sulphur-rich layer on the surface as a possible reason for the discrepancy. The presence of elemental sulphur and sulphur-rich iron minerals, such as marcasite, on the surface of oxidized pyrrhotite has been confirmed by other workers (**Jambor, 1994; Steger, 1982**).

Analysis of the data in Figures 4.25 to 4.30 suggests that between 3 and 9 times more oxygen was consumed than could be accounted for by the amount of sulphate produced. This implies that only 10 to 30% of the oxygen was consumed by the complete oxidation of pyrrhotite to sulphate according to Equation 2.2. The balance of the oxygen may be accounted for by partial oxidation reaction mechanisms such as;



or



In comparison to the findings of **Janzen (1996)**, 10 to 30% complete oxidation to sulphate seems reasonable. Detailed analysis of the oxidized surface, using a technique such as auger electron spectroscopy or X-ray photoelectron spectroscopy, would be required to verify the presence of a sulphur-enriched layer on the surface.

The discrepancy between oxygen consumption and sulphate release rates could also be due to the incomplete recovery of sulphate due to storage in the rock sample in the form of secondary solids at micro sites. Sulphate could be stored as a number of secondary minerals including gypsum ( $\text{CaSO}_4 \cdot 2\text{H}_2\text{O}$ ), melanterite ( $\text{FeSO}_4 \cdot 7\text{H}_2\text{O}$ ) and jarosite ( $\text{KFe}_3(\text{SO}_4)_2(\text{OH})_6$ ). Due to the relatively short time scale

of the tests small amounts of sulphate were produced in most cases. An average of approximately 20 mg of sulphate was generated for each test. Small losses of sulphate mass can translate into large errors in the observed rate of sulphate release. Recovery of the entire mass of sulphate could be difficult to achieve if the leaching step is too short to allow the complete dissolution of the secondary precipitates. However, because sulphate recovery was not problematic for samples with pyrite as the dominant sulphide mineral, incomplete oxidation of the pyrrhotite sulphide appears to be a more plausible hypothesis for the differences between oxygen consumed and sulphate produced.

Comparison of Figures 4.30 and 4.31 highlights the apparent difference between pyrite and pyrrhotite oxidation. The amount of sulphate collected at the end of each test correlated well with the measured oxygen consumption rates of rock samples containing pyrite, given the stoichiometry in Equation 2.1 (*i.e.* 1.75 moles of oxygen consumed for every mole of sulphate produced). The slope of the best-fit line in Figure 4.31 was 0.91, which is very close to the predicted 1 :1 correspondence between oxygen consumption rate and sulphate release.

The experimental results indicate that there is a distinct difference between pyrite and pyrrhotite with regard to oxygen consumption rate. Partial oxidation of pyrrhotite appears to be a significant contributor to the overall consumption of oxygen but this does not seem to be the case with pyrite. This is consistent with previous studies on pyrrhotite (Janzen, 1996; Steger, 1982) and pyrite (Moses *et al.*, 1987).

## **5.8 Comparison of Rates with those in the Literature**

Table 5.5 lists a number of intrinsic oxidation rate values that have been reported in the literature. Oxidation rates have been reported for materials containing variable amounts of pyrite or pyrrhotite and this is reflected in the wide range of equivalent

oxygen consumption rates calculated from the reported data. The oxygen consumption rates measured for waste rock samples in this investigation are on the same order of magnitude. The lowest rates were determined for the 10 cm size materials and had values ranging from  $4.7 \times 10^{-11}$  to  $7.8 \times 10^{-11}$  moles  $\text{O}_2 \cdot \text{kg}^{-1} \cdot \text{s}^{-1}$  (1.4 to 2.3 mg  $\text{SO}_4 \cdot \text{kg}^{-1} \cdot \text{week}^{-1}$ ). The highest rates were those measured on the 0.7 cm size materials inoculated with *T. ferrooxidans* and ranged from  $8.1 \times 10^{-9}$  to  $2.8 \times 10^{-8}$  moles  $\text{O}_2 \cdot \text{kg}^{-1} \cdot \text{s}^{-1}$  (235 to 813 mg  $\text{SO}_4 \cdot \text{kg}^{-1} \cdot \text{week}^{-1}$ ).

Table 5.5: Literature values of intrinsic oxidation rates

Source	% S <sup>2-</sup>	Rate (as quoted)	Rate* (moles O <sub>2</sub> •kg <sup>-1</sup> •s <sup>-1</sup> )	Rate** (mg SO <sub>4</sub> •kg <sup>-1</sup> •week <sup>-1</sup> )
Bennett, et al., 1994	~1% as Py	0.25x10 <sup>11</sup> kg O <sub>2</sub> •m <sup>-3</sup> •s <sup>-1</sup>	1x10 <sup>-11</sup>	0.3
Lapakko, 1994	0.63-1.41% as Py-Cp mixture	2 to 10 mmol SO <sub>4</sub> •t <sup>-1</sup> •d <sup>-1</sup> (field)	4.5x10 <sup>-11</sup> to 2.3x10 <sup>-10</sup>	1.3 to 6.7
		25 to 66x10 <sup>-14</sup> mol SO <sub>4</sub> •g <sup>-1</sup> •s <sup>-1</sup> (lab)	5.0x10 <sup>-10</sup> to 1.3x10 <sup>-9</sup>	14.5 to 38.3
Lapakko, 1994	6 % as Po	5.6 to 13x10 <sup>-12</sup> mol SO <sub>4</sub> •g <sup>-1</sup> •s <sup>-1</sup>	1.1 to 2.6x10 <sup>-8</sup>	325 to 755
Strömberg, 1994	0.57 % as Py	7.6 x10 <sup>-12</sup> kg O <sub>2</sub> •kg <sup>-1</sup> •s <sup>-1</sup> (lab)	2.4x10 <sup>-10</sup>	7.0
		2x10 <sup>11</sup> kg O <sub>2</sub> •m <sup>-3</sup> •s <sup>-1</sup> (field)	3.2x10 <sup>-10</sup>	9.3
Harries and Ritchie, 1981	3% as Py	1.9x10 <sup>-7</sup> kg SO <sub>4</sub> •m <sup>-2</sup> •s <sup>-1</sup>	4.8x10 <sup>-10</sup>	13.8
THIS STUDY	Variable As Py and Po	4 x10 <sup>-11</sup> to 2 x 10 <sup>-6</sup> moles O <sub>2</sub> •kg <sup>-1</sup> •s <sup>-1</sup>	4x10 <sup>-11</sup> to 2 x 10 <sup>-6</sup>	1.4 to 58,000

**nb** Py = pyrite, Po = pyrrhotite, Cp = chalcopyrite  
calculated as equivalent oxygen consumption rate

**\*\*** calculated as equivalent sulphate release rate

## 6. Summary of Conclusions

The oxygen consumption method has been successfully adapted for use with waste rock. Measured rates were in the range of  $4 \times 10^{-11}$  mol  $O_2 \cdot kg^{-1} \cdot s^{-1}$  to  $1.8 \sim 10^{-6}$  mol  $O_2 \cdot kg^{-1} \cdot s^{-1}$ .

The rate of oxygen consumption of inoculated and uninoculated samples was expressed as a function of particle size, sulphur content and temperature using a multivariable linear regression approach. Particle size was the most significant factor in determining the rate of oxygen consumption of uninoculated samples. All three variables had equal weight as predictors of the oxygen consumption rate of inoculated samples.

Field monitoring of sulphate loading rates from the Whistle Mine waste rock pile compared very well with potential loading rates predicted from oxygen consumption measurements performed in the laboratory.

The oxygen consumption rate was determined to be a function of  $l/d^n$ , where  $n$  was generally between 0.8 and 1.6 for uninoculated rock samples and between 0.3 and 0.7 for inoculated samples. The dependence of oxygen consumption rate on particle size suggests that attention should be focused on rock particles smaller than 2 cm. In addition, these results suggest that efforts to minimize fragmentation of waste rock materials during blasting and handling may be effective at lowering risk of reactivity in waste designated for disposal on the land surface if there is some potential for even minimal sulphide oxidation. Although there is little potential for such control with highly oxidized or altered host rock, many rock types, such as those associated with Ni-Cu deposits in Canada, are hard and competent so that strategies can be applied to minimize fragmentation and hence, minimize the production of fines.

In general, the rate of oxygen consumption increased at higher temperatures, however, the temperature dependence of the oxygen consumption rate was confounded by **occasional** anomalous behaviour of the oxygen sensors at temperatures below 20°C. Temperature had a more pronounced effect on oxygen consumption rates for samples that had been inoculated with acidophilic bacteria.

The rate of oxygen consumption exhibited a much stronger linear correlation with sulphur content after inoculation than before, which implies that the bacteria are oxidizing the sulphur moiety directly. Only one rock type, Faro waste rock, which contained significant amounts of sphalerite (**ZnS**) and galena (**PbS**), did not fit the expected trend in oxygen consumption rate with sulphur content. Evidence suggests that galvanic interactions between sphalerite, galena and pyrite may hinder the rate of oxygen consumption and lead to the preferential oxidation and release of lead and zinc.

Inoculation with *T. ferrooxidans* resulted in an increase in the oxygen consumption rate by a factor of 2 to 10 for pyrrhotite samples at temperatures of 20 and 30°C. Inoculation did not enhance the oxygen consumption rate of samples at temperatures below 20°C. This observation is not conclusive, however, because the bacteria may not have been acclimatized to the lower temperature environments. Inoculation of the pyrite bearing samples resulted in greater relative increases in oxygen consumption rates. Although uninoculated rates of pyrite oxidation are generally much lower than those for pyrrhotite, the inoculated rates for both sulphide minerals are similar.

The measured oxygen consumption rate is consistently higher than the amount of sulphate recovered after testing for rock samples containing pyrrhotite. Partial oxidation of the sulphur moiety and incomplete recovery of sulphate

could account for this. The oxygen consumption rate correlated well with the sulphate released from samples containing pyrite.

The ability to conduct multiple measurements within a 2 to 3 day period allowed the development of a substantial data base of rates for several rock types and for materials under different conditions. Statistical analysis of the kinetic data was conducted and important relationships that affect oxidation rates were investigated. The Oxygen Consumption Method provides an effective tool to conduct practical and detailed investigations of the reactivity of sulphide waste rock.

## References

Bennett, J.W., Gibson, D.K., Ritchie, A.I.M., Tan, Y., Broman, P.G., and Jönsson, H. (1994) Oxidation rates and pollution loads in drainage; correlation of measurements in a pyritic waste rock dump. *In* Proceedings of the Third International Conference on the Abatement of Acidic Drainage vol 1, pp 400-409 (Pittsburgh, PA, Apr 24-29)

Boggs, S. (1987) 'Principles of Sedimentology and Stratigraphy' Merrill Publishing, Columbus OH

Choquette, M. and Glinas, P. (1994) Mineralogical transformations associated with AMD production in a waste rock dump: La Mine Doyon South Waste Rock Dump. Report prepared for **CANMET**

Coastech Research Inc. (1989) Investigation of prediction techniques for acid mine drainage. DDS contract # 23440-7-9178/01-SQ

Davis, B.S., Fortin, D. and Beveridge, T.J. (1995) Acidophilic bacteria, acid mine drainage and Kidd Creek Mine tailings. *In* Proceedings of Sudbury '95: Mining and the Environment. (Sudbury, Ontario, May 28-June 1) pp 69-78

Dickie, A. (1995) A Future Denied? A special report on mining in Canada. Supplement to September 1995 *Report* on Business Magazine

Elberling, B., Nicholson, R.V. and David, D.J. (1993) Field evaluation of sulphide oxidation rates. *Nordic Hydrology* **24**(5), pp 23-338

Elberling, B., Nicholson, R.V., Reardon, E.J. and Tibble, P.A. (1994) Evaluation of sulphide oxidation rates: a laboratory study comparing oxygen fluxes and rates of oxidation product release. *Canadian Geotechnical Journal* **31**, pp 375-383

Elberling, B. and Nicholson, R.V. (1996) Field determination of sulphide oxidation rates in mine tailings. *Wafer Resources Research* **32:6**, pp 1773-1784

Evangelou, V.P. and Zhang, Y.L. (1995) A review; pyrite oxidation mechanisms and acid mine drainage prevention. *Critical Reviews in Environmental Science and Technology* **25**, pp141-199

Gélinas, P., Choquette, M., Lefebvre, R., Isabel, D., Leroueil, S., Locat, J., Bérubé, M.-A., Thériault, D. et Masson, A. (1991) Evaluation du drainage minier acide et des barrières sèches pour les haldes de stériles: Etude du site de La Mine Doyon. Rapport **GREGI 91-19** version préliminaire

Golder Associates (1996) Whistle Mine waste rock pile monitoring field and laboratory measurements (progress report 1 and year 2 work plan). MEND Project report PWGSC file # 02888.23440-5-1 125

Golder Associates (1997) Whistle Mine waste rock pile monitoring field and laboratory measurements (draft final report). MEND Project report PWGSC file # 028SQ.23440-5-1125

Gould, W.D., B  chard, G. and Lortie, L. (1994) The nature and role of microorganisms in the tailings environment. In Short Course Handbook on Environmental Geochemistry of Sulphide Mine-Wastes. Jambor, J.L. and Blowes, D.W., Eds. pp 185-199

Harries, J.R. and Ritchie, A.I.M. (1981) The use of temperature profiles to estimate the pyritic oxidation rate in a waste rock dump from an open-cut mine. *Water, Air and Soil Pollution* 15, pp 405-423

Jambor, J.L. (1994) Mineralogy of sulphide-rich tailings and their oxidation products. In Short Course Handbook on Environmental Geochemistry of Sulphide Mine-Wastes. Jambor, J.L. and Blowes, D.W., Eds. Geological Society of Canada, Nepean, Ontario. pp 59-1 02

Janzen, M.P. (1996) "Role of ferric iron, trace metal content and crystal structure on pyrrhotite oxidation" **M.Sc.** Thesis, Department of Earth Science, University of Waterloo

Kleinmann, R.L.P., Crerar, D.A and Pacilli, R.R. (1981) Biogeochemistry of acid mine drainage and a method to control acid formation. *Mining Engineering* 33, pp 300-304

Kwong, E.C.M. (1995a) "**Abiotic** and biotic pyrrhotite dissolution" **M.A.Sc.** Thesis, Department of Chemical Engineering, University of Waterloo

Kwong, J.Y.T. (1995b) Influence of galvanic sulphide oxidation on mine water chemistry. In Proceedings of Sudbury '95: Mining and the Environment. (Sudbury, Ontario, May 28-June 1) pp 477-483

Lapakko, K.A. and Antonson, D.A. (1994) Oxidation of sulfide minerals present in Duluth Complex rock: a laboratory study. In ACS Symposium Series 550 - Environmental geochemistry of sulphide oxidation. Alpers, C.N. and Blowes, D.W., Eds. pp 593-607

Lapakko, K.A. (1994) Comparison of Duluth complex rock dissolution in the laboratory and field. In Proceedings of the third International Conference on the Abatement of Acidic Drainage vol 4, pp 419-428 (Pittsburgh, PA, Apr 24-29)

Lasaga, A.C. (1981) Rate laws of chemical reactions. In Reviews in Mineralogy, Volume 8: Kinetics of geochemical processes, Lasaga, A.C. and Kirkpatrick, R.J., Eds. pp 1-67

Lee, G.F., and Stumm, W. (1960) Determination of ferrous iron in the presence of ferric iron with bathophenanthroline., *Journal of AWWA*, 52, pp 1567-1573

**McKibben, M.A. and Barnes, H.L.** (1986) Oxidation of pyrite in low temperature acidic solutions: rate laws and surface textures. *Geochimica et Cosmochimica Acta* 50, pp 1509-1520

Morin, K., Gerencher, E., Jones, C.E., Konasewich, D.E. and Harries, J.R. (1990) Critical literature review of acid drainage from waste rock. Draft report to MEND

Morin, K.A. and Hutt, N.M. (1994) Observed preferential depletion of neutralization potential over sulphide minerals in kinetic test: Site-specific criteria for safe **NP/AP** ratios. In Proceedings of the third International Conference on the Abatement of Acidic Drainage vol 1, pp 148-156 (Pittsburgh, PA, Apr 24-29)

Moses, C.O., Nordstrom, D.K., Herman, J.S. and Mills, A.A. (1987) Aqueous pyrite oxidation by dissolved oxygen and ferric iron. *Geochimica et Cosmochimica Acta* 51, pp 1561-1571

Natarajan, K.A. (1990) "Electrochemical aspects of bioleaching of base-metal sulphides." In Microbial Mineral Recovery, Ehrlich, H. and Brierley, C, Eds., pp 79-106

Nicholson, R.V., Gillham, R.W. and Reardon, E.J. (1988) Pyrite oxidation in carbonate-buffered solution: 1. Experimental kinetics. *Geochimica et Cosmochimica Acta* 52, pp 1077-1085

Nicholson, R.V. (1994) Iron-sulphide oxidation mechanisms: laboratory studies. In Short Course Handbook on Environmental Geochemistry of Sulphide Mine-Wastes. Jambor, J.L. and Blowes, D.W., Eds. Geological Society of Canada, Nepean, Ontario. pp 163-183

Nicholson, R.V. and Scharer, J.M. (1994) Laboratory studies of pyrrhotite oxidation kinetics. In ACS Symposium Series 550 - Environmental geochemistry of sulphide oxidation. Alpers, C.N. and Blowes, D.W., Eds. pp 14-30

Nicholson, R.V., Elberling, B. and Williams, G. (1995) A new oxygen consumption technique to provide rapid assessment of tailings reactivity in the field and the laboratory. In Proceedings of Sudbury '95: Mining and the Environment. (Sudbury, Ontario, May 28-June 1)

Norecol Environmental Consultants (1988) Cinola Gold Project Stage II Report. Report prepared for City Resources (Canada) Limited

Nordstrom, D.K. (1982) Aqueous pyrite oxidation and the consequent formation of secondary iron minerals. **In** Soil Science Society of America Special Publication No. 10: Acid Sulphate Weathering. Nordstrom, D.K., Ed. pp 37-56

Olson, G.J. (1991) Rate of bioleaching by *Thiobacillus ferrooxidans*: results of an interlaboratory comparison. *Applied Environmental Microbiology* 57, pp 642-644

Rimstidt, J.D., Chermak, J.A. and **Gagen**, P.M. (1994) Rates of reaction of galena, sphalerite, chalcopyrite, and arsenopyrite with **Fe(III)** in acidic solutions. **In** ACS Symposium Series 550 - Environmental geochemistry of sulphide oxidation. Alpers, C.N. and Blowes, D.W., Eds. pp 2-13

Ritchie, A.I.M. (1994a) The waste rock environment. **In** Short Course Handbook on Environmental Geochemistry of Sulphide Mine-Wastes. **Jambor**, J.L. and Blowes, D.W., Eds. Geological Society of Canada, Nepean, Ontario. pp 133-161

Ritchie, A.I.M. (1994b) Sulphide oxidation mechanisms: controls and rates of oxygen transport. **In** Short Course Handbook on Environmental Geochemistry of Sulphide Mine-Wastes. **Jambor**, J.L. and Blowes, D.W., Eds. Geological Society of Canada, Nepean, Ontario. pp 185-199

Robertson Geoconsultants Inc. (1997) Anvil Range Mining Complex - Integrated comprehensive abandonment plan. Prepared for Anvil Range Mining Corporation.

SRK (B.C.) Inc (1989) Draft Acid Mine Drainage Technical Guide: Volume 1 - Technical Guide. Prepared in association with Norecol Environmental Consultants and Gormley Process Engineering for the B.C. AMD Task Force (Report 660020).

Steger, H.F. (1982) Oxidation of sulphide minerals VII. Effect of temperature and relative humidity on the oxidation of pyrrhotite. *Chemical Geology*, 35 pp281-295

Sheremata, T.W., Yanful, E.K., St-Arnaud, L.C. and **Payant**, S.C. (1991) Flooding and lime addition for the control of acidic drainage from mine waste rock: a comparative laboratory study. **In** Proceedings of the first Canadian Conference on Environmental Geotechnics. (Montreal, Quebec, May 14-16)

Sobek, A.A., **Schuller**, W.A., Freeman, J.R. and Smith, R.M. (1978) Field and laboratory methods applicable to overburden and minesoils. EPA 600/2-78-054

Stromberg, B. and **Banwart**, S. (1994) Kinetic modelling of geochemical processes at the Aitik mining waste rock site in northern Sweden. *Applied Geochemistry* 9, pp583-595

Stromberg, B., **Banwart**, S., Bennett, J.W. and Ritchie, A.I.M. (1994) Mass balance assessment of initial weathering processes derived from oxygen consumption rates in waste sulfide ore. In Proceedings of the third International Conference on the Abatement of Acidic Drainage vol 2, pp 363-370 (Pittsburgh, PA, Apr 24-29)

Stumm, W. and Morgan, J., (1981) "Aquatic Chemistry: An introduction emphasizing chemical equilibria in natural waters" 2<sup>nd</sup> ed., Wiley and Sons. New York.

Synergetic Technology (1996) Physical mechanisms in acid mine drainage waste rock piles Phase I Part 1: Physical and geostatistical aspects of acid rock drainage. Draft report prepared for MEND and Environment Canada

Tibble, P.A. and Nicholson, R.V. (1997) Oxygen Consumption on Sulphide Tailings and Tailings Covers: Measured Rates and Applications. In Proceedings of the Fourth International Conference on Acid Rock Drainage. pp 647-661 (Vancouver, BC, May 31-Jun 6)

Watzlaf, G.R. (1988) Chemical inhibition of iron-oxidizing bacteria in waste rock and sulfide tailings and effect on water quality. In Proceedings of the 1988 Mine Drainage and Surface Mine Reclamation Conference. (Pittsburgh, PA, Apr 17-22)

Wheatherell, C. (1997) personal communication.

White III, **W.W.**, and Jeffers, T.H. Chemical predictive modeling of acid mine drainage from metallic sulfide-bearing waste rock. In ACS Symposium Series 550 - Environmental geochemistry of sulphide oxidation. **Alpers**, C.N. and Blowes, D.W., Eds. pp 608-630

## Appendix A: Measured Oxygen Consumption Rates

Table A.1 : Measured Oxygen Consumption Rates of Whistle Waste Rock from Initial Tests

Rock Type	Size (mm)	%S	Temperature (°C)	Corrected Rate (mol O <sub>2</sub> kg <sup>-1</sup> s <sup>-1</sup> )
High S	22	4.81	20	1.7E-09
High S	22	4.81	20	2.1 E-09
High S	14	5.01	20	1.7E-09
High S	14	5.01	20	7.8E-09
High S	7	6.04	30 w/T.f.	4.4E-08
High S	7	6.04	30	1.5E-08
High S	7	6.04	20	3.6E-09
High S	7	6.04	10	4.5E-09
Med S	22	1.94	20	1.1E-09
Med S	14	1.85	20	9.1 E-10
Med S	7	1.76	30 w/T.f.	2.3E-08
Med S	7	1.76	30	2.6E-09
Med S	7	1.76	20	N/D
Med S	7	1.76	10	4.2E-10
Low s	22	2.32	20	6.1 E-10
LOWS	14	2.71	30	8.6E-10
Low s	7	2.31	30 w/T.f.	2.1E-08
Low s	7	2.31	30	5.5E-10
Low s	7	2.31	30	4.4E-09
Low s	7	2.31	10	1.0E-09
Massive S	25*	22.3	20 w/T.f.	5.0E-08
Massive S	25*	22.3	20	3.4E-08
Massive S	25*	22.3	20	3.4E-08
Massive S	25*	22.3	20	3.5E-08
Massive S	22	22.0	20	9.2E-09
Massive S	10*	22.3	20	6.7E-08
Massive S	7	22.3	30 w/T.f.	3.3E-08
Massive S	7	22.3	30	7.3E-09
Massive S	7	22.3	30	5.2E-09
Massive S	7	22.3	30	3.5E-09
Massive S	7	22.3	30	2.3E-09
Massive S	7	22.3	10	6.1E-09
Massive S	0.074	22.3	20	1.8E-06
Massive S	0.074	22.3	20	9.4E-07
Pink Gran	22	0.14	30	N/D

NOTE: shaded cells indicate rates based on tremulous data,  
N/D denotes a value below the detection limit

\*estimated particle size, not measured

Table A.2: Measured Oxygen Consumption Rates of Voisey's Bay Eastern Deeps, Western Extension and Ovoid Samples

Sample	Date	%S	Corrected R a t e (mol O <sub>2</sub> kg <sup>-1</sup> s <sup>-1</sup> )
ED-TROC-1	11-Oct	0.505	9.3E-10
ED-TROC-1(R)	17-Oct	0.505	7.0E-10
ED-TROC-2	11-Oct	1.535	6.5E-10
ED-TROC-3	11-Oct	3.085	2.0E-09
ED-TROC-3 (R)	17-Oct	3.085	1.8E-09
ED-TROC-4	11-Oct	0.625	3.6E-10
WE-TROC-5	22-Oct	0.385	3.3E-09
WE-TROC-5 (R)	24-Oct	0.385	3.1E-09
WE-TROC-6	22-Oct	1.57	2.7E-09
WE-TROC-6 (R)	24-Oct	1.57	4.1E-09
WE-TROC-7	22-Oct	2.35	3.0E-09
WE-TROC-7 (R)	24-Oct	2.35	4.3E-09
ED-GNEISS-1	11-Oct	0.29	1.5E-09
ED-GNEISS-2	11-Oct	0.03	7.1E-10
ED-GNEISS-2 (R)	17-Oct	0.03	2.7E-10
ED-ORTHO-1	11-Oct	0.63	2.2E-10
ED-ORTHO-1 (R)	17-Oct	0.63	1.2E-09
WE-PARA-1	22-Oct	0.35	1.0E-09
WE-PARA-1 (R)	24-Oct	0.35	2.8E-09
VB-GRAN-1	22-Oct	0.2	9.2E-10
VB-GRAN-1 (R)	24-Oct	0.2	1.1E-09
OVOID-COL 18	15-Oct	0.12	2.0E-09
OVOID-COL 18 (R)	17-Oct	0.12	3.3E-10
OVOID-COL19	15-Oct	2.02	1.2E-09
OVOID-HC1	15-Oct	0.02	1.2E-09
OVOID-HC1 (R)	17-Oct	0.02	N/D
OVOID-HC2	15-Oct	1.22	1.2E-09
OVOID-HC3	15-Oct	0.09	5.0E-10
OVOID-HC3 (R)	17-Oct	0.09	N/D
OVOID-HC4	15-Oct	0.49	N/D
OVOID-HC5	15-Oct	0.24	7.9E-10
OVOID-HC5 (R)	17-Oct	0.24	4.4E-10
OVOID-HC6	15-Oct	0.01	N/D
OVOID-HC7	15-Oct	0.05	N/D
OVOID-HC7 (R)	17-Oct	0.05	N/D
OVOID-HC8	15-Oct	24.14	2.5E-08

NOTE: all of the above tests were performed on the 8 mm size fraction at 30°C,  
 N/D denotes a value below the detection limit,  
 (R) indicates replicate test using the same sample under similar conditions, at a later  
 time, usually within 2 to 3 weeks of the original test

Table A.3: Measured Oxygen Consumption Rates of Voisey's Bay Eastern Deeps and Western Extension Samples with three size fractions

Description	Size (mm)	%S	Corrected Rate (mol O <sub>2</sub> kg <sup>-1</sup> s <sup>-1</sup> )
ED-TROC-1 +1/2	16	0.505	N/D
ED-TROC-1 +1/2 (R)	16	0.505	N/D
ED-TROC-1 -1/2 +4m	8	0.505	9.30E-10
ED-TROC-1 -1/2 +4m (R)	8	0.505	7.00E-10
ED-TROC-1 -10 +30m	1	0.505	5.00E-09
ED-TROC-1 -10 +30m (R)	1	0.505	5.70E-08
ED-TROC-3 +1/2	16	3.085	6.70E-10
ED-TROC-3 +1/2	16	3.085	6.70E-10
ED-TROC-3 +1/2	16	3.085	9.30E-10
ED-TROC-3 -1/2 +4m	8	3.085	2.00E-09
ED-TROC3 -1/2+4m (R)	8	3.0851	1.80E-09
ED-TROC-3 -10 +30m	1	3.085	1.50E-09
ED-TROC3 -10 +30m (R)	1	3.085	5.70E-08
WE-TROC-5 +1/2	16	0.385	4.7E-10
WE-TROC-5 +1/2	16	0.385	6.50E-11
WE-TROC-5 -1/2 +4m	8	0.385	3.3E-09
WE-TROC-5 -1/2 +4m (R)	8	0.385	3.1E-09
WE-TROC-5 -10 +30m	1	0.385	4.70E-09
WE-TROC-7 +1/2	16	2.35	1.2E-09
WE-TROC-7 +1/2	16	2.35	1.7E-09
WE-TROC-7 -1/2 +4m	8	2.35	3.00E-09
WE-TROC-7 -1/2 +4m (R)	8	2.35	4.3E-09
WE-TROC-7 -10 +30m	1	2.35	3.60E-09
WE-TROC-7 -10 +30m (R)	1	2.35	6.80E-09

NOTE: all of the above tests were performed at 30°C,  
 N/D denotes a value below the detection limit,  
 (R) indicates replicate tests performed using the same sample under similar conditions,  
 at a later time, usually within 2 to 3 weeks of the original test

Table A.4: Measured Oxygen Consumption Rate of **Voisey's Bay COMPs** at **30°C**

Description	Size (mm)	%S	Rate (mol O <sub>2</sub> kg <sup>-1</sup> s <sup>-1</sup> )
COMP 1	8	0.71	2.1E-09
COMP 1 (R)	8	0.71	2.3E-09
COMP 2	8	0.3	2.4E-09
COMP 2 (R)	8	0.3	4.7E-09
COMP 3	8	4.22	1.5E-09
COMP 3 (R)	8	4.22	1.1E-09
COMP 4	8	5.86	2.6E-09
COMP 4 (R)	3	5.86	3.6E-09
		1.37	3.7E-09
COMP 1 (R)	3	1.37	6.6E-09
COMP 2	3	0.64	2.8E-09
COMP 2 (R)	3	0.64	2.1E-09
COMP 3	3	3.76	8.4E-09
COMP 3 (R)	3	3.76	6.7E-09
COMP 4	3	3.43	1.2E-08
COMP 4 (R)	3	3.43	1.1E-08
COMP 1	1	1.42	N/D
COMP 2	1	0.39	N/D
COMP 3	1	3.031	N/D
COMP 4	1	2.69	N/A
COMP 1	0.3	0.72	N/D
COMP 2	0.3	0.33	1.3E-08
COMP 2 (R)	0.3	0.33	8.1E-09
COMP 3	0.3	6.01	N/D
COMP 4	0.3	3.35	3.6E-08

NOTE: (R) indicates replicate test using same sample under similar conditions, at a later time, usually within 2 to 3 weeks of the original test, N/D denotes a value below the detection limit, N/A means that no coherent trend was established over the course of the test

Table A.5: Measured Oxygen Consumption Rate of **Voisey's Bay COMPs** at 20°C

Description	Size (mm)	%S	Rate (mol O <sub>2</sub> kg <sup>-1</sup> s <sup>-1</sup> )
COMP 1	8	0.71	1.1E-09
COMP 1 (R)	8	0.71	8.8E-10
COMP 2	8	0.3	2.4E-09
COMP 2 (R)	8	0.3	9.5E-11
COMP 3	8	4.22	1.3E-09
COMP 3 (R)	8	4.22	4.6E-10
COMP 4	8	5.86	2.4E-09
COMP 4 (R)	8	5.86	2.3E-09
COMP 1	3	1.37	1.7E-09
COMP 2	3	0.64	5.5E-09
COMP 2	3	0.64	9.9E-10
COMP 3	3	3.76	6.3E-09
COMP 4	3	3.43	1.2E-08
COMP 4 (R)	3	3.43	3.6E-09
COMP 1	1	1.42	2.6E-07
COMP 1 (R)	1	1.42	1.5E-07
COMP 2	1	0.39	1.2E-07
COMP 2 (R)	1	0.39	7.8E-08
COMP 3	1	3.03	1.9E-07
COMP 3 (R)	1	3.03	6.3E-08
COMP 4	1	2.69	1.9E-07
COMP 4 (R)	1	2.69	1.3E-07
COMP 1	0.31	0.72	2.1E-07
COMP 1 (R)	0.3	0.72	1.3E-07
COMP 2	0.3	0.33	1.7E-08
COMP 2 (R)	0.3	0.33	6.0E-08
COMP 3	0.3	6.01	7.2E-08
COMP 3 (R)	0.3	6.01	9.8E-08
COMP 4	0.3	3.35	1.6E-07
COMP 4 (R)	0.3	3.35	3.1E-07

NOTE: (R) indicates replicate test using same sample under similar conditions, at a later time, usually within 2 to 3 weeks of the original test

Table A.6: Measured Oxygen Consumption Rate of Voisey's Bay **COMPs** at 10°C

Description	Size (mm)	%S	Rate (mol O <sub>2</sub> kg <sup>-1</sup> s <sup>-1</sup> )
COMP 1	8	0.71	1.1E-09
COMP 2	8	0.3	9.9E-11
COMP 3	8	4.22	N/D
COMP 4	8	5.86	3.5E-09
COMP 1	3	1.55	1.5E-09
COMP 2	3	0.64	3.3E-09
COMP 3	3	3.76	1.1E-09
COMP 4	3	3.43	5.4E-09
COMP 1	1	1.42	1.3E-08
COMP 2	1	0.39	N/D
COMP 3	1	3.03	2.5E-08
COMP 3 (R)	1	3.03	4.2E-08
COMP 4	1	2.69	3.0E-08
COMP 4 (R)	1	2.69	4.5E-09
COMP 1	0.3	0.72	5.7E-08
COMP 1 (R)	0.31	0.721	1.7E-08
COMP 2	0.3	0.33	2.9E-08
COMP 2 (R)	0.3	0.33	4.5E-08
COMP 3	0.3	6.01	6.7E-08
COMP 3 (R)	0.3	6.01	2.8E-08
COMP 4	0.3	3.35	5.8E-08
COMP 4 (R)	0.3	3.35	1.3E-08
COMP 4 (R)	0.3	3.35	2.1E-08

NOTE: (R) indicates replicate test using same sample under similar conditions, at a later time, usually within 2 to 3 weeks of the original test, N/D denotes a value below the detection limit

Table A.7: Measured Oxygen Consumption Rate of **Voisey's Bay COMPs** at 4°C

Description	Size (mm)	%S	Rate (mol O <sub>2</sub> kg <sup>-1</sup> s <sup>-1</sup> )
COMP 1	8	0.71	6.2E-10
COMP 2	8	0.3	7.2E-11
COMP 3	8	4.22	3.3E-10
COMP 4	8	5.86	1.0E-09
COMP 1	3	1.37	3.4E-10
COMP 2	3	0.64	N/D
COMP 3	3	3.76	2.1E-09
COMP 4	3	3	1.4E-09
COMP 1	1	1.42	2.5E-08
COMP 2	1	0.39	1.5E-08
COMP 3	1	3.03	N/D
COMP 4	1	2.69	4.6E-08
COMP 1	0.3	0.72	2.0E-08
COMP 2	0.3	0.33	5.8E-08
COMP 3	0.3	6.01	3.1E-08
COMP 4	0.3	3.35	6.7E-08

NOTE: N/D denotes a value below the detection limit

Table A.8: Measured Oxygen Consumption Rate of **Voisey's Bay COMPs** at **30°C** inoculated with *T. ferrooxidans*

Description	Size (mm)	%S	Rate (mol O <sub>2</sub> kg <sup>-1</sup> s <sup>-1</sup> )
COMP1	8	0.71	3.9E-09
COMP2	8	0.3	3.9E-09
COMP3	8	4.22	N/D
COMP4	8	5.86	N/D
COMP1	3	1.37	N/D
COMP2	3	0.64	8.6E-09
COMP3	3	3.76	1.3E-08
COMP4	3	3.43	2.1E-08
COMP1	1	1.42	3.7E-08
COMP2	1	0.39	N/D
COMP3	1	3.03	4.5E-08
COMP4	1	2.69	1.5E-08
COMP1	0.3	0.72	2.3E-08
COMP2	0.3	0.33	2.2E-08
COMP3	0.3	6.01	1.6E-07
COMP4	0.3	3.35	1.1E-07

NOTE: (R) indicates replicate test using same sample. under similar conditions, at a later time, usually within 2 to 3 weeks of the original test, N/D denotes a value below the detection limit

Table A.9: Measured Oxygen Consumption Rate of Voisey's Bay COMPs at 10°C inoculated with *T. ferrooxidans*

Description	Size (mm)	%S	Rate (mol O <sub>2</sub> kg <sup>-1</sup> s <sup>-1</sup> )
COMP1	8	0.711	8.9E-10
COMP2	8	0.3	5.4E-10
COMP3	8	4.22	N/D
COMP4	8	5.86	N/D
COMP1	3	1.37	1.2E-09
COMP2	3	0.64	2.1E-09
COMP3	3	3.76	1.7E-09
COMP4	3	3.43	2.6E-09
COMP1	1	1.42	N/D
COMP2	1	0.39	4.4E-09
COMP3	1	3.03	4.8E-09
COMP4	1	2.69	6.4E-09
COMP1	0.3	0.72	6.7E-09
COMP2	0.3	0.33	6.4E-09
COMP3	0.3	6.01	6.5E-09
COMP4	0.3	3.35	3.2E-09

NOTE: N/D denotes a value below the detection limit

Table A. 10: Measured Oxygen Consumption Rate of **Voisey's Bay COMPs** at 4°C inoculated with *T. ferrooxidans*

Description	Size (mm)	%S	Rate (mol O <sub>2</sub> kg <sup>-1</sup> s <sup>-1</sup> )
COMP1	8	0.71	1.4E-09
COMP2	8	0.3	3.7E-10
COMP3	8	4.22	N/D
COMP4	8	5.86	N/D
COMP1	3	1.37	N/D
COMP2	3	0.64	2.1E-09
COMP3	3	3.76	3.7E-09
COMP4	3	3.43	6.2E-09
COMP1	1	1.42	1.7E-08
COMP2	1	0.39	6.6E-10
COMP3	1	3.03	1.3E-08
COMP4	1	2.69	1.2E-08
COMP1	0.3	0.72	1.0E-08
COMP2	0.3	0.33	N/D
COMP3	0.3	6.01	6.2E-09
COMP4	0.3	3.35	1.2E-08

NOTE: N/D denotes a value below the detection limit

Table A.11: Measured Oxygen Consumption Rates of 6 Rock Types at 30°C

MATERIAL	Date	Size (mm)	% s	Rate (mol O <sub>2</sub> kg <sup>-1</sup> s <sup>-1</sup> )
Faro	31-Jan	16	19.5	N/A
Faro	12-Feb	16	19.5	N/A
Faro	31-Jan	8	18.7	1.4E-09
Faro	12-Feb	8	18.71	N/A
Faro	31-Jan	3	18.41	3.3E-09
Faro	12-Feb	3	18.4	1.3E-09
Mine Doyon	31-Jan	16	6.09	N/A
Mine Doyon	12-Feb	16	6.09	5.8E-09
Mine Doyon	31-Jan	8	5.79	1.5E-10
Mine Doyon	12-Feb	8	5.79	1.8E-09
Mine Doyon	31-Jan	3	12.4	N/A
Mine Doyon	12-Feb	3	12.4	2.1E-09
Whistle high S	31-Jan	8	3.77	4.3E-09
Whistle high S	12-Feb	8	3.77	5.6E-09
Whistle high S	31-Jan	3	3.89	1.8E-08
Whistle high S	12-Feb	3	3.89	1.5E-08
Whistle low S	31-Jan	8	1.71	N/A
Whistle low S	12-Feb	8	1.71	2.5E-09
Whistle low S	31-Jan	3	2.23	N/D
Whistle low S	12-Feb	3	2.23	5.6E-09
Pamor	31-Jan	8	0.67	N/D
Pamor	12-Feb	8	0.67	N/D
Pamor	31-Jan	3	0.49	1.9E-10
Pamor	12-Feb	3	0.49	5.6E-09
KZK	31-Jan	8	0.74	N/D
KZK	12-Feb	8	0.74	7.6E-11
KZK	31-Jan	3	0.99	1.5E-09
KZK	12-Feb	3	0.99	2.0E-09

NOTE: N/D designates a value below detection limit, N/A means that no coherent trend was established over the course of the test

Table A.1 2: Measured Oxygen Consumption Rates of 6 Rock Types at 20°C

MATERIAL		Size (mm)	% s	Rate (mol O <sub>2</sub> kg <sup>-1</sup> s <sup>-1</sup> )
Faro	31-Jan	15.6	19.5	N/A
Faro	12-Feb	15.6	19.5	N/A
Faro	31-Jan	7.77	18.7	5.9E-10
Faro	12-Feb	7.77	18.7	N/D
Faro	31-Jan	3.1	18.4	1.4E-09*
Faro	12-Feb	3.1	18.4	1.5E-09
Mine Doyon	31-Jan	15.6	6.09	N/A
Mine Doyon	12-Feb	15.6	6.09	N/A
Mine Doyon	31-Jan	7.77	5.79	5.3E-10*
Mine Doyon	12-Feb	7.77	5.79	2.3E-11
Mine Doyon	31-Jan	3.1	12.4	3.0E-09*
Mine Doyon	12-Feb	3.1	12.4	1.3E-09
Whistle high S	31-Jan	7.77	3.77	1.9E-09
Whistle high S	12-Feb	7.77	3.77	6.3E-10
Whistle high S	31-Jan	3.1	3.89	4.0E-09
Whistle high S	12-Feb	3.1	3.89	2.8E-09
Whistle low S	31-Jan	7.77	1.7	3.9E-10*
Whistle low S	12-Feb	7.77	1.7	3.3E-10
Whistle low S	31-Jan	3.1	2.23	N/A
Whistle low S	12-Feb	3.1	2.23	3.7E-10
Pamor	31-Jan	7.77	0.67	2.9E-10
Pamor	12-Feb	7.77	0.67	N/D
Pamor	31-Jan	3.1	0.49	1.1E-09
Pamor	12-Feb	3.1	0.49	N/D
KZK	31-Jan	7.77	0.74	N/D
KZK	12-Feb	7.77	0.74	N/D
KZK	31-Jan	3.1	0.991	3.4E-10
KZK	12-Feb	3.1	0.991	4.8E-10

NOTE: \* calculated from 16 hours of data, N/D designates a value below detection limit, N/A means that no coherent trend was established over the course of the test

Table A.1 3: Measured Oxygen Consumption Rates of 6 Rock Types at 10°C

MATERIAL	Date	Size (mm)	%S	Rate (mol O <sub>2</sub> kg <sup>-1</sup> s <sup>-1</sup> )
Faro	10-Feb	15.6	19.5	4.51E-11
Faro	10-Feb	7.77	18.7	N/D
Faro	10-Feb	3.1	18.41	1.48E-09
Mine Doyon	10-Feb	15.6	6.09	2.72E-09
Mine Doyon	10-Feb	7.77	5.79	4.84E-10
Mine Doyon	10-Feb	3.1	12.4	1.57E-09
Whistle high S	10-Feb	7.77	3.77	2.19E-09
Whistle high S	10-Feb	3.1	3.89	4.85E-09
Whistle low S	10-Feb	7.77	1.7	9.75E-10
Whistle low S	10-Feb	3.1	2.23	2.05E-09
Pamor	10-Feb	7.77	0.67	1.22E-10
Pamor	10-Feb	3.1	0.49	8.55E-10
KZK	10-Feb	7.77	0.74	3.32E-10
KZK	10-Feb	3.1	0.99	8.88E-10

NOTE: N/D designates a value below detection limit, N/A means that no coherent trend was established over the course of the test

Table A.1 4: Measured Oxygen Consumption Rates of 6 Rock Types at 20°C inoculated with *T. ferrooxidans*

MATERIAL	Date	Size (mm)	%S	Rate (mol O <sub>2</sub> kg <sup>-1</sup> s <sup>-1</sup> )
Faro	28-Feb	15.6	19.5	7.67E-10
Faro	28-Feb	7.77	18.7	2.26E-09
Faro	28-Feb	3.1	18.4	3.89E-09
Mine Doyon	28-Feb	15.6	6.09	1.43E-08
Mine Doyon	28-Feb	7.77	5.79	1.71E-08
Mine Doyon	28-Feb	3.1	12.41	4.29E-08
Whistle high S	28-Feb	7.77	3.77	5.03E-09
Whistle high S	28-Feb	3.1	3.89	1.42E-08
Whistle low S	28-Feb	7.77	1.7	3.02E-09
Whistle low S	28-Feb	3.1	2.23	8.97E-09
Pamor	28-Feb	7.77	0.67	N/D
Pamor	28-Feb	3.1	0.49	2.0E-09*
KZK	28-Feb	7.77	0.74	1.10E-09
KZK	28-Feb	3.1	0.99	N/A

NOTE: \* based on erratic data, N/D designates a value below detection limit, N/A means that no coherent trend was established over the course of the test

## Appendix B: Oxygen Consumption Rate vs. Nominal Particle Size for Voisey's Bay COMP Samples

figure B.I: Oxygen Consumption Rate vs Size  
COMP 1, 30°C

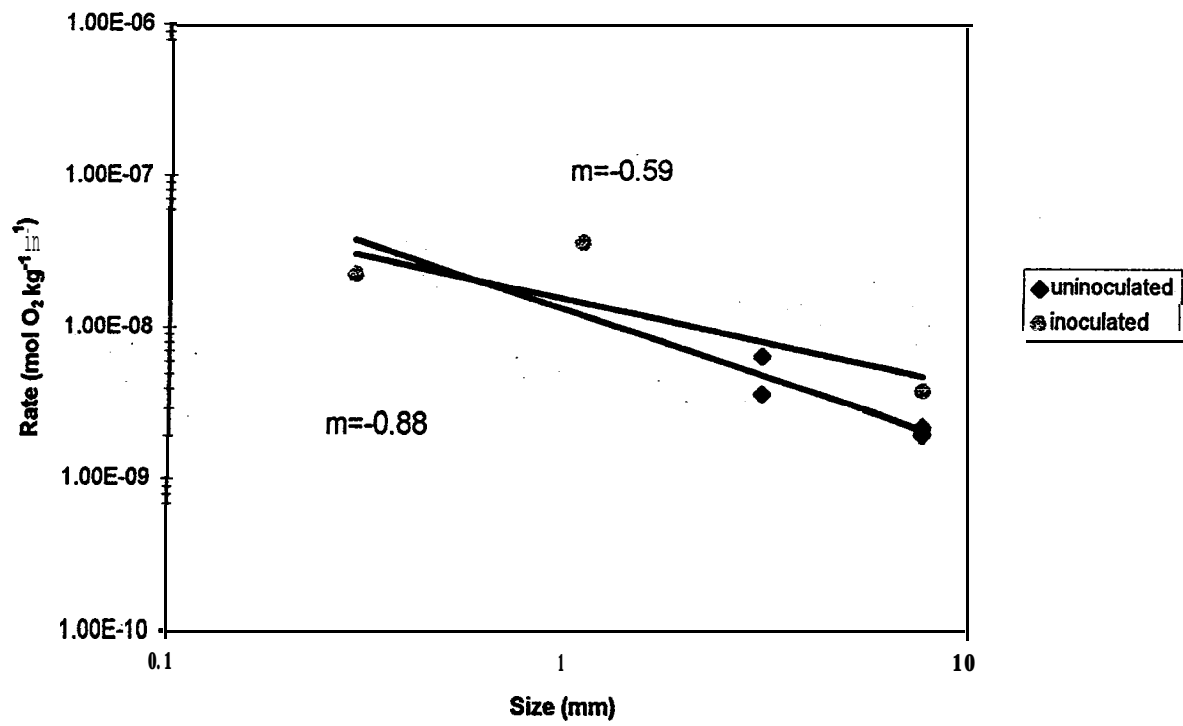


Figure B.2: Oxygen Consumption Rate vs Size

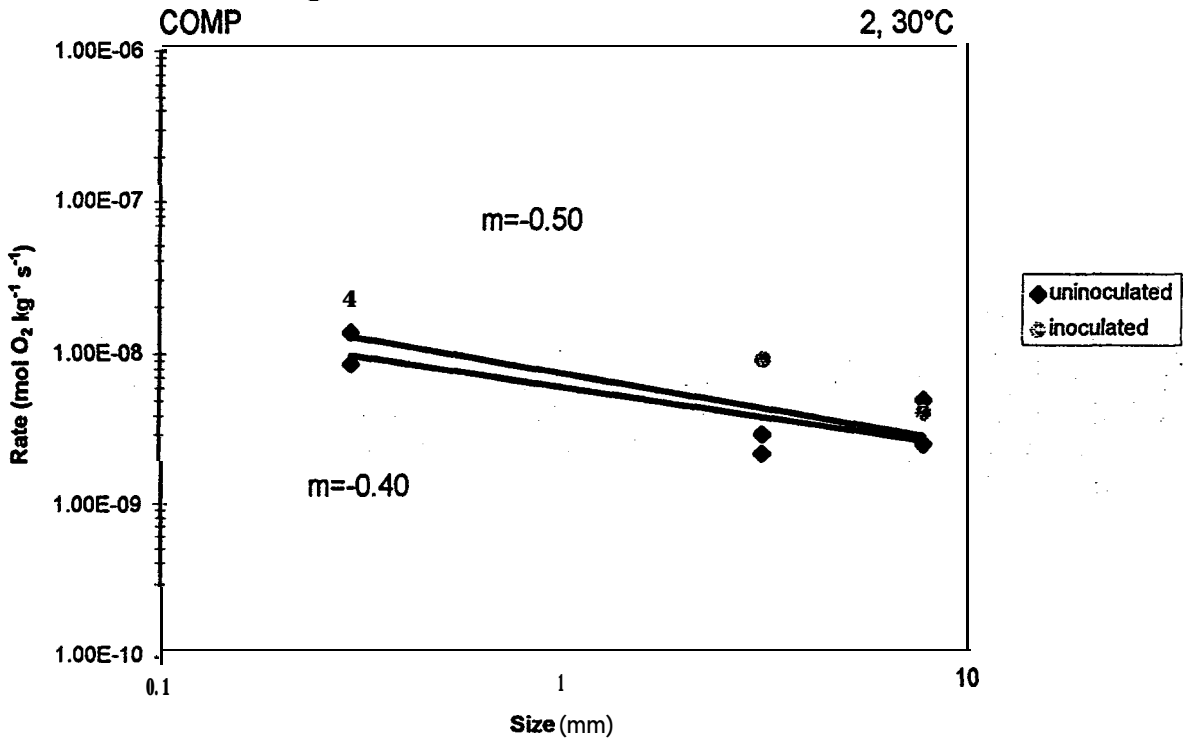


Figure 8.3: Oxygen Consumption Rate vs Size  
COMP 3, 30°C

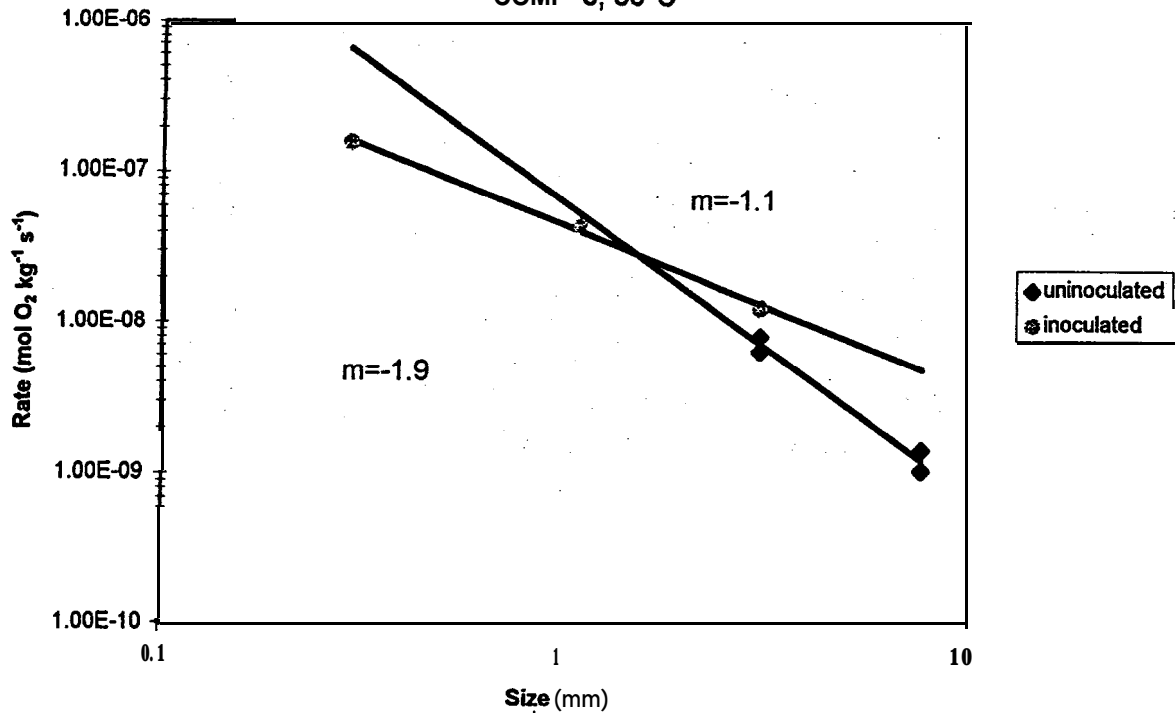


Figure B.4: Oxygen Consumption Rate vs Size  
COMP 4, 30°C

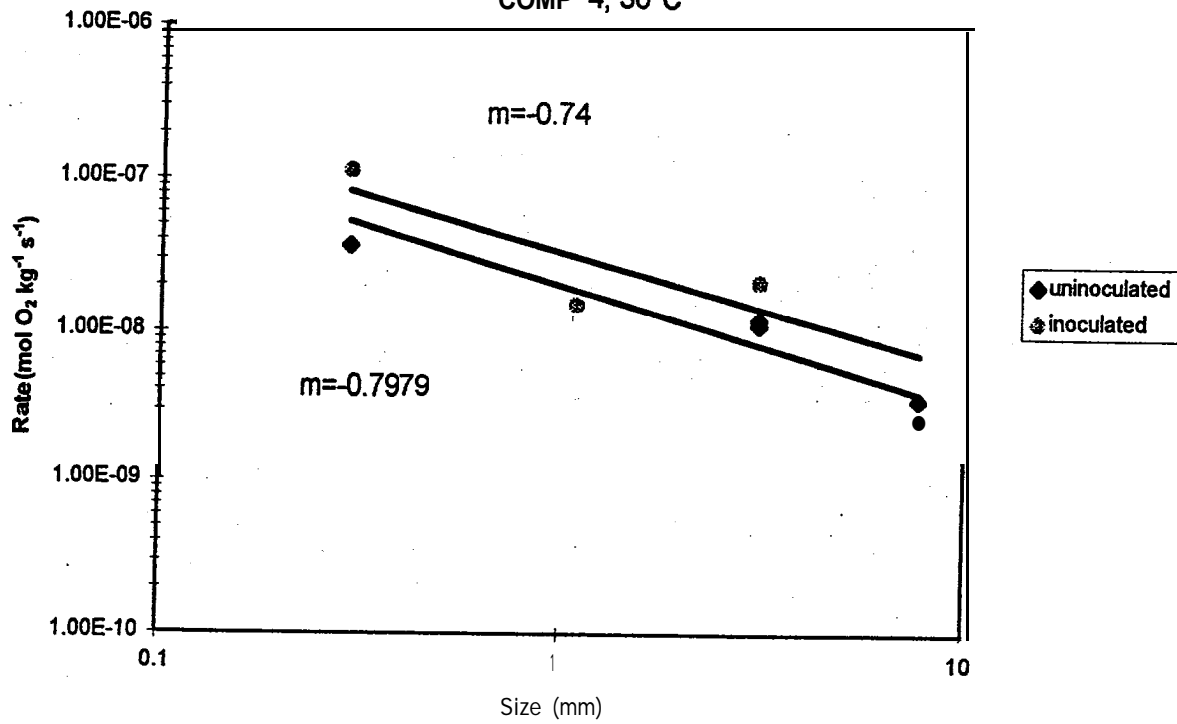


Figure B.5: Oxygen Consumption Rate vs Size  
COMP 1, 20°C

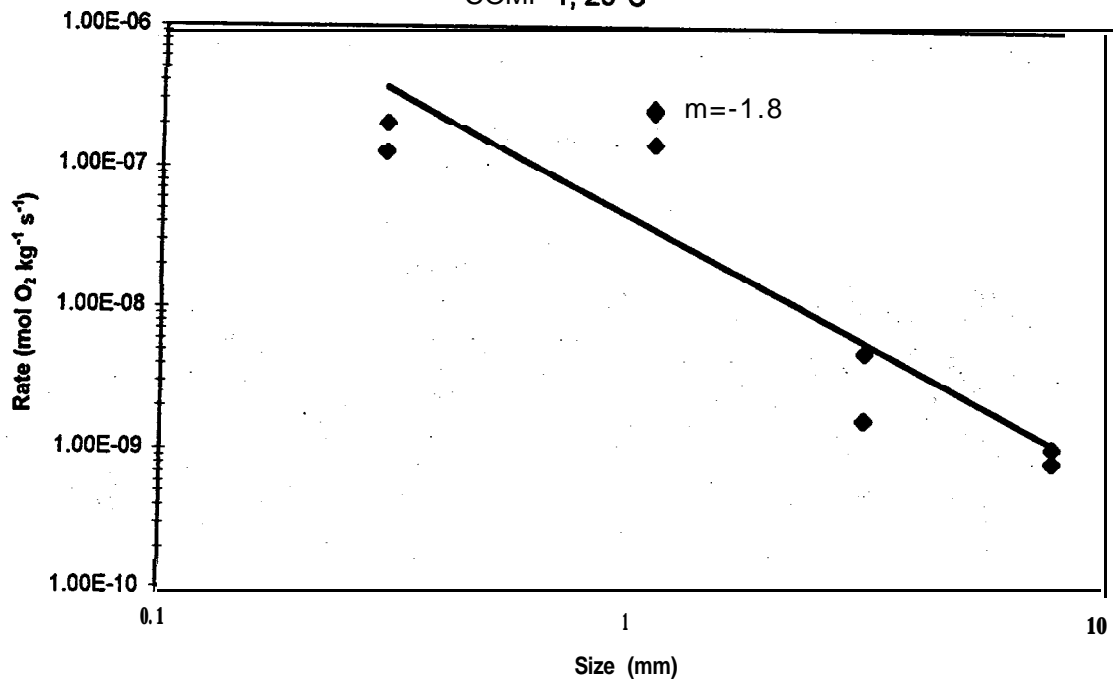


Figure B.6: Oxygen Consumption Rate vs Size  
C O M P 2, 20°C

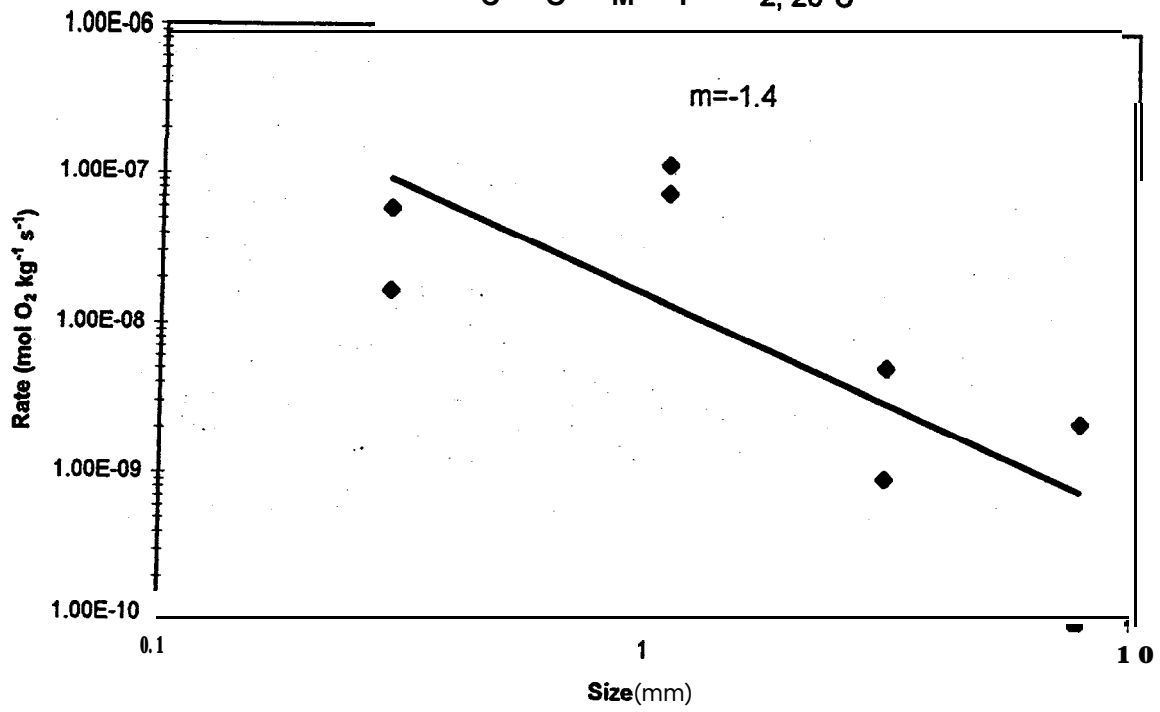


Figure B.7: Oxygen Consumption Rate vs Size  
COMP3, 20°C

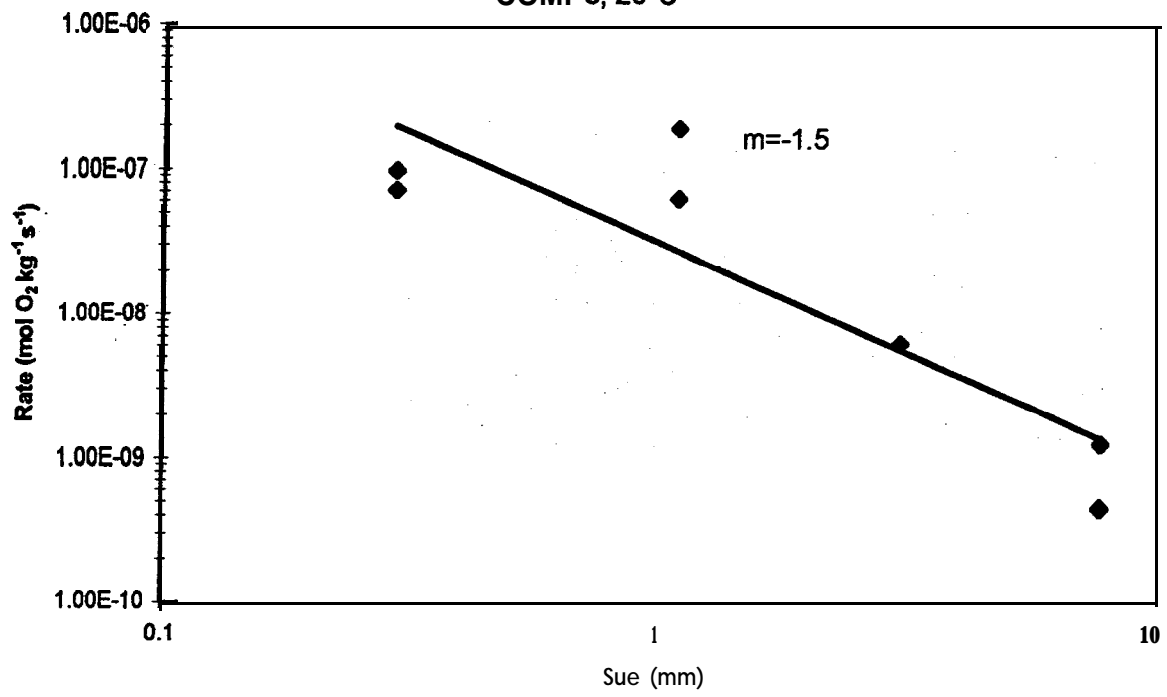


Figure 8.8: Oxygen Consumption Rate vs Size  
COMB 4, 20°C

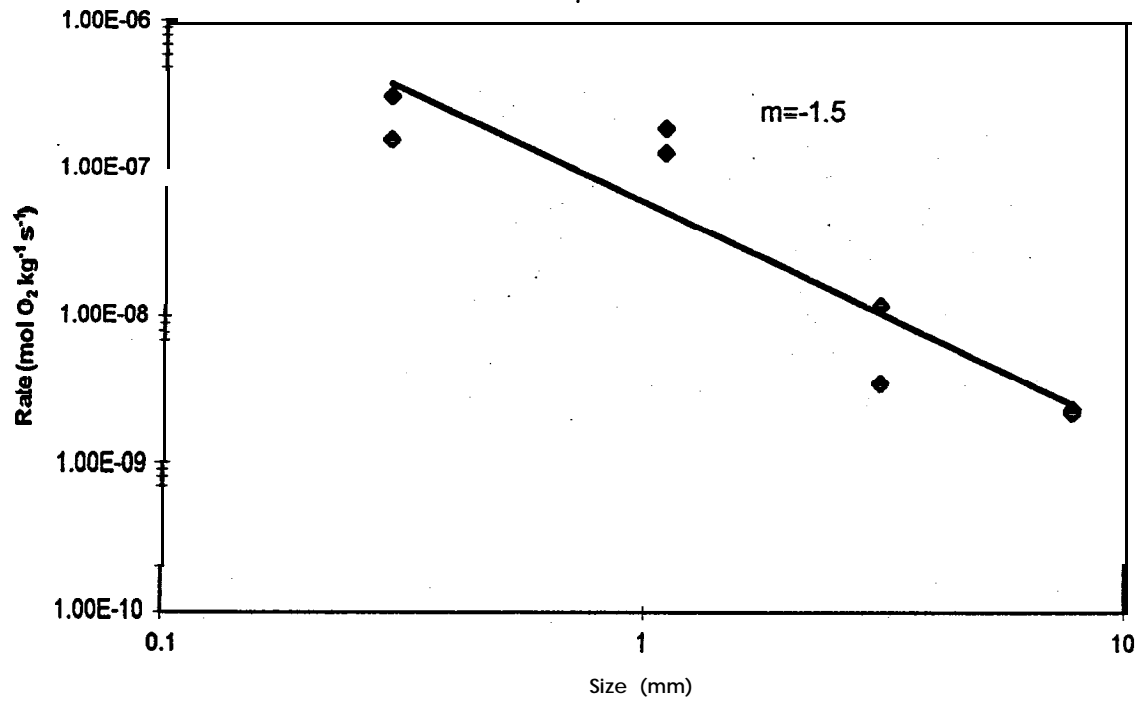


Figure B.9: Oxygen Consumption Rate vs Size

COMP 1. 10°C

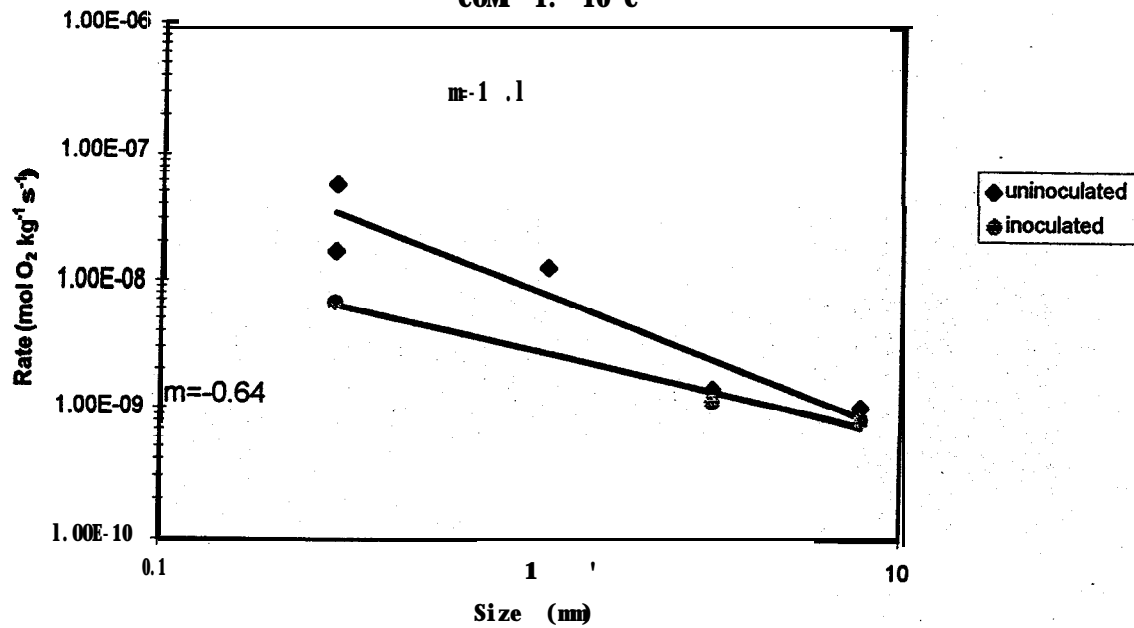


Figure B.10: Oxygen Consumption Rate vs Size  
COMP 2, 10°C

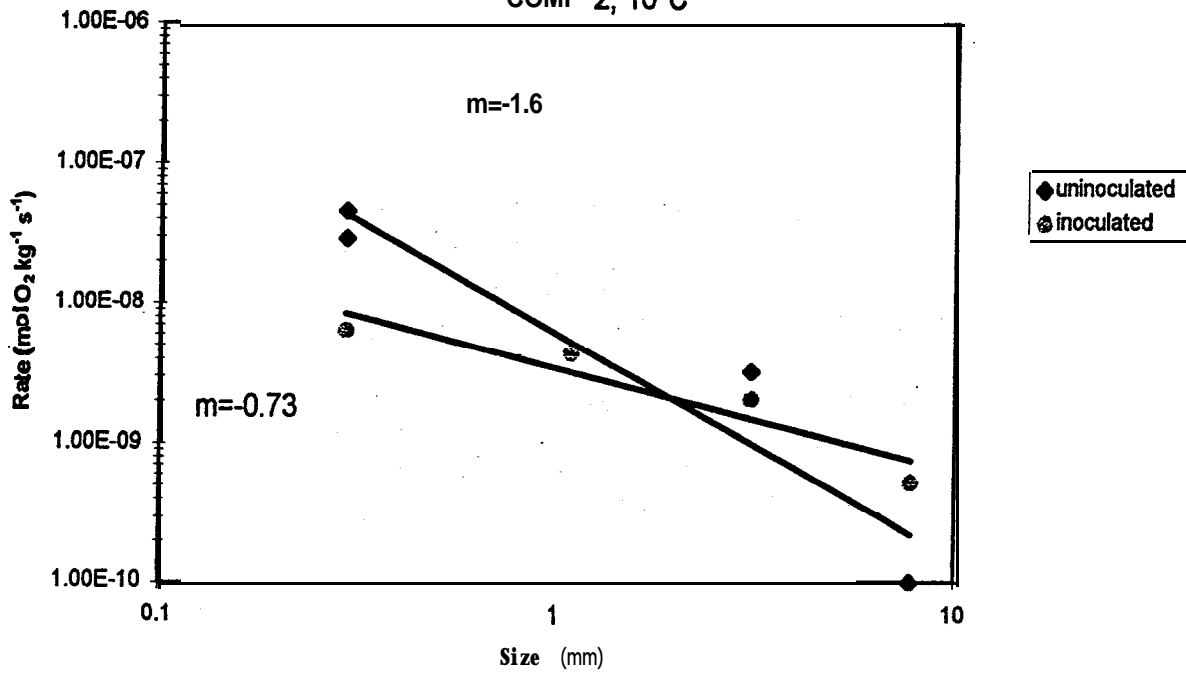


Figure B.II: Oxygen Consumption Rate vs Size  
COMP 3, 10°C

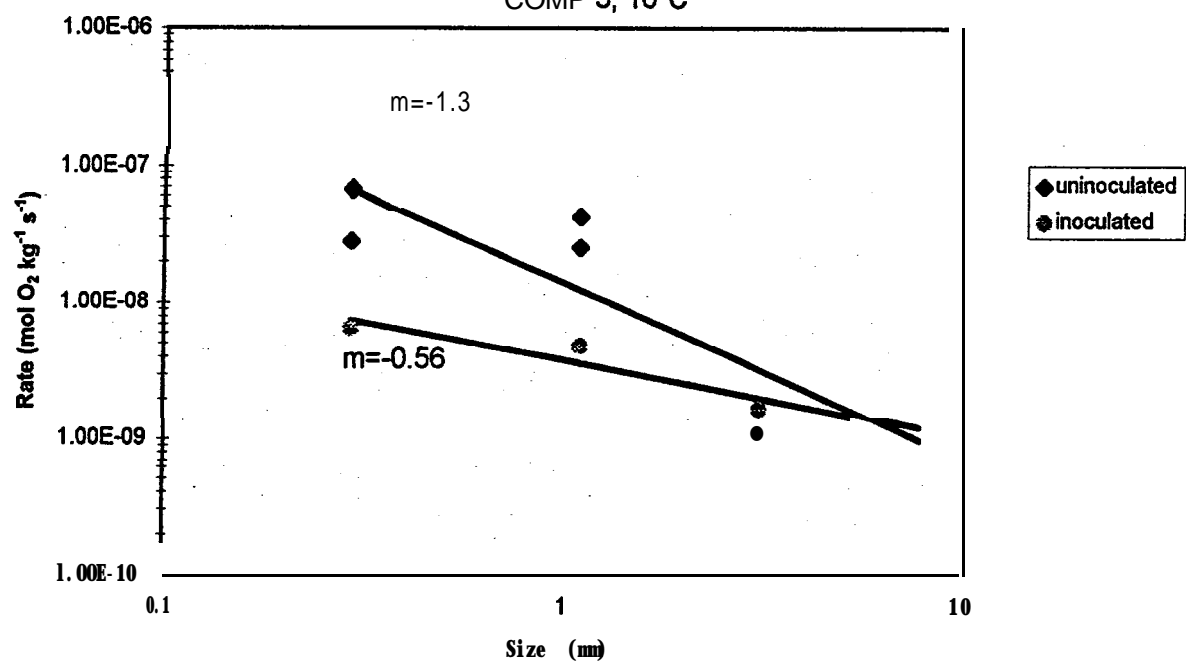


Figure 8.12: Oxygen Consumption Rate vs Size  
COMP 4, 10°C

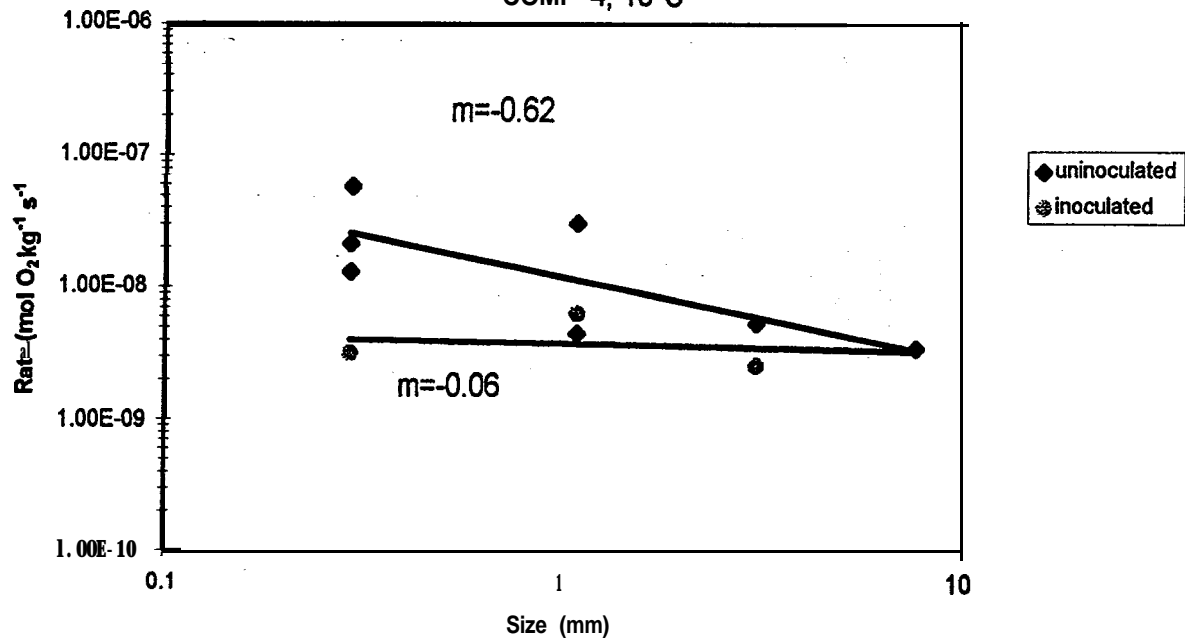


Figure 8.13: Oxygen Consumption Rate vs Size  
COMP1, 4°C

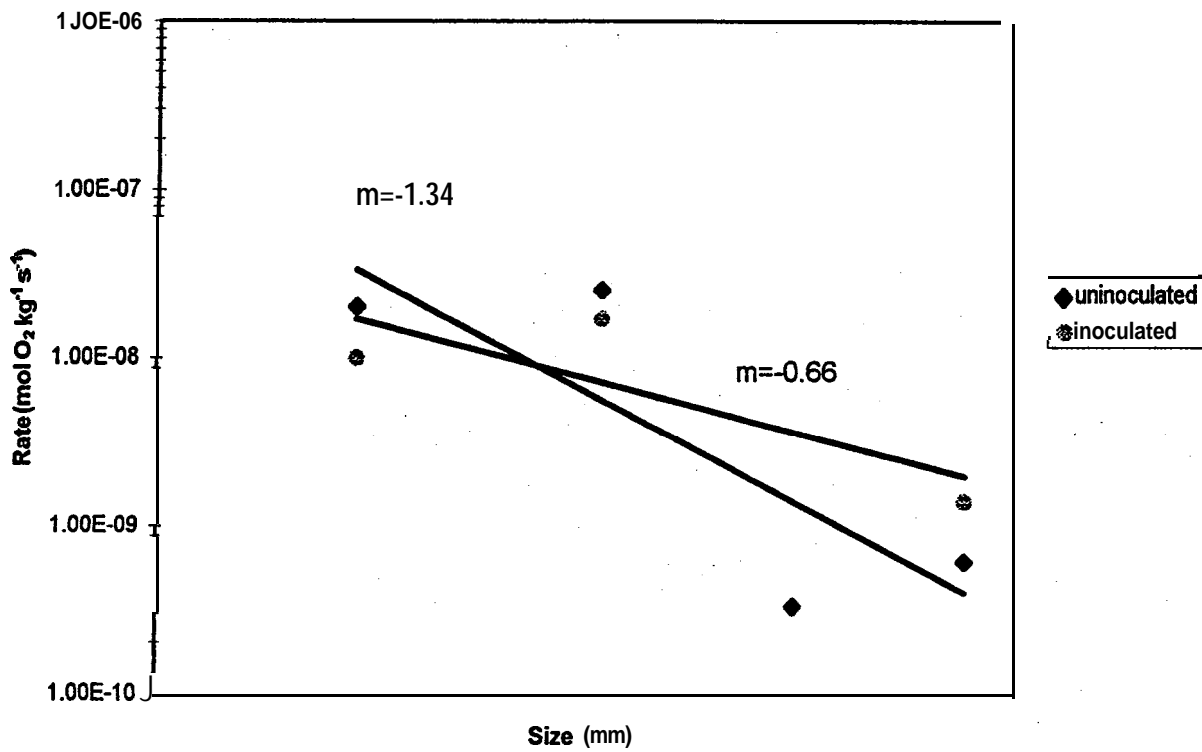


Figure 8.14: Oxygen Consumption Rate vs Size  
COMP2,4°C

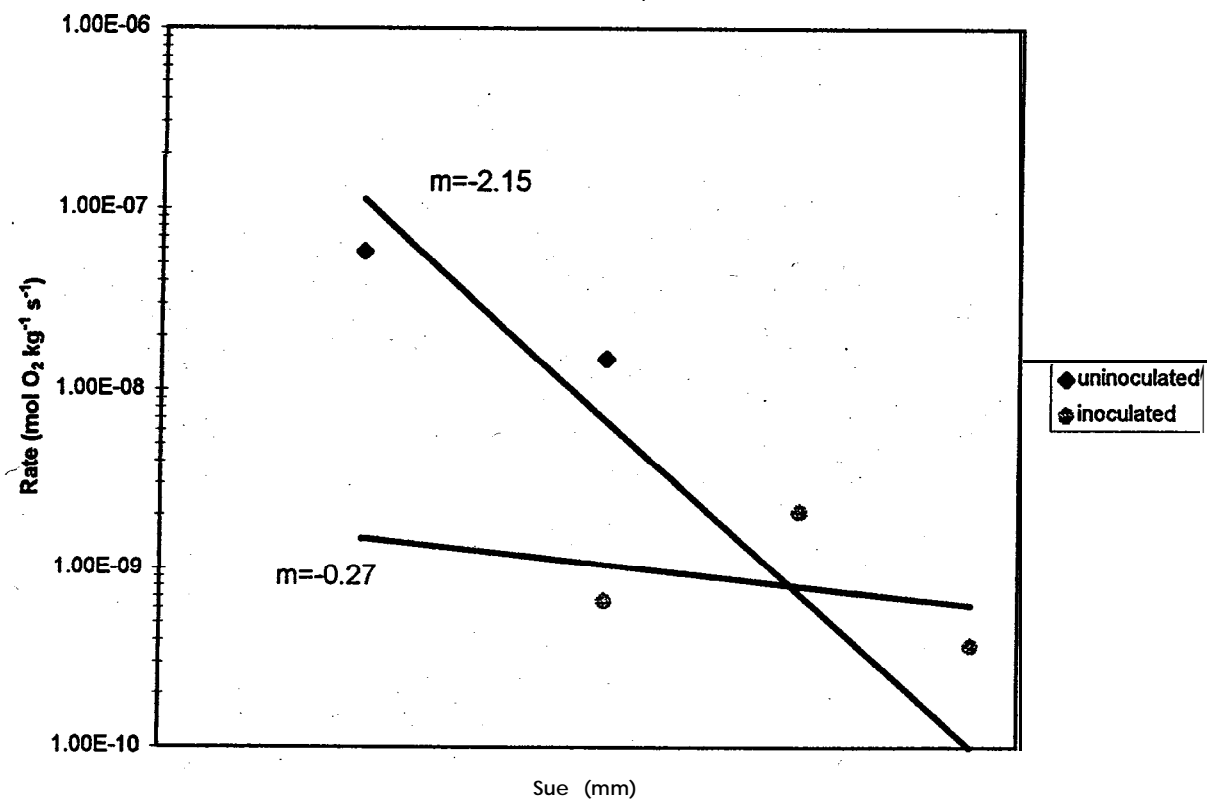


Figure B.15: Oxygen Consumption Rate vs Size  
COMP3, 4°C

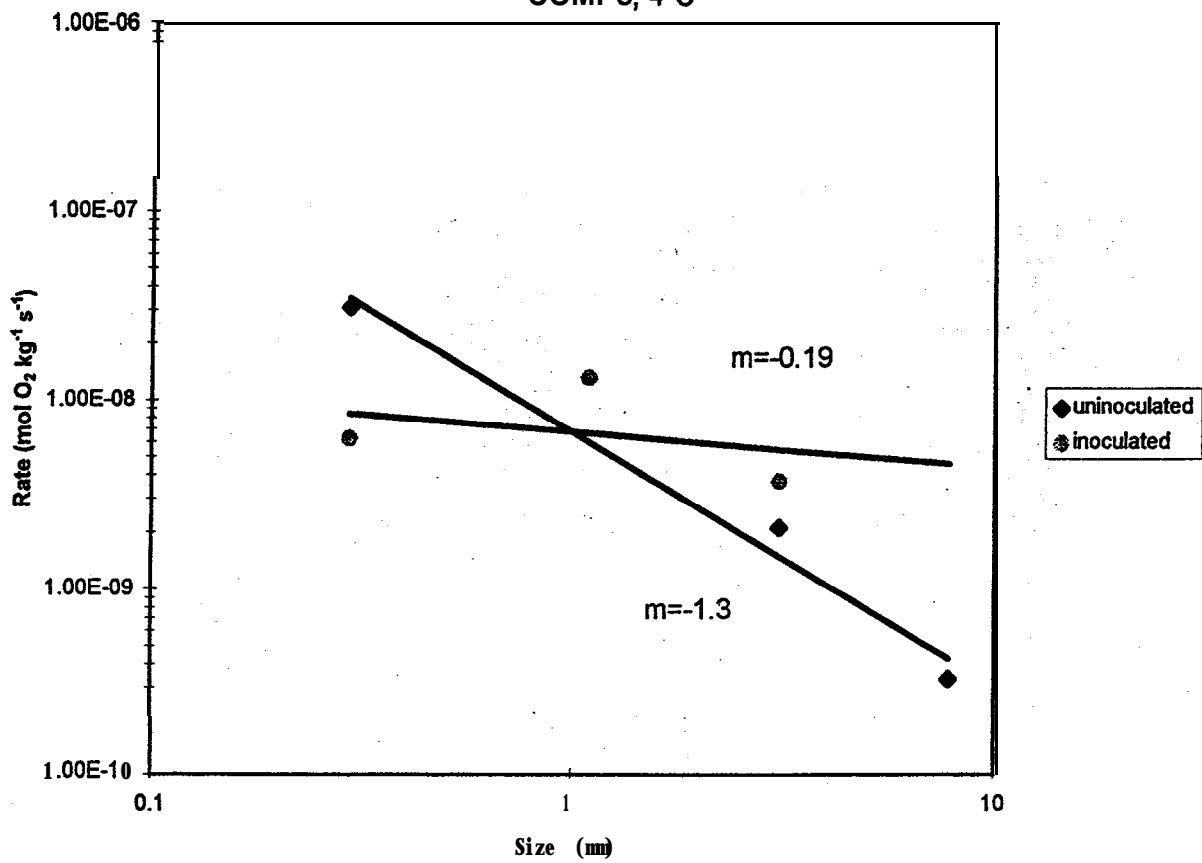
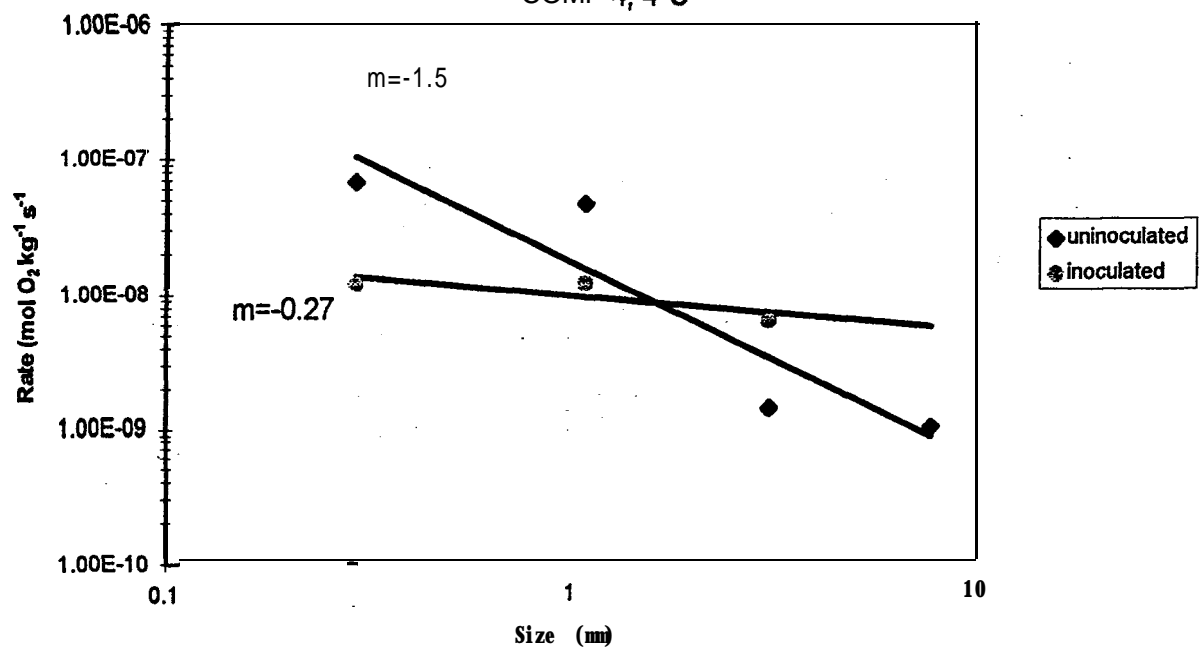


Figure B.16: Oxygen Consumption Rate vs Size  
COMP 4, 4°C



## Appendix C: Arrhenius Plots

Figure C.I: Arrhenius Plot for Whistle massive Snorite  
7 mm size fraction

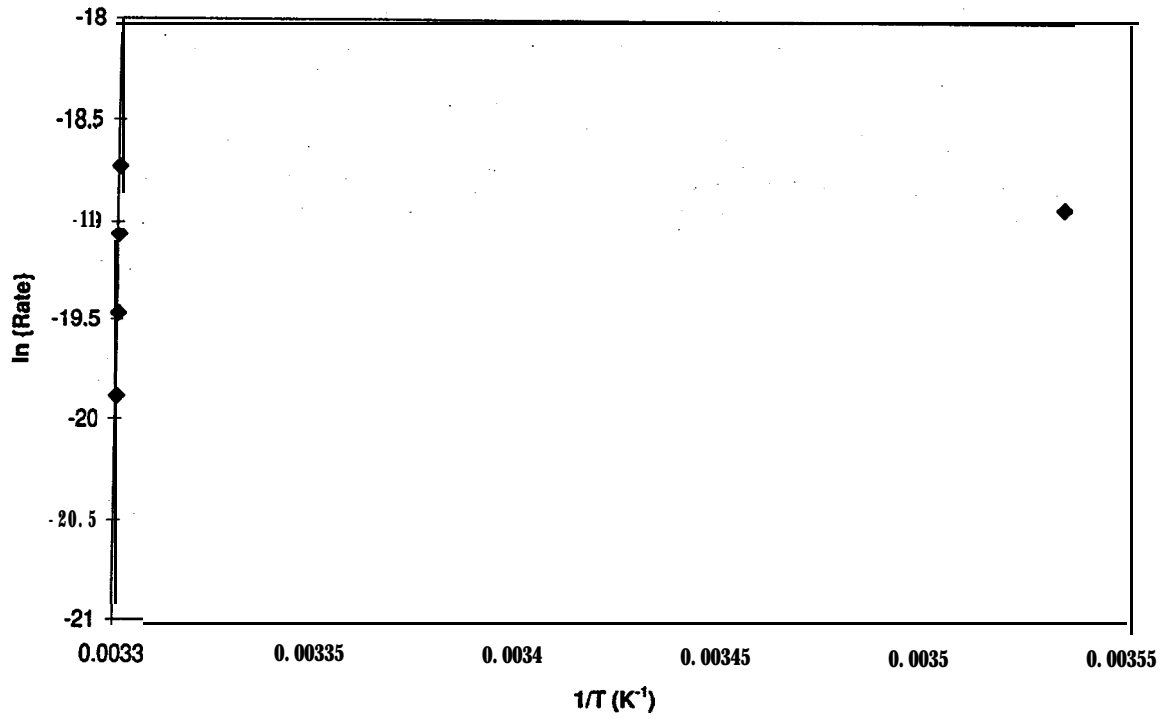
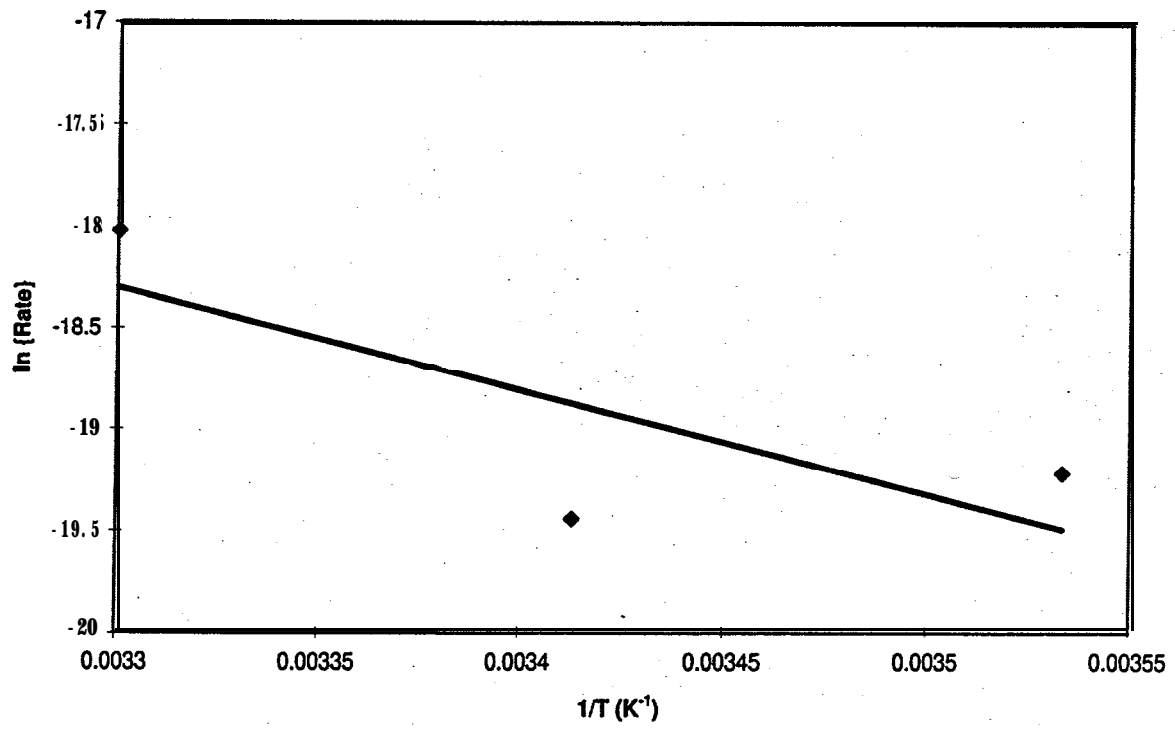


Figure C.2: Arrhenius Plot for Whistle high Snorite  
7 mm size fraction



**Figure C.3: Arrhenius Plot for Whistle medium Snorite**  
7 mm size fraction

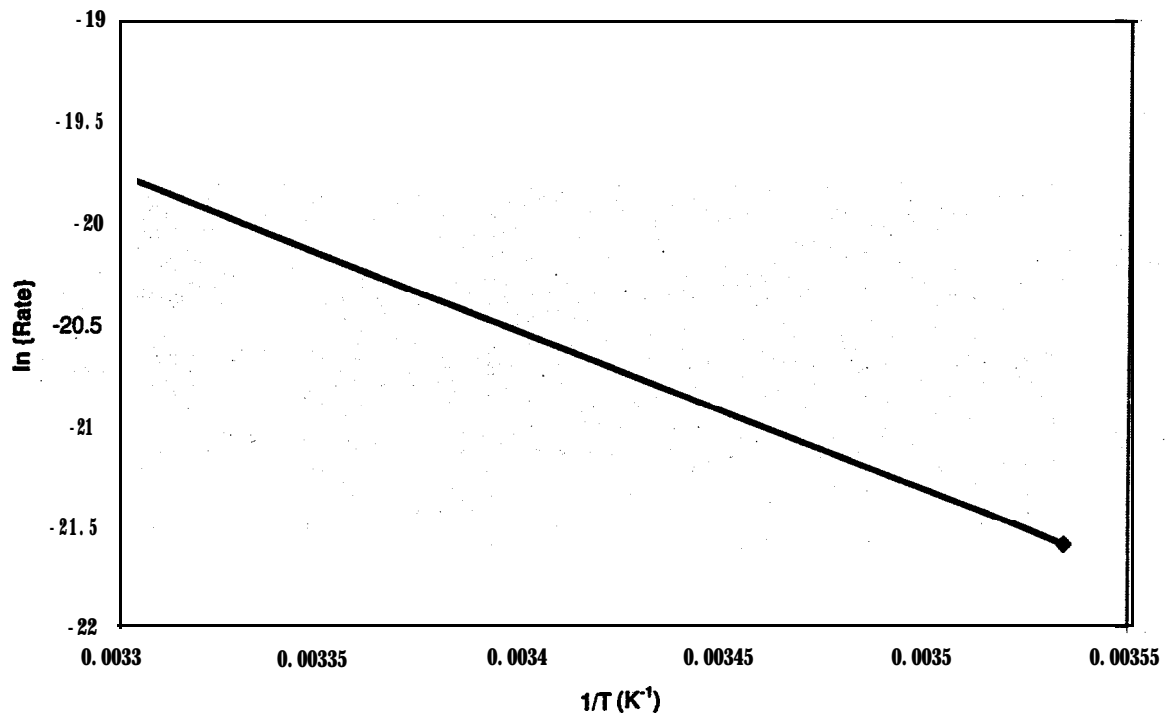


Figure C.4: Arrhenius Plot for Whistle low Snorite  
7 mm size fraction

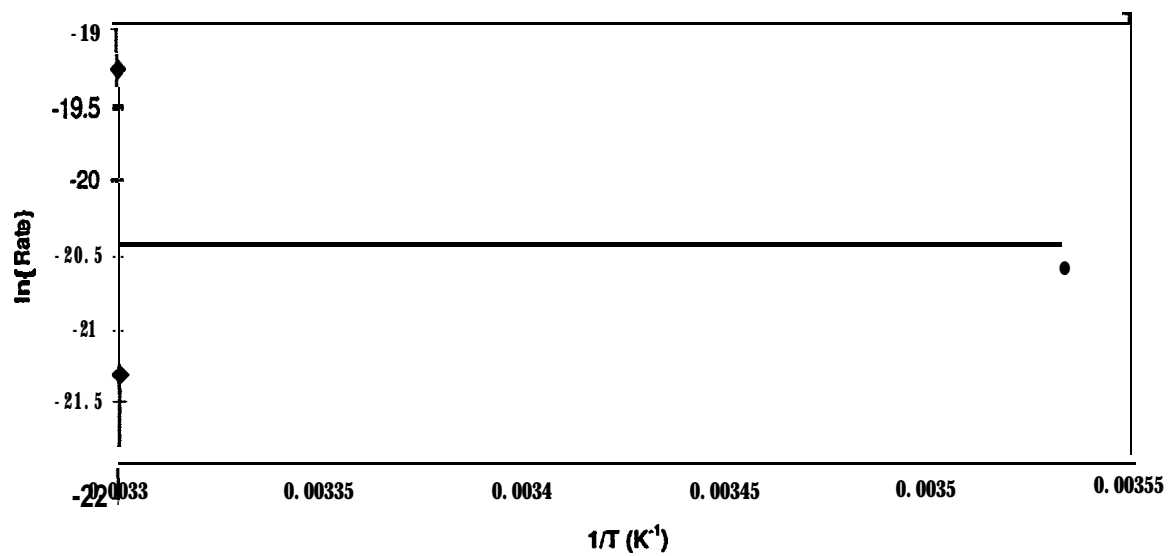


Figure C.5: Arrhenius plot for Voisey's BayCOMPs  
8 mm size fraction

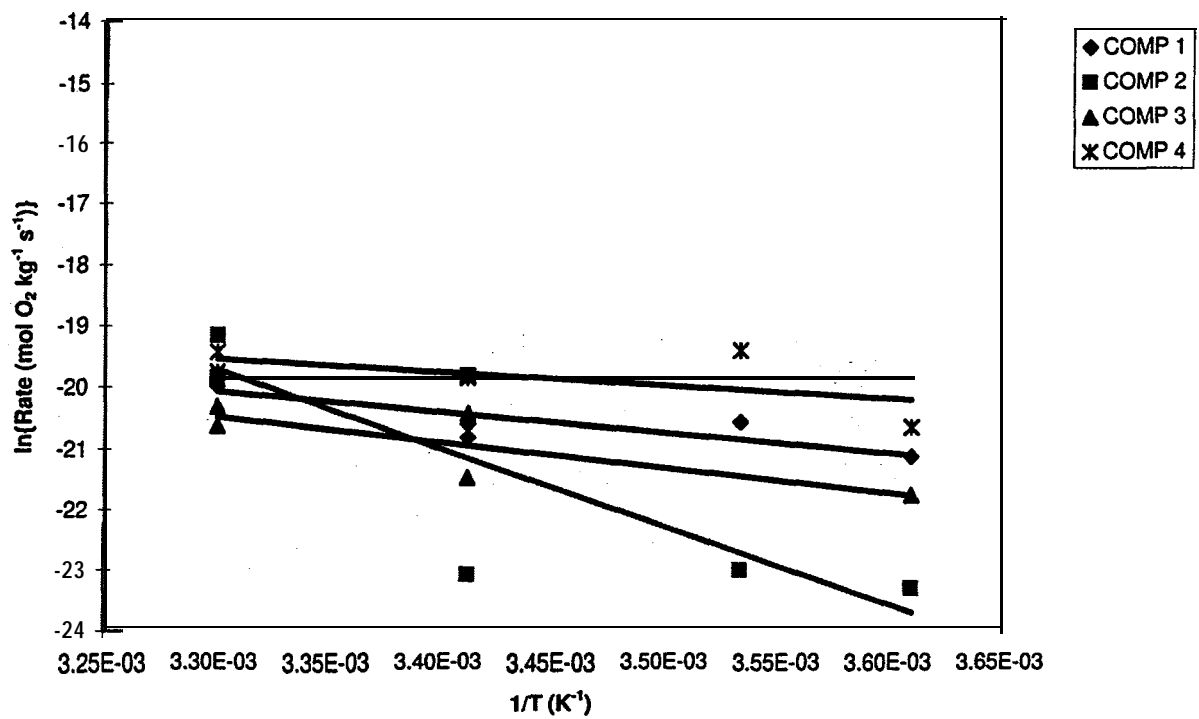


Figure C.6: Arrhenius plot for Voisey's BayCOMPs  
3 mm size fraction

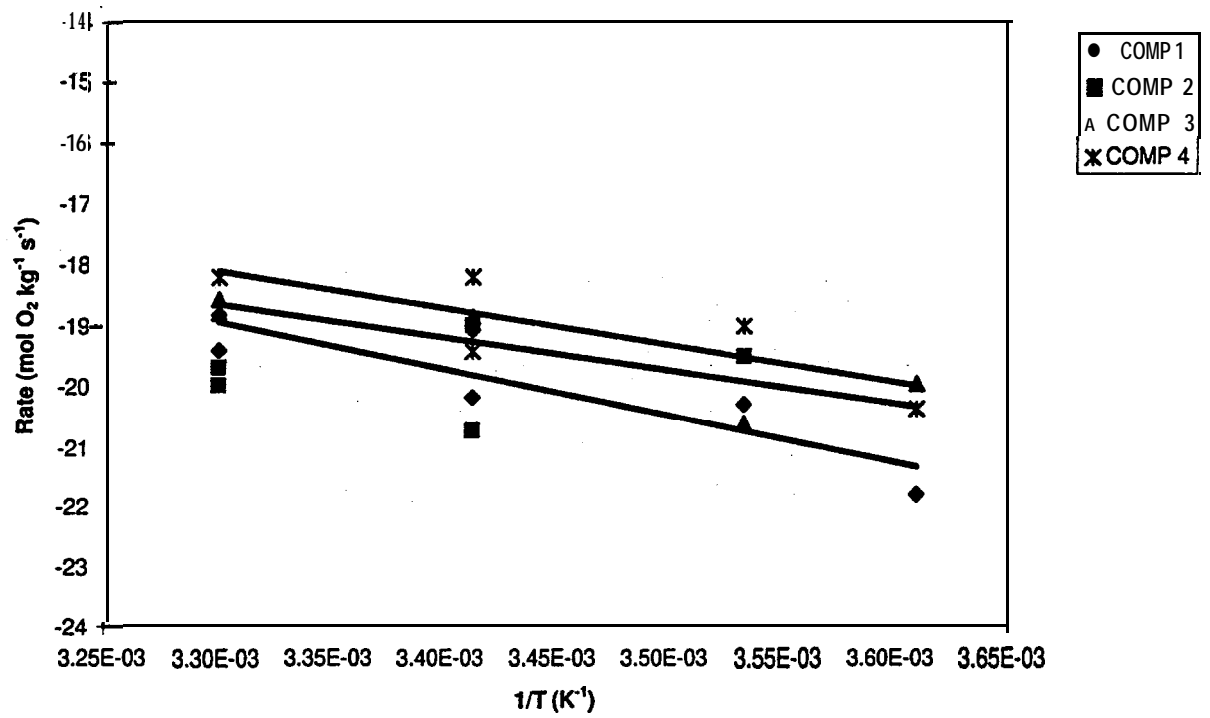


Figure C.7: Arrhenius plot for Voisey's BayCOMPs  
1 mm size fraction

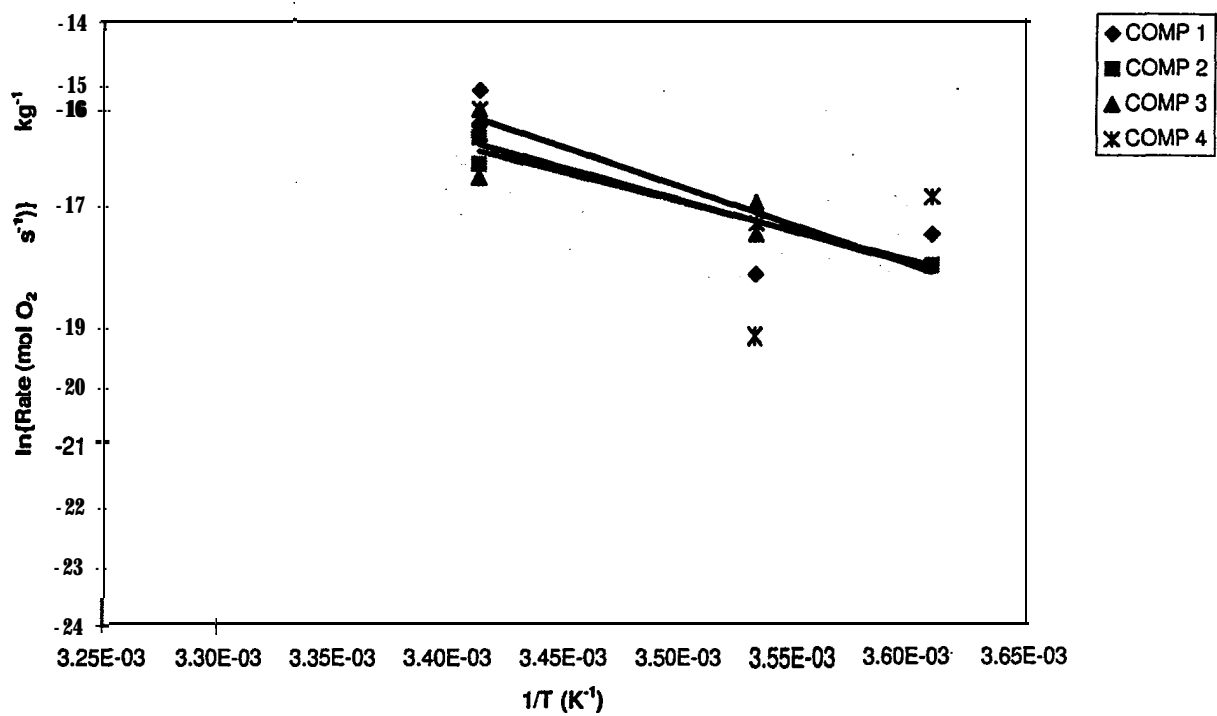


Figure C.8: Arrhenius plot for Voisey's BayCOMPs  
0.3 mm size fraction

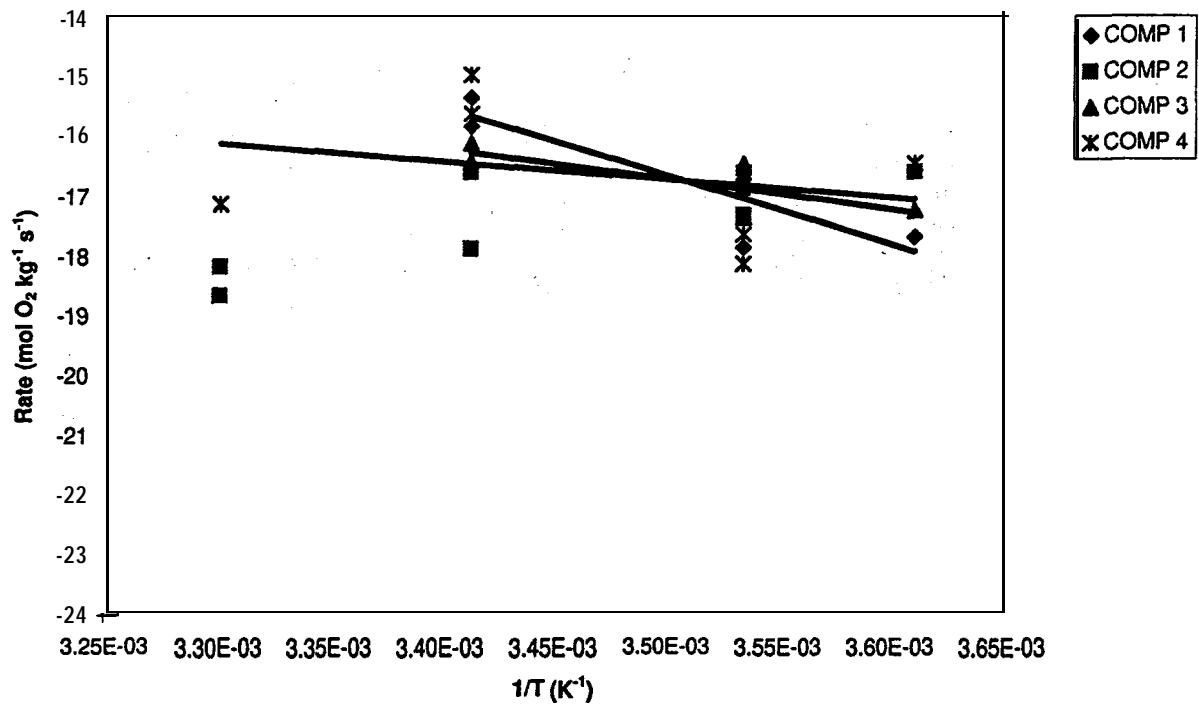


Figure C.9: Arrhenius Plot for Faro Waste Rock

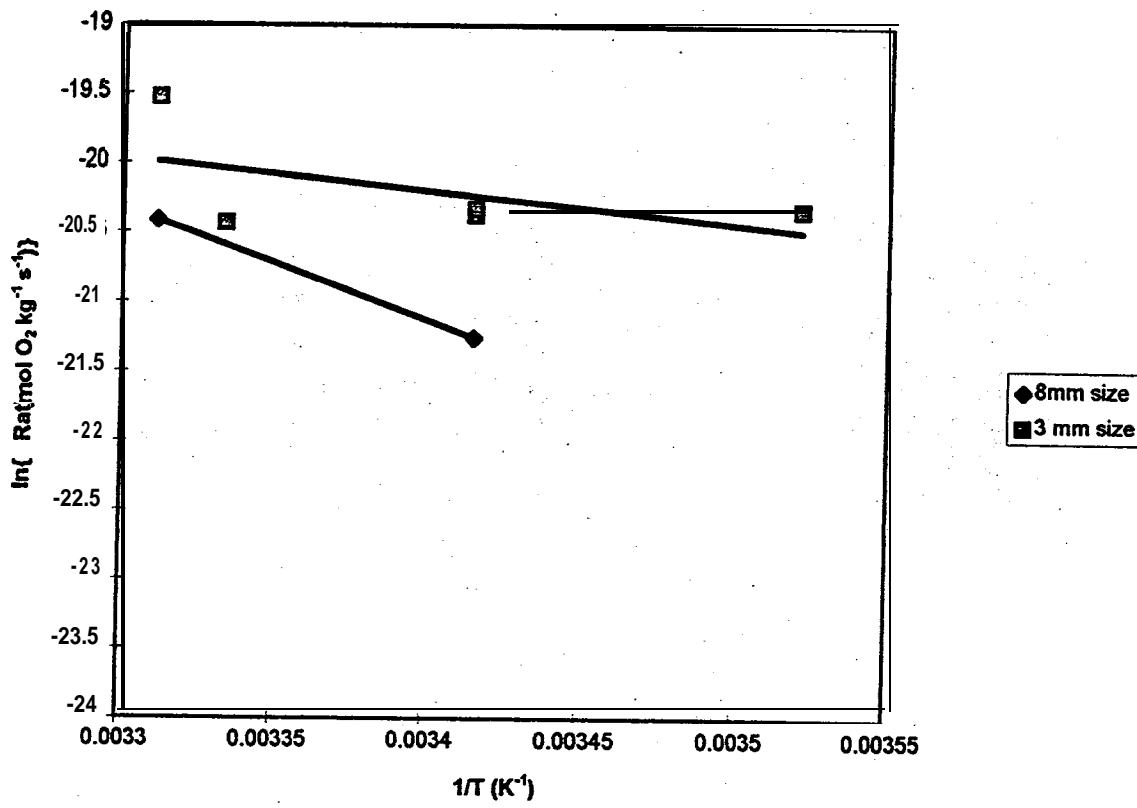


Figure C.10: Arrhenius Plot for Mine Doyon Waste Rock

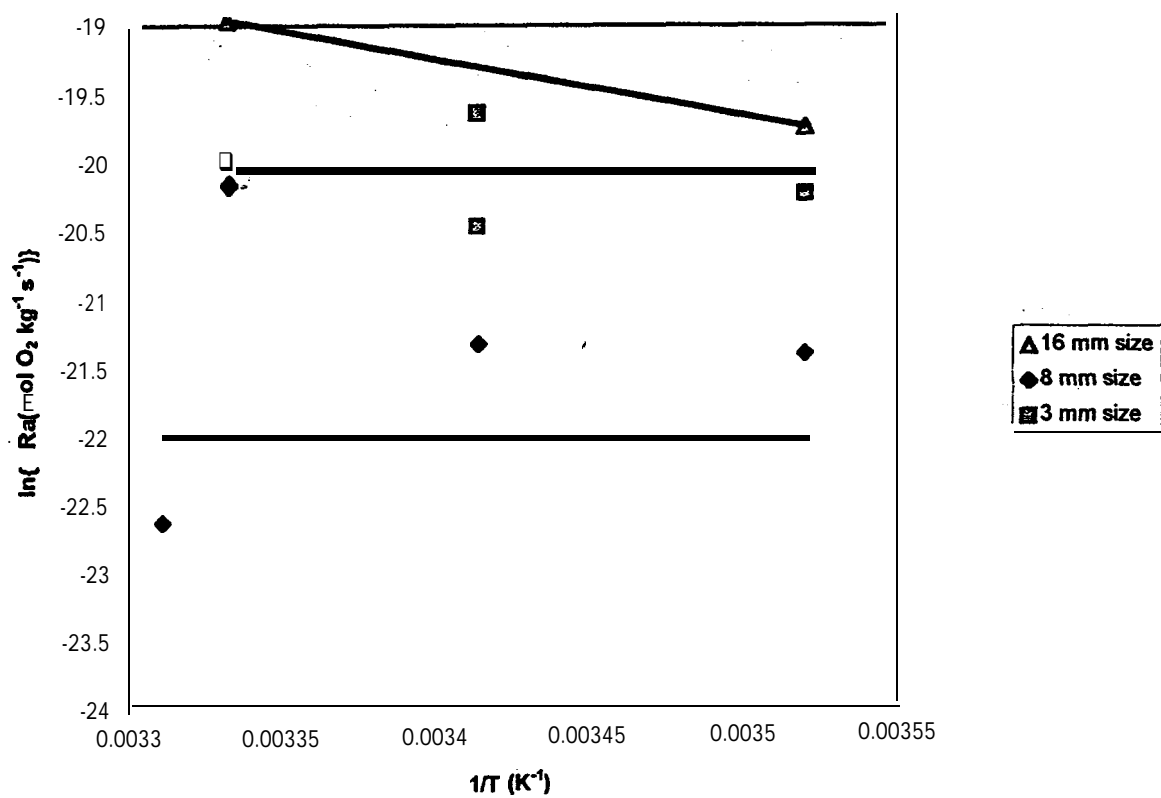


Figure C.11: Arrhenius Plot for Whistle high S Waste Rock

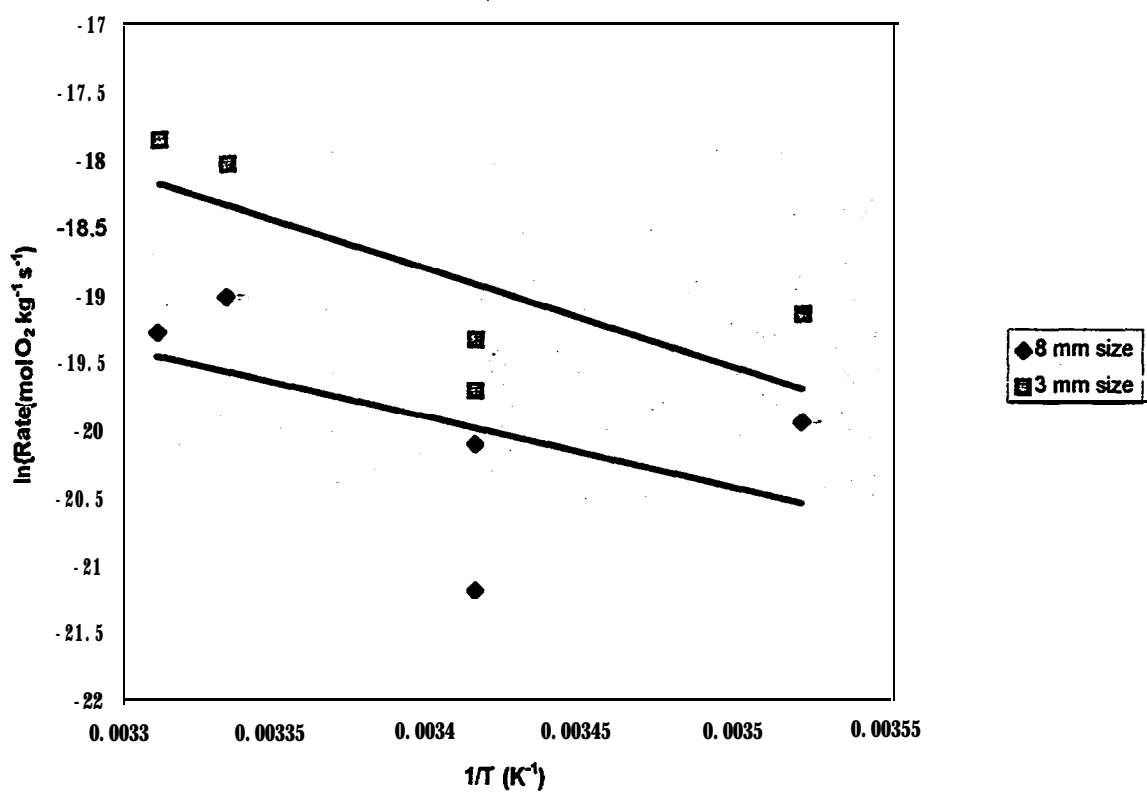


Figure C.12: Arrtmnius Plot for Whistle low S Waste Rock

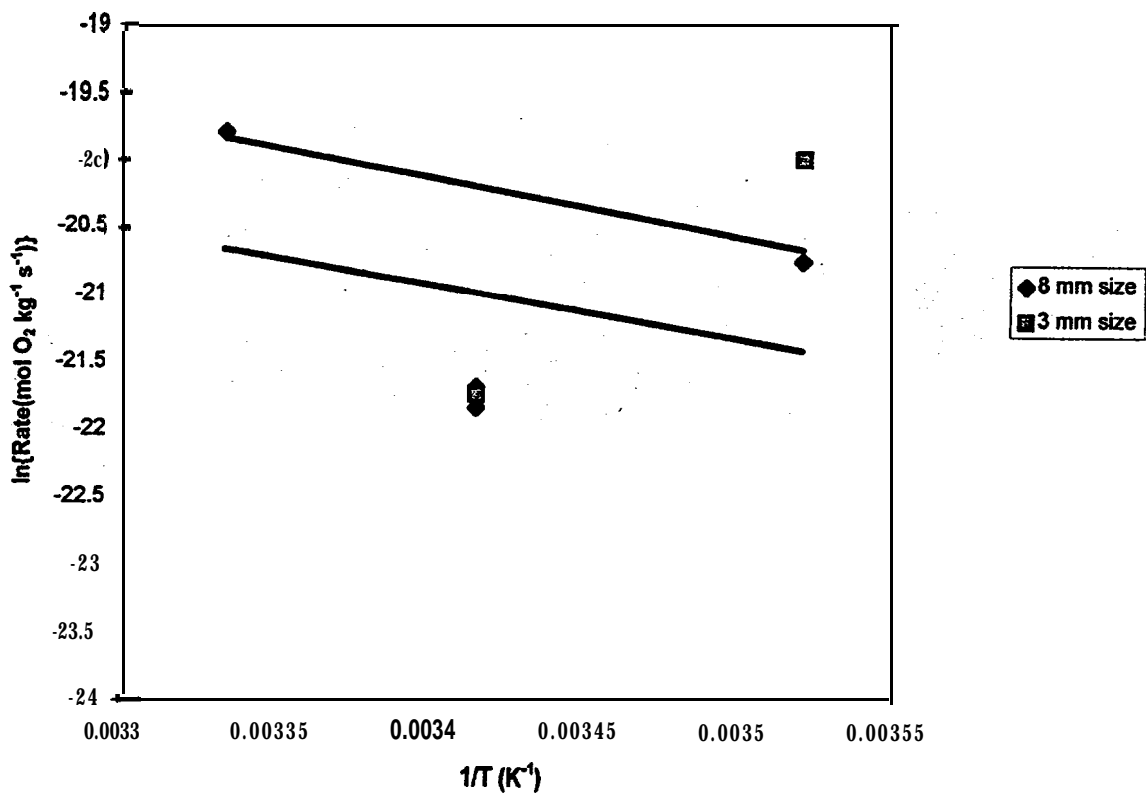


Figure C.13: Arrhenius Plot for Pamour Waste Rock

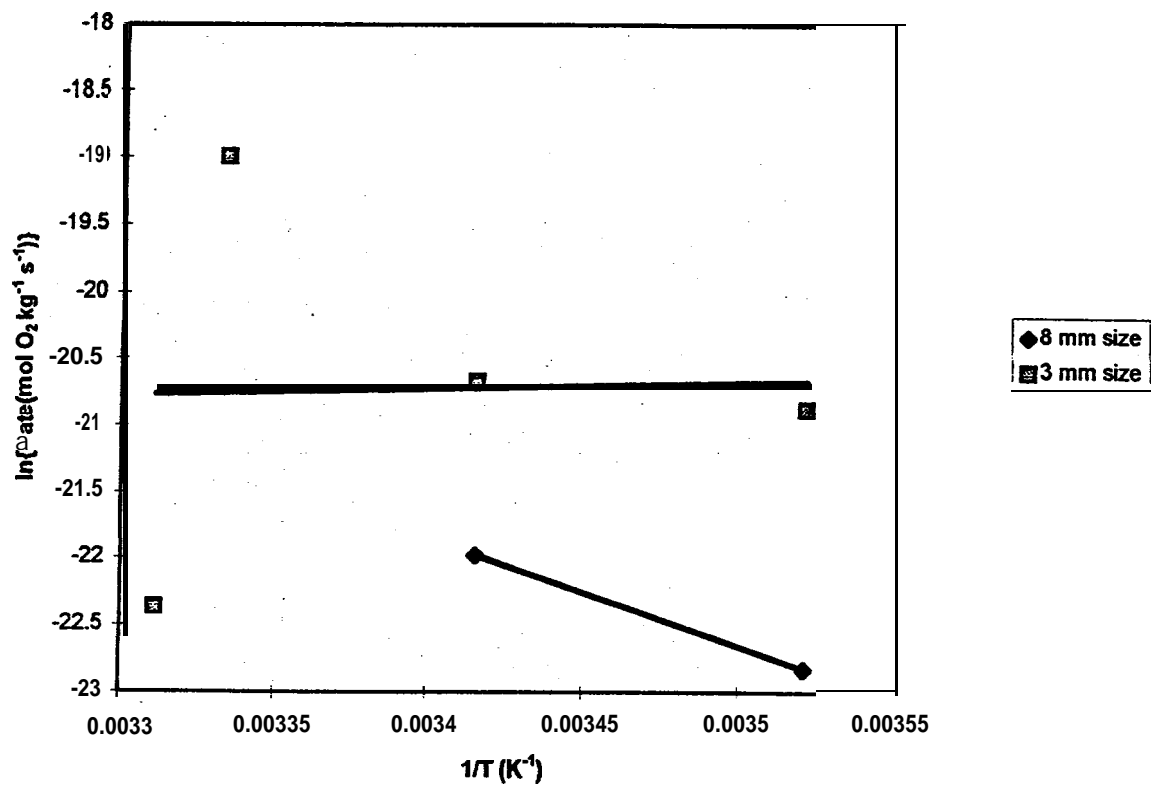
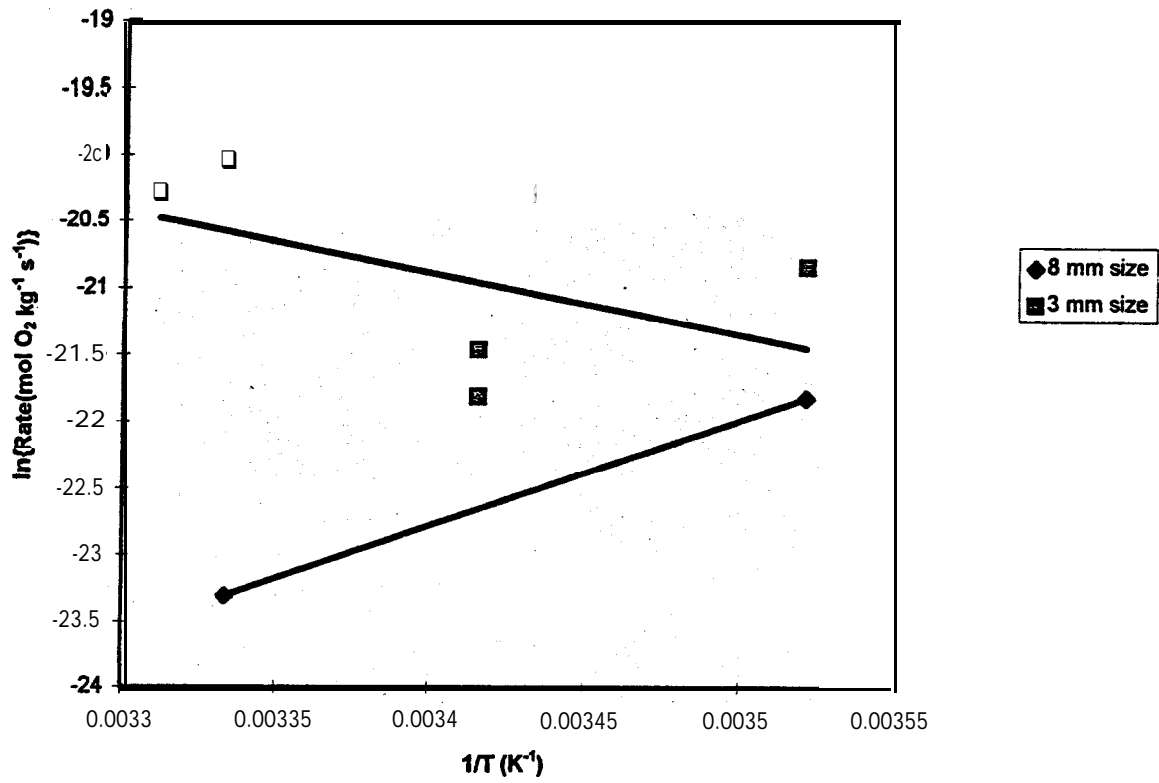


Figure C.14: Arrhenius Plot for KZK Waste Rock



## **Appendix D: Oxygen Consumption Rate vs. Sulphur Content for Voisey's Bay COMP Samples**

Figure D.1: Oxygen Consumption Rate vs %S  
Voisey's Bay COMPs, 30°C

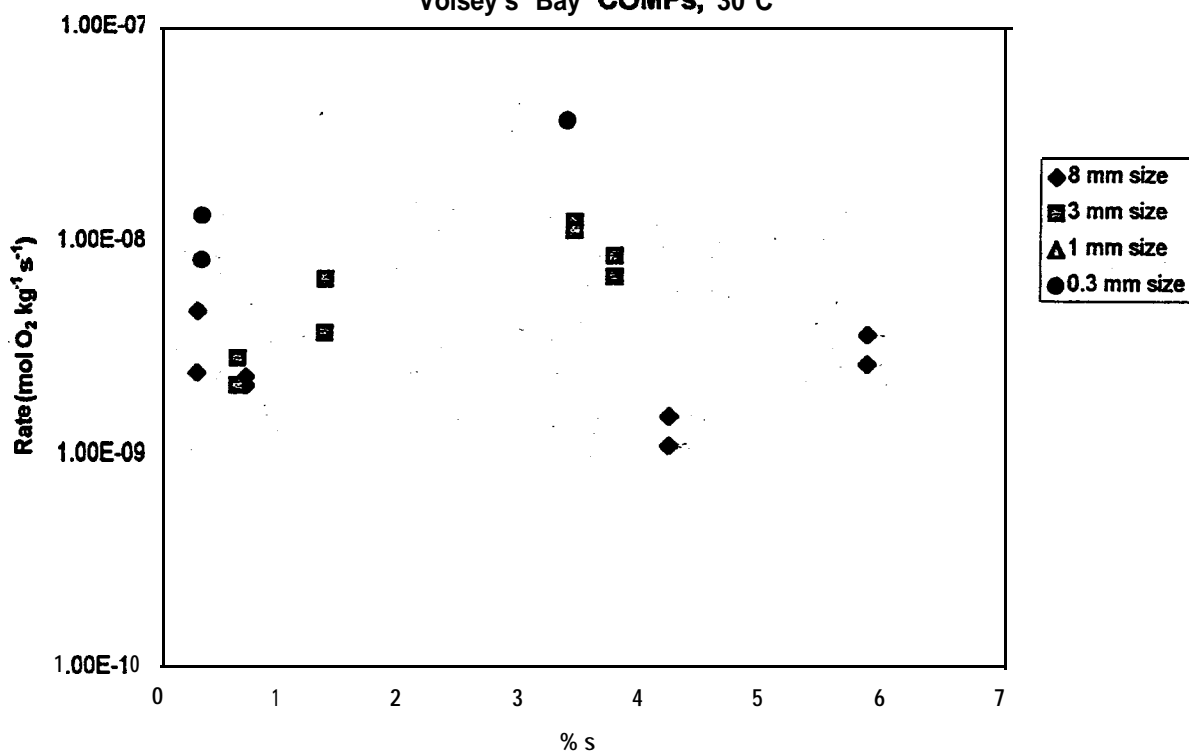


Figure D.2: Oxygen Consumption Rate vs %S  
Voisey's Bay COMPs, 20°C

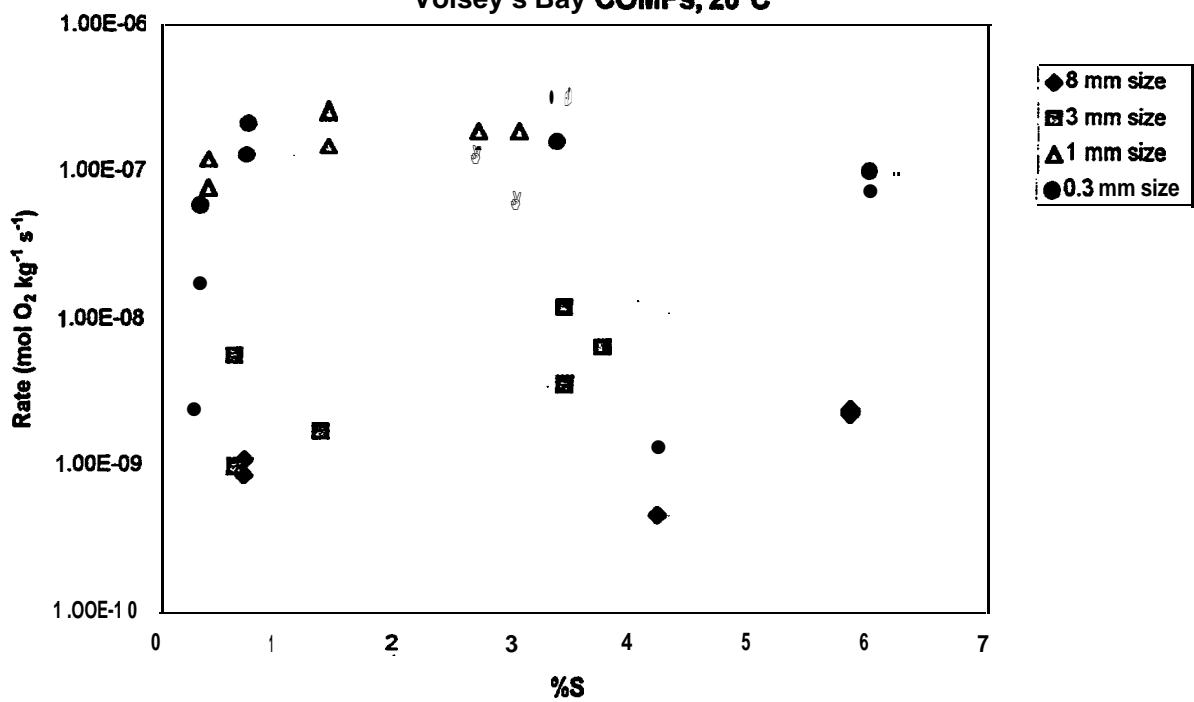


Figure D.3: Oxygen Consumption Rate vs %S  
Voisey's Bay COMPs, 10°C

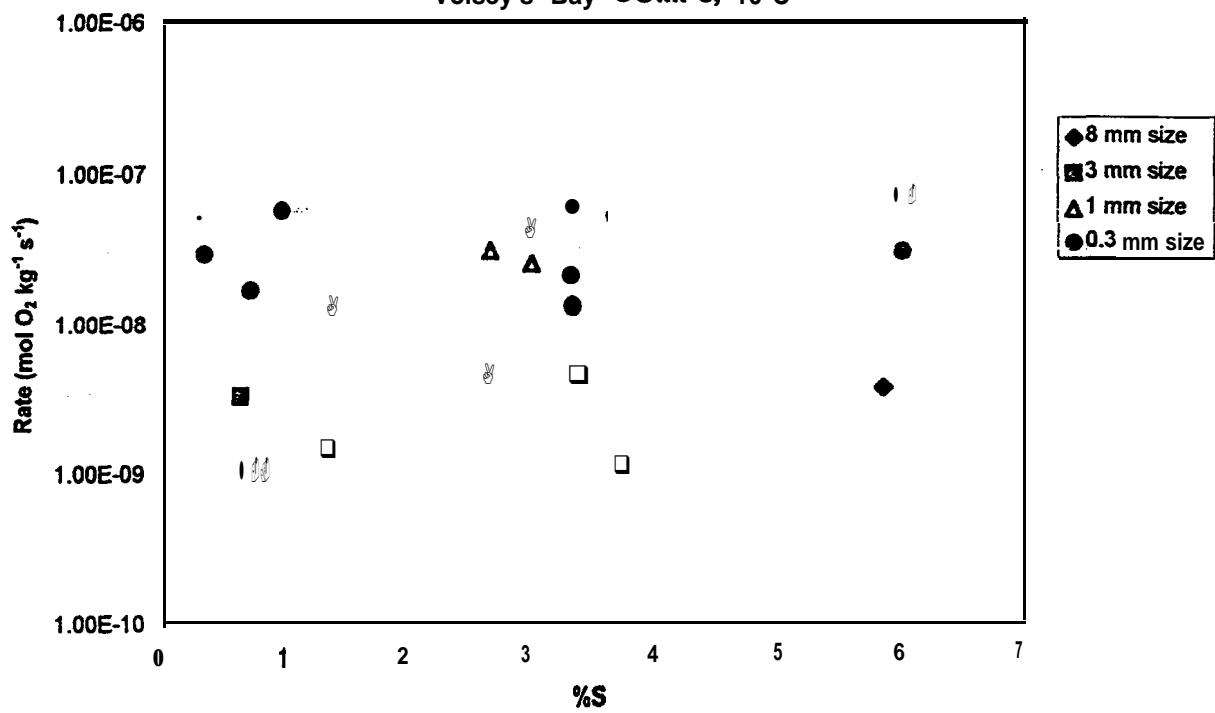


Figure D.4: Oxygen Consumption Rate vs %S  
Voisey's Bay COMPs, 4°C

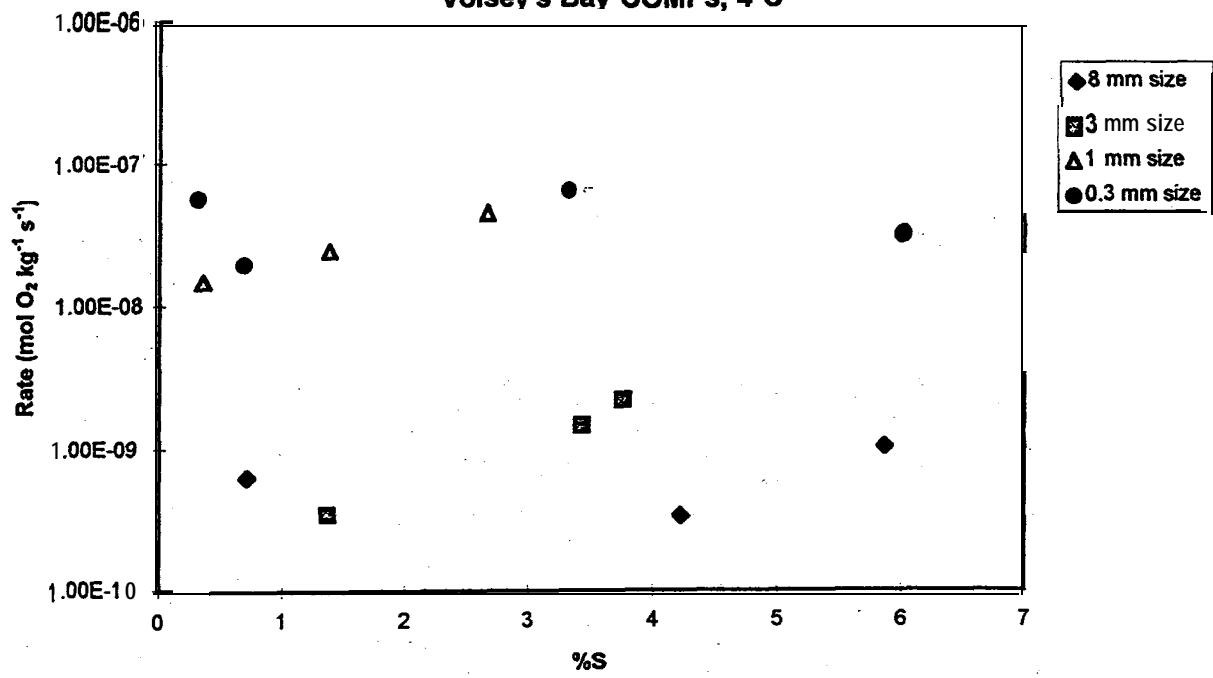


Figure D.5: Oxygen Consumption Rate vs %S  
Voisey's Bay COMPs inoculated at 30°C

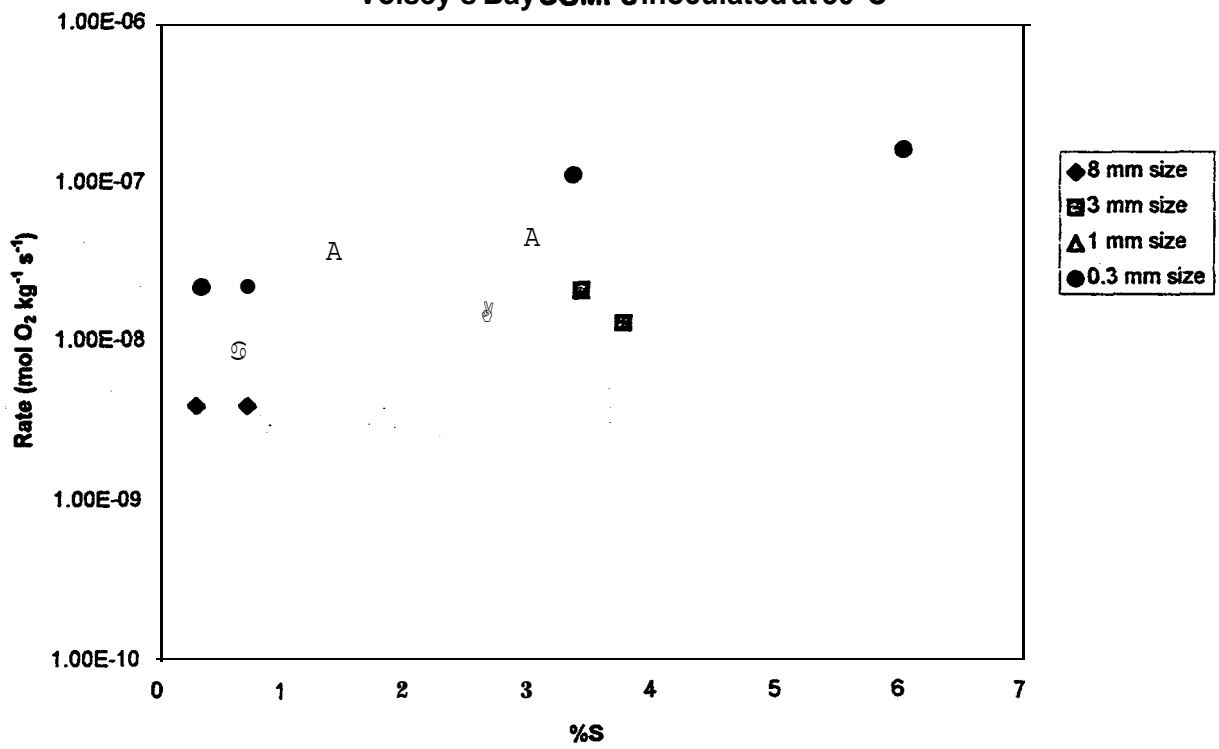


Figure D.6: Oxygen Consumption Rate vs %S  
 Voisey's Bay COMPs inoculated at 10°C

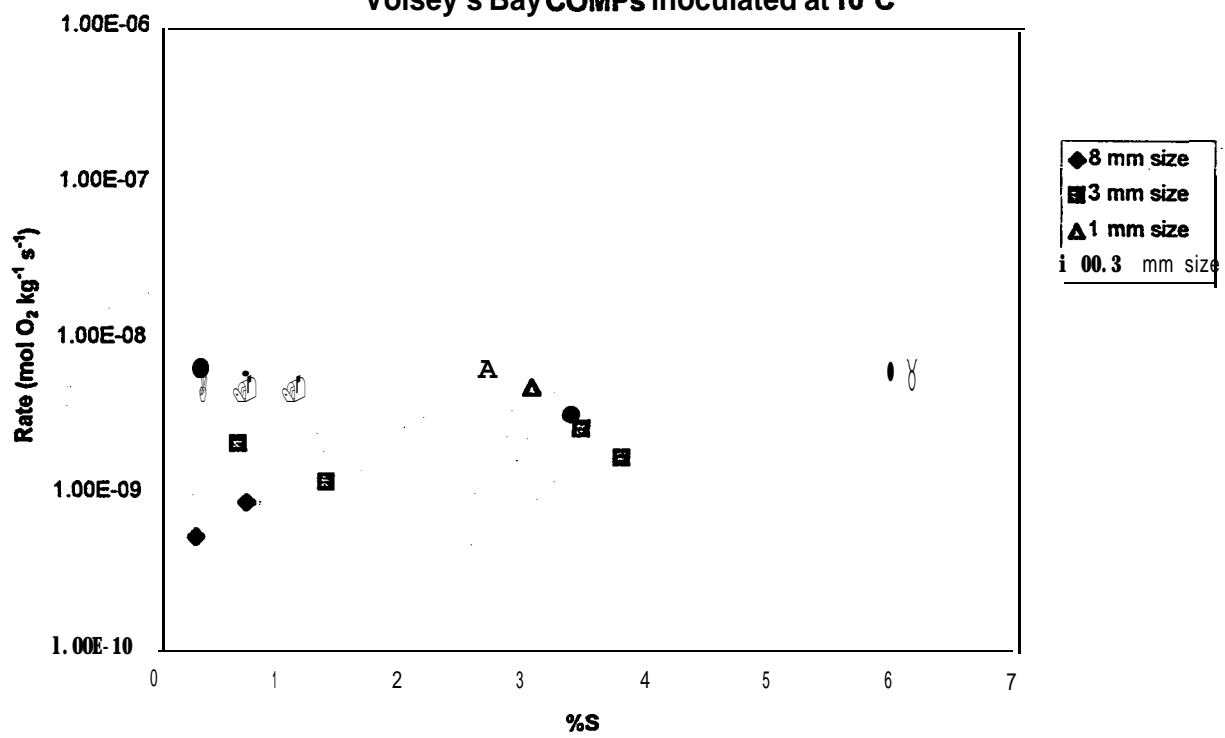
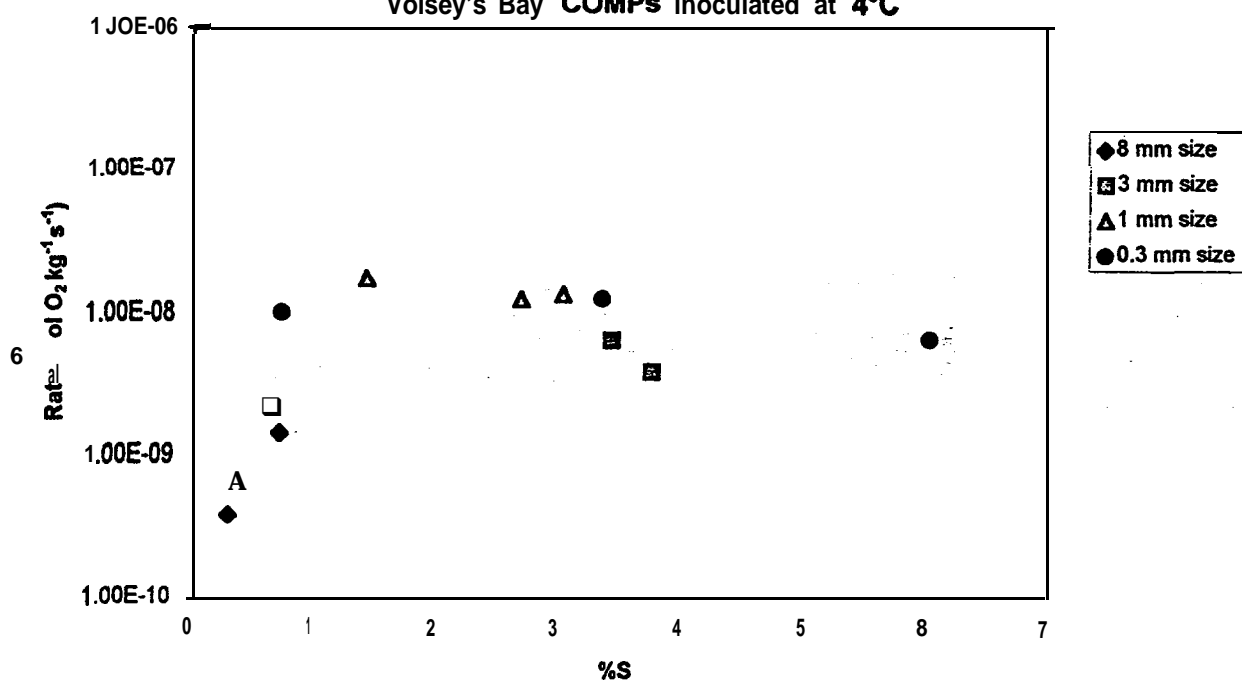


Figure D.7: Oxygen Consumption Rate vs KS  
Voisey's Bay COMPs inoculated at 4°C



## Appendix E: Normalized Oxygen Concentration vs. Time for 17L Tests

Figure E.I: Normalized Oxygen Concentration vs. Time

Whistle massive S, 87.2 mm size, 20°C

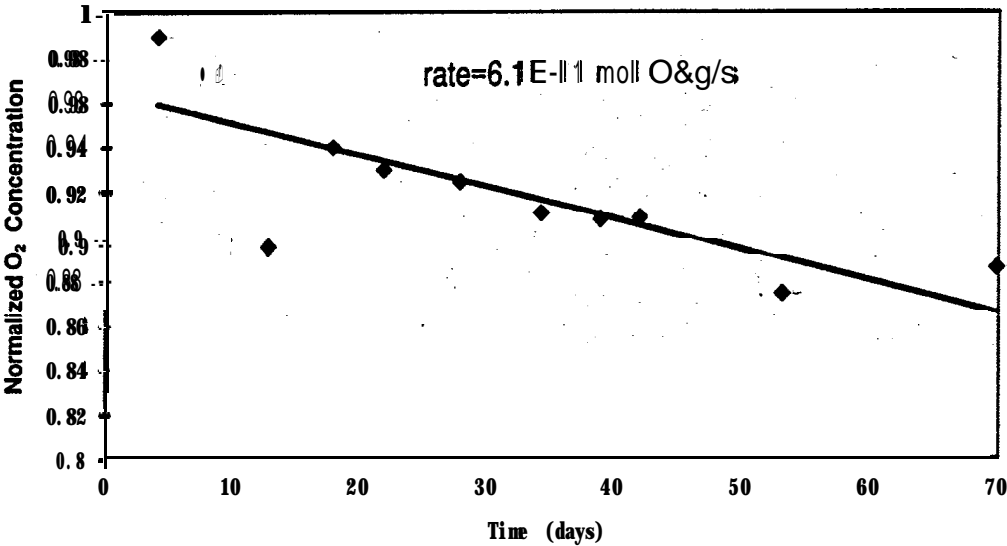


**Figure E.2: Normalized Oxygen Concentration vs. Time**  
Whistle High S Norite, 87.1 mm diameter, 20°C

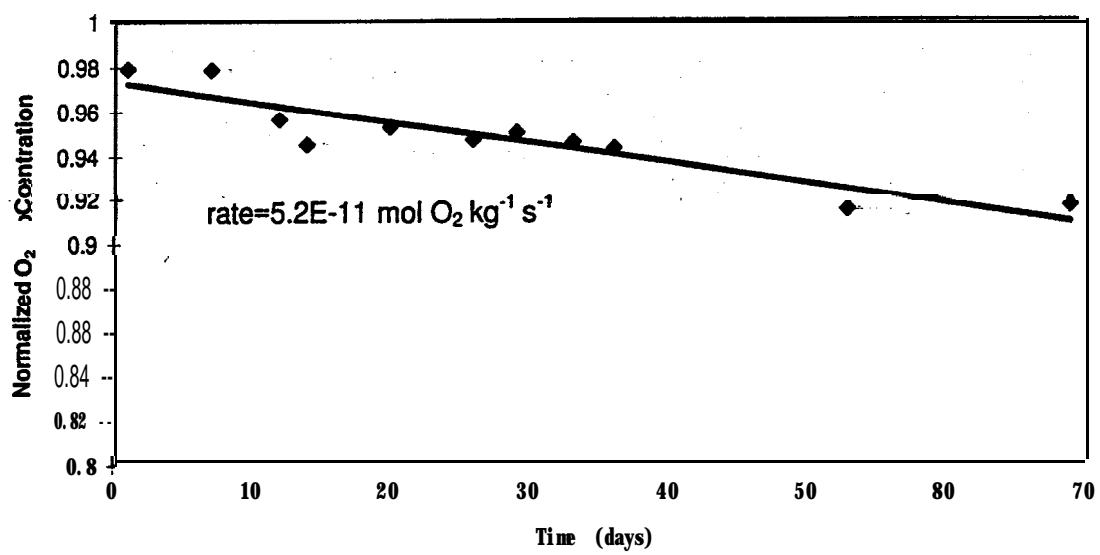


Figure E.3: Normalized Oxygen Concentration vs. Time  
Whistle Medium S Norite, 95.6 mm size, 20°C

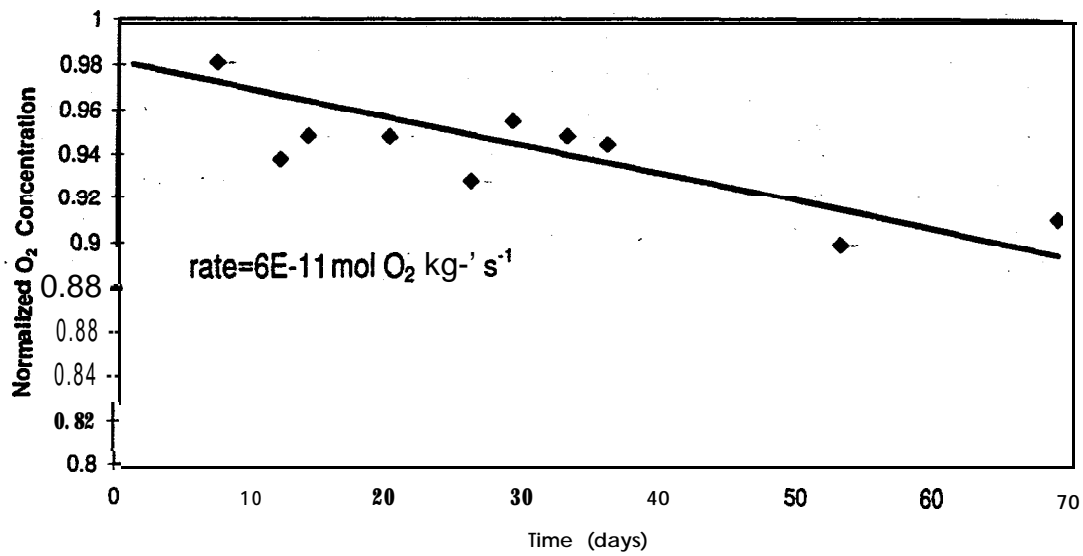
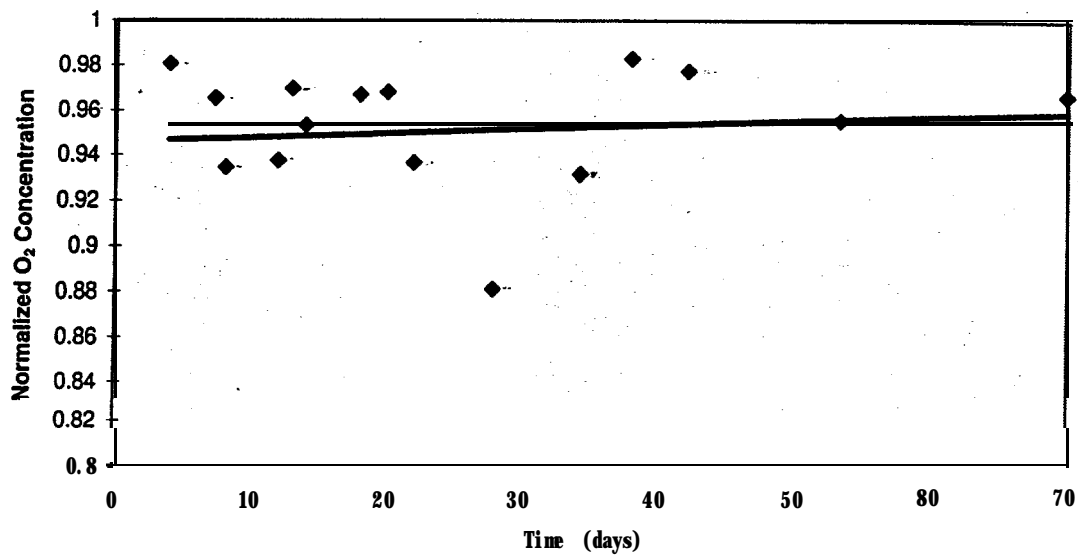


Figure E.4: Normalized Oxygen Concentration vs. Time  
Whistle Low S Norite, 83.9 mm size, 20°C



## Appendix F: Summary of Statistical Output from SYSTAT®

SYSTAT Output for Multivariable Regression Analysis of Uninoculated  
Rocks: **Voisey's** Bay COMP Samples

TUE 5/20/97 3:49:10 PM

SYSTAT VERSION 6.0.1  
COPYRIGHT (C) 1996, SPSS INC.

Welcome to SYSTAT!

>IMPORT 'N:\TEMP\NLIN.XLS' / TYPE=EXCEL  
IMPORT successfully completed.

>EDIT

>regress

>model y = constant + x1 + x2 + x3

>estimate .

Dep Var: Y N: 54 Multiple R: 0.862 Squared multiple R: 0.743

Adjusted squared multiple R: 0.728 Standard error of estimate: 1.034

Effect	Coefficient	Std Error	Std Coef	Tolerance	t	P(2 Tail)
CONSTANT	-4.034	4.438	0.0		-0.909	0.
X1	-1.339	0.113	-0.854	0.981	-11.794	0.
x2	0.293	0.138	0.153	0.998	2.126	0.
x3	-4044.090	1274.201	-0.230	0.982	-3.174	0.

Analysis of Variance

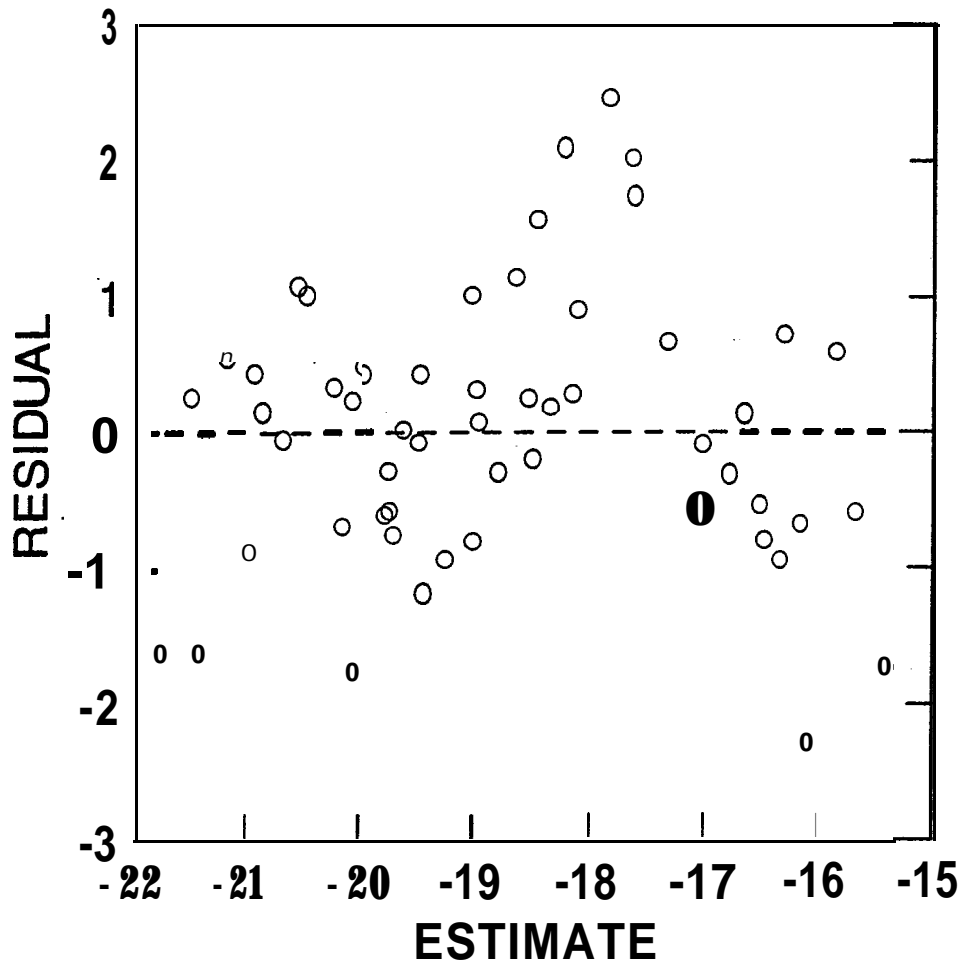
Source	Sum-of-Squares	DF	Mean-Square	F-Ratio	P
Regression	154.483	3	51.494	48.177	0.000
Residual	53.443	50	1.069		

Durbin-Watson D Statistic 1.268  
First Order Autocorrelation 0.317

NOTE: y = ln(Rate), X1 = ln(Particle Size in mm), X2 = ln(Sulphur Content in %),  
x3 = 1/(Temperature in K)

# Plot of Residuals against Predicted Values

from linear regression model of uninoculated rates  
Voisey's Bay COMP Samples



SYSTAT Output for Multivariable Regression Analysis of Inoculated  
 Rock: **Voisey's** Bay **COMP** Samples

>IMPORT 'N:\TEMP\BACRATE.XLS' / TYPE=EXCEL  
 IMPORT successfully completed.

>regress

>model y = constant + x1 + x2 + x3

>estimate

Dep Var: Y N: 37 Multiple R: 0.869 Squared multiple R: 0.754

Adjusted squared multiple R: 0.732 Standard error of estimate: 0.714

Effect il)	Coefficient	Std Error	Std Coef	Tolerance	t	P(2 Ta
CONSTANT 658	1.406	3.145	0.0	.	0.447	0.
X1 000	-0.566	0.105	-0.488	0.914	-5.407	0.
x2 002	0.423	0.124	0.307	0.915	3.408	0.
x3 000	-5825.957	902.468	-0.557	0.999	-6.456	0.

Analysis of Variance. .

Source	Sum-of-Squares	DF	Mean-Square	F-Ratio	P
Regression	<b>51.727</b>	<b>3</b>	17.242	33.783	0.000
Residual	16.843	33	0.510		

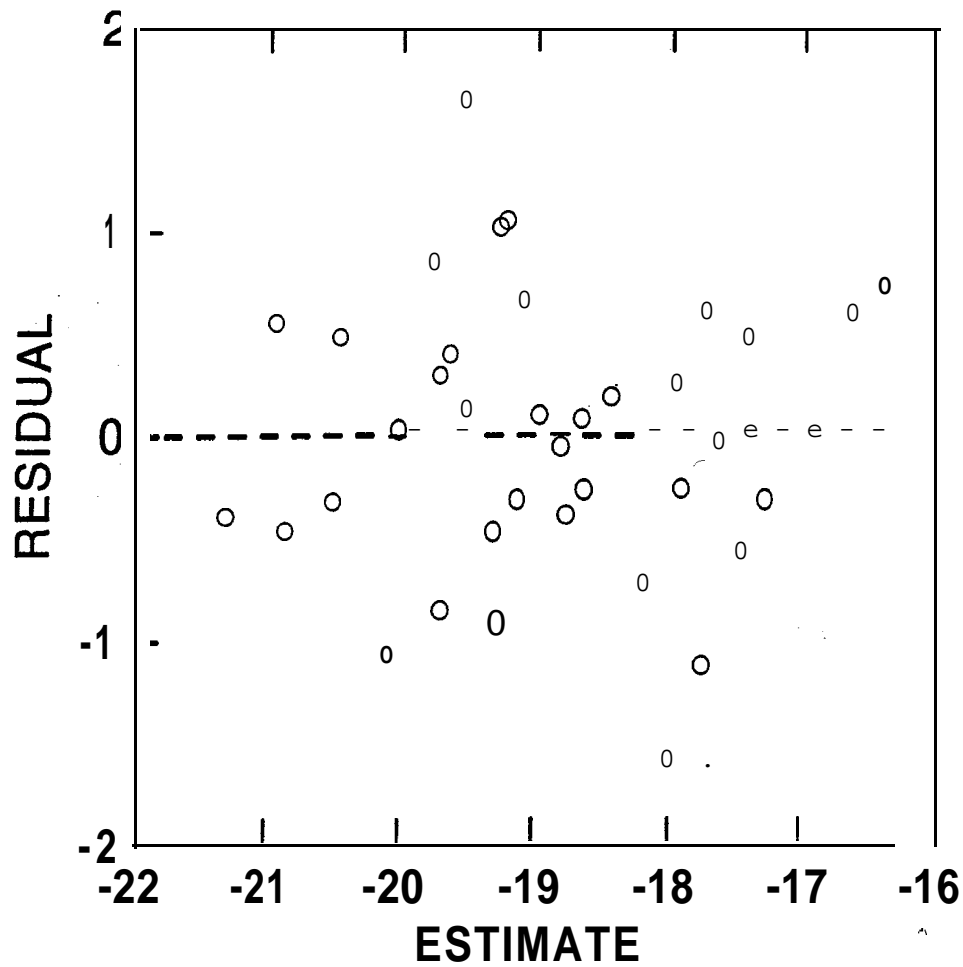
-----  
 --

Durbin-Watson D Statistic 2.379  
 First Order Autocorrelation -0.198

NOTE: Y = ln(Rate), X1 = ln(Particle Size in mm), X2 = ln(Sulphur Content in %), x3 = 1/(Temperature in K)

# Plot of Residuals against Predicted Values

from linear regression model of inoculated rates  
Voisey's Bay COMP Samples



## Appendix G: Analytical Reports

**ACTLABS**

**ACTIVATION  
LABORATORIES LTD**

---

Invoice No.: 10901  
Work Order: 10972  
Invoice Date: 02-AUG-96  
Date Submitted: 10-JUL-96  
Your Reference: NONE  
Account Number: 1498

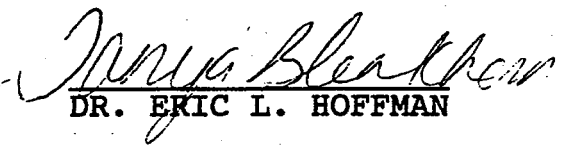
UNIVERSITY OF WATERLOO  
DEPT. OF EARTH SCIENCES  
WATERLOO, ONTARIO  
N2L 3G1

ANALYST: MARK ANDERSON

**CERTIFICATE OF ANALYSIS**  
-----

LECO  
901B - AQUA REGIA - ICP

CERTIFIED BY :

*per*   
DR. ERIC L. HOFFMAN

SAMPLE DESCRIPTION	S
WM1	4.81
WM2	5.01
WM3	6.04
WM4	1.94
WM5	1.85
WM6	1.76
WM7	2.32
WM8	2.71
WM9	2.31

# LAKEFIELD RESEARCH LIMITED

Box 4300, 185 Concession St., Lakefield, Ontario, K0L 2H0  
Phone : 705-652-2038 FAX : 705-652-6441

Environmental Services

Lakefield, November 10, 1996

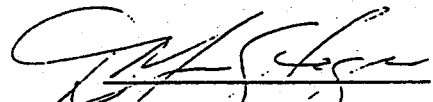
Date Rec. : October 28, 1996  
LR. Ref. : OCT7064.R96  
Reference : LR 9606819  
Project : 7777-296

## CERTIFICATE OF ANALYSIS

No.	Sample ID	S %	S= %
6	Analysis Date	01.11.96	06.11.96
7	Analysis Time	06:44	15:56
9	Comp 1-1/2+4m	0.71	0.64
10	Comp 1-4+10m	1.37	1.26
11	Comp 1-10+30m	1.42	1.35
12	Comp 1-30+100m	0.72	0.64
13	Comp 1-100+140m	1.55	1.34
14	Comp 2-1/2+4m	0.30	0.24
15	Comp 2-4+10m	0.64	0.55
16	Comp 2-10+30m	0.39	0.28
17	Comp 2-30+100m	0.33	0.02
18	Comp 2-100+140m	0.63	0.50
19	Comp 3-1/2+4m	4.22	3.97
20	Comp 3-4+10m	3.76	3.16
21	Comp 3-10+30m	3.03	2.51
22	Comp 3-30+100m	6.01	4.92
23	Comp 3-100+140m	6.13	4.92
24	Comp 4-1/2+4m	5.86	5.20
25	Comp 4-4+10m	3.43	2.97
26	Comp 4-10+30m	2.69	2.47
27	Comp 4-30+100m	3.35	2.93
28	Comp 4-100+140m	4.30	3.74
--	Check -- Replicate		
29	Comp 2-100+140m	0.63	0.53
30	Comp 4-100+140m	4.33	3.72

Sample Date: October 28, 1996

Sample Received: October 28, 1996 @ 1600

  
D. Masson Szogran

Lakefield, November 12, 1996

Date Rec. : September 25, 1996  
 LR. Ref. : SEP7134.R96  
 Reference : Hum Cell Init.ABA  
 Project : 7-296

## CERTIFICATE OF ANALYSIS

### Initial EPA ABA Modified

No.	Sample ID	Constant	Normality of HCl	HCL added mL	NaOH to pH=7.0	HCl (mL) Consumed	NP *	MPA *
9	ED-TROC-1	1.0076	0.5061	40	32.80	7.0	88.6	9.4
10	ED-TROC-1 D	1.0076	0.5061	40	33.00	6.8	86.0	17.2
11	ED-TROC-2	1.0076	0.5061	40	29.05	10.7	135.4	32.8
12	ED-TROC-2 D	1.0076	0.5061	40	29.40	10.4	131.6	46.6
13	ED-TROC-3	1.0076	0.5061	40	30.90	8.9	112.6	90.3
14	ED-TROC-3 D	1.0076	0.5061	40	31.30	8.5	107.5	81.6
15	ED-TROC-4	1.0076	0.5061	40	26.30	13.5	170.8	15.9
16	ED-TROC-4 D	1.0076	0.5061	40	24.10	15.7	198.6	14.1
17	ED-ORTHO-1	1.0076	0.5061	40	36.15	3.6	45.6	15.9
18	ED-ORTHO-1 D	1.0076	0.5061	40	36.10	3.6	45.6	14.4
-- Check --								
19	ED-TROC-2	1.0076	0.5061	40	29.30	10.5	132.9	34.1

No.	Sample ID	CMNP *	NP/MPA *	Paste pH units	S %	S= %	CO3 %	SO4 %
9	ED-TROC-1	79.2	9.4	9.66	0.37	0.30	0.4	< 0.4
10	ED-TROC-1 D	68.8	5.0	9.69	0.64	0.55	0.4	< 0.4
11	ED-TROC-2	102.6	4.1	9.65	1.30	1.05	0.4	< 0.4
12	ED-TROC-2 D	85.0	2.8	9.45	1.77	1.49	0.3	< 0.4
13	ED-TROC-3	22.3	1.2	9.49	3.24	2.89	0.4	< 0.4
14	ED-TROC-3 D	25.9	1.3	9.43	2.92	2.61	0.4	< 0.4
15	ED-TROC-4	154.9	10.7	9.72	0.67	0.51	0.4	< 0.4
16	ED-TROC-4 D	184.5	14.1	9.65	0.58	0.45	0.4	< 0.4
17	ED-ORTHO-1	29.7	2.9	9.56	0.68	0.51	0.3	< 0.4
18	ED-ORTHO-1 D	31.2	3.2	9.62	0.58	0.46	0.3	< 0.4
-- Check --								
19	ED-TROC-2	98.8	3.9	9.76	1.34	1.09	0.4	< 0.4

# LAKEFIELD RESEARCH LIMITED

Box 4300, 185 Concession St., Lakefield, Ontario, K0L 2H0  
 Phone : 705-652-2038 FAX : 705-652-6441

Environmental Services

Lakefield, November 12, 1996

Date Rec. : October 2, 1996  
 LR. Ref. : OCT7008.R96  
 Reference : Hum Cell Init.ABA  
 Project : 7-296

## CERTIFICATE OF ANALYSIS

### Initial EPA ABA Modified

Element	ED-GNEISS-1	ED-GNEISS-1 D	ED-GNEISS-2	ED-GNEISS-2 D	ED-GNEISS-1
Constant	0.9950	0.9950	0.9950	0.9950	0.9950
Normality (of HCl)	0.5061	0.5061	0.5061	0.5061	0.5061
HCL added [mL]	40	40	40	40	40
Initial [pH]	0.96	0.96	0.94	0.95	1.05
NaOH to [pH=7.0]	34.50	34.60	37.80	37.85	35.10
HCl (mL) [Consumed]	5.7	5.6	2.4	2.3	5.1
NP [*]	72.1	70.9	30.4	29.1	64.5
MPA [*]	4.1	13.1	0.9	1.3	4.1
CNNP [*]	68.0	57.8	29.5	27.8	60.4
NP/MPA [*]	17.6	5.4	33.8	22.4	15.7
Paste pH [units]	9.81	9.73	9.88	9.81	9.86
Fizz Rate [1-4]	3	3	3	3	3
S [%]	0.13	0.45	0.03	0.03	0.13
S- [%]	0.06	0.29	0.01	0.03	0.03
CO3 [%]	0.4	1.2	< 0.1	0.2	< 0.1
SO4 [%]	< 0.4	0.6	0.7	< 0.4	< 0.4

Constant (C) = (mL acid in blank) / (mL base in blank)  
 mL acid consumed = (mL acid added) - (mL base added x C)

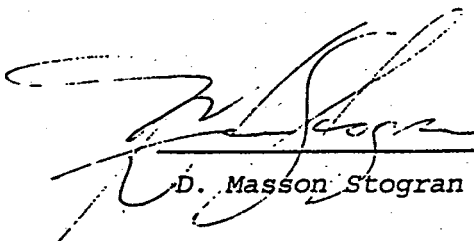
\*NP (Neutralization Potential)  
 = (mL acid consumed) x (25) x (N of acid)

\*MPA (Maximum Potential Acidity)  
 = % Sulphide Sulphur x 31.25

\*CNNP (Common Net Neutralization Potential)  
 = NP - MPA

\*Results expressed as tonnes CaCO3 eq/1000 tonnes material

Sample(s) Received: Oct. 2, 1996



D. Masson Stogran

Environmental Services

Lakefield, November 12, 1996

Analyst: Richard Wagner

Date Rec. : October 15, 1996

LR. Ref. : OCT7041.R96

Reference : Modified ABA

Project : 7777-296

## CERTIFICATE OF ANALYSIS

### EPA Modified ABA - Initial Hum. Cell

No.	Sample ID	Constant	Normality of HCl	HCl added mL	NaOH to pH=7.0	HCl (mL) Consumed	NP *	MPA *
9	WE-TROC-5	1.0076	0.5061	40	32.40	7.4	93.6	..
10	WE-TROC-5 D	1.0076	0.5061	40	31.60	8.2	103.8	..
11	WE-TROC-6	1.0076	0.5061	40	30.90	8.9	112.6	..
12	WE-TROC-6 D	1.0076	0.5061	40	29.45	10.3	130.3	..
13	WE-TROC-7	1.0076	0.5061	40	30.50	9.3	117.7	..
14	WE-TROC-7 D	1.0076	0.5061	40	30.70	9.1	115.1	..
15	WE-PARA-1	1.0076	0.5061	40	35.00	4.7	59.5	..
16	WE-PARA-1 D	1.0076	0.5061	40	35.00	4.7	59.5	..
17	VB-GRAN-1	1.0076	0.5061	40	37.00	2.7	34.2	..
18	VB-GRAN-1 D	1.0076	0.5061	40	36.65	3.1	39.2	..
-- Check --								
19	WE-TROC-7	1.0076	0.5061	40	30.75	9.0	113.9	..

No.	Sample ID	CNNP *	NP/MPA *	Paste pH units	S %	S= %	CO3 %	SO4 %
9	WE-TROC-5	..	..	9.10	0.44	0.24	0.4	< 0.40
10	WE-TROC-5 D	..	..	9.24	0.33	0.21	0.4	< 0.40
11	WE-TROC-6	..	..	9.28	1.71	1.40	0.3	< 0.40
12	WE-TROC-6 D	..	..	9.26	1.43	1.13	0.4	< 0.40
13	WE-TROC-7	..	..	9.29	2.24	1.91	0.4	< 0.40
14	WE-TROC-7 D	..	..	9.14	2.46	2.14	0.5	< 0.40
15	WE-PARA-1	..	..	9.16	0.38	0.27	1.1	< 0.40
16	WE-PARA-1 D	..	..	9.27	0.32	0.22	0.4	< 0.40
17	VB-GRAN-1	..	..	9.73	0.12	0.05	0.4	< 0.40
18	VB-GRAN-1 D	..	..	9.56	0.28	0.11	0.2	< 0.40
-- Check --								
19	WE-TROC-7	..	..	9.34	2.26	1.93	0.4	< 0.40

**ACTLABS**

**ACTIVATION  
LABORATORIES LTD**

---

Invoice No.: 12466  
Work Order: 12539  
Invoice Date: 03-MAR-97  
Date Submitted: 07-FEB-97  
Your Reference: NONE  
Account Number: 1496

UNIVERSITY OF WATERLOO  
DEPT. OF EARTH SCIENCES  
WATERLOO, ONTARIO  
N2L 3G1

CONTACT: RON NICHOLSON

**CERTIFICATE OF ANALYSIS**  
-----

SAMPLES were submitted for analysis.

The following analytical packages were requested. Please see  
current fee schedule for elements and detection limits.

PORT 12466 S, SO4, CO2 - LECO  
PORT 12466 B PKG 1E OPTION 1-AQUA REGIA ICP

This report may only be reproduced in its entirety without the  
express consent of ACTIVATION LABS. If no instructions were received  
a copy will be received within 90 days from the date of this report, excess  
material will be discarded. Our liability is limited solely to the  
analytical cost of these analyses.

CERTIFIED BY :



DR. E. L. HOFFMAN

SAMPLE DESCRIPTION	S %	CO2 %	SO4 %
FAROI-1	19.5	0.051	1.15
FAROI-2	18.7		
FAROI-3	18.4		
DOYN-1	6.09	0.124	0.716
DOYN-2	5.79		
DOYN-3	12.4		
WMHS-1	3.77	0.070	0.917
WMHS-2	3.89		
WMLS-1	1.70	0.070	0.524
WMLS-2	2.23		
PAMR-1	0.670	4.14	1.02
PAMR-2	0.485		
KZK-1	0.738	1.79	0.399
KZK-2	0.994		

Invoice No.: 12466  
Work Order: 12539  
Invoice Date: 03-MAR-97  
Date Submitted: 07-FEB-97  
Your Reference: NONE  
Account Number: 1496

UNIVERSITY OF WATERLOO  
SCHOOL OF EARTH SCIENCES  
WATERLOO, ONTARIO  
N2L 2G1

CONTACT: RON NICHOLSON

CERTIFICATE OF ANALYSIS  
-----

SAMPLES were submitted for analysis.

The following analytical packages were requested. Please see  
current fee schedule for elements and detection limits.

RT 12466 S, SO4, CO2 - LECO  
RT 12466 B PKG 1E OPTION 1-AQUA REGIA ICP

This report may only be reproduced in its entirety without the  
express consent of ACTIVATION LABS. If no instructions were received  
all results will be received within 90 days from the date of this report, excess  
material will be discarded. Our liability is limited solely to the  
analytical cost of these analyses.

CERTIFIED BY :



DR. E. L. HOFFMAN